



**Parametric Studies on the Behaviour of Reinforced Soil Retaining Walls  
under Static and Dynamic Loadings**

**Brian Oluwatobi Oyegbile**

**Advisor**

**Prof. V.N. Georgiannou**

A dissertation submitted to the postgraduate school of civil engineering in partial fulfilment of the requirements for the degree of Master of Science in civil engineering, The National Technical University, Athens.

**July 2011**

## CERTIFICATION

Parametric Studies on the Behaviour of Reinforced Soil Retaining Walls under Static and Dynamic Loadings

A Dissertation Presented to Post Graduate School of Civil Engineering in Partial Fulfilment of the Requirements for the Award of Master of Science in Civil Engineering

By:

Brian Oluwatobi Oyegbile

X

\_\_\_\_\_  
Advisor (Name)

X

\_\_\_\_\_  
Signature and Date

X

\_\_\_\_\_  
Internal Examiner (Name)

X

\_\_\_\_\_  
Signature and Date

X

\_\_\_\_\_  
External Examiner (Name)

X

\_\_\_\_\_  
Signature and Date

## **ACKNOWLEDGEMENT**

This study was carried out under the supervision of my Advisor Professor V.N. Georgiannou, School of Civil Engineering, National Technical University of Athens, Athens, Greece.

I would like to express my sincere gratitude to my Advisor Professor V.N. Georgiannou for her guidance and support throughout the study period. My acknowledgement is due to the Director of ADERS program Professor Papakradakakis M. for his help, support and valuable advice throughout my study. My sincere appreciations go to my friends Thang, Yannis and Nikos for assisting me in some technical matters and giving me valuable suggestions during my study.

I will also have to thank my family and other colleagues for their supports and encouragements throughout my study at the prestigious National Technical University of Athens, Athens, Greece.

## **ABSTRACT**

Nowadays Geosynthetics have been used as a routine reinforcement in earth structures such as reinforced soil retaining walls (mechanically stabilized earth (MSE) walls), column-supported embankments, soil slopes, and paved/unpaved roads. Reinforced soil structures are both economically and technically vary advantageous over their conventional counterparts, especially under poor soil conditions and when there are property line limitations. Various researchers have carried out extensive investigations into the mechanisms of reinforcement of the above-mentioned applications; especially the geosynthetic-soil interactions and they have subsequently considered them into design methods.

This dissertation presents case studies and analyses of reinforced soil retaining walls were carried out. The behaviour of the walls under static and dynamic loadings was investigated numerically with the aid of finite element program-Plaxis and EERA Shake 91. The finite-element analyses provide relevant information on the mechanical behaviour of the wall that was otherwise difficult to obtain from the limit equilibrium based current design approaches. Practical implications of the findings of this study are highlighted along with the role of numerical modelling in the analysis and design of geosynthetic-reinforced retaining walls.

## LIST OF SYMBOLS

Tensile Force of the Soil Reinforcement	$T$
At Rest Lateral Earth Pressure Coefficient	$k_o$
Active Lateral Pressure Coefficient	$k_a$
Angle of Internal Friction of Sliding Surface	$\phi$
Maximum Tensile Force	$T_{max}$
Angle of Vertical Wall Inclination	$\theta$
Stiffness of Soil Reinforcement	$k$
Longitudinal Strain of Soil Reinforcement	$\varepsilon_h$
Factor of Safety	$F_s$
Weight of Sliced Blocks	$W$
Length of Sliding Plane in Sliced Block	$b$
Cohesion of Sliding Surface	$c$
Inclination of Sliding Surface with Horizontal	$\alpha$
Sliding Moment of Soil Reinforced Wall	$M_D$
Resisting Moment of Soil Reinforced Wall	$M_R$
Resisting Moment of Geogrids	$\Delta M_R$
Radius of Slip Surface	$R$
Sum of Tensile Strengths of Geogrids	$T_i$
Horizontal Earth Pressure	$P_H$
Axial Stiffness of Soil Reinforcement	$EA$
Saturated Unit Weight of Soil	$\gamma_{sat}$
Unsaturated Unit Weight of Soil	$\gamma_{unsat}$
Horizontal Permeability	$k_x$
Vertical Permeability	$k_y$
Young's Modulus	$E$
Poisson's Ratio	$\nu$
Dilatancy Angle	$\Psi$
Interface Strength Reduction Factor	$R_{inter}$

Maximum Bending Moment	$M_p$
Maximum Axial Force	$N_p$
Flexural Rigidity	$EI$
Weight of the Plate	$w$

## TABLE OF CONTENTS

<b>CHAPTER 1 .....</b>	<b>1</b>
<b>INTRODUCTION.....</b>	<b>1</b>
<b>1.1 General.....</b>	<b>1</b>
<b>1.2 Objectives and Scope of Study.....</b>	<b>4</b>
<b>1.2.1 Numerical Analysis of Reinforced Soil Retaining Walls for Appropriate Geometry and Load .....</b>	<b>4</b>
<b>1.2.2 Numerical Analysis of Reinforced Soil Retaining Walls for Appropriate Geogrids Stiffness Selection .....</b>	<b>5</b>
<b>CHAPTER 2 .....</b>	<b>8</b>
<b>DEVELOPMENT OF REINFORCED EARTH STRUCTURES AND THEIR UNDERLYING PRINCIPLES .....</b>	<b>8</b>
<b>2.1 General.....</b>	<b>8</b>
<b>2.2 History and Development of Reinforcing Systems.....</b>	<b>9</b>
<b>2.3 Types of Reinforcing Materials.....</b>	<b>12</b>
<b>2.3.1 Inextensible Reinforcement.....</b>	<b>13</b>
<b>2.3.2 Extensible Reinforcement.....</b>	<b>14</b>
<b>2.3.3 Miscellaneous.....</b>	<b>14</b>
<b>2.4 Concept and Mechanism of Reinforced Soils .....</b>	<b>15</b>

<b>2.5 Behaviour of Reinforced Soil Structures .....</b>	<b>16</b>
<b>2.5.1 Vertical and Horizontal Soil Stress Distribution.....</b>	<b>17</b>
<b>2.5.2 Forces in Reinforcements .....</b>	<b>18</b>
<b>2.5.3 Horizontal Displacement .....</b>	<b>19</b>
<b>2.5.4 The Role of Face Rigidity .....</b>	<b>20</b>
<b>2.6 Typical Current Design Methods .....</b>	<b>21</b>
<b>2.6.1 Force Equilibrium Methods .....</b>	<b>22</b>
<b>2.6.1 Slope Stability Methods .....</b>	<b>24</b>
<b>2.6.3 Failure Modes .....</b>	<b>28</b>
<b>2.7 Finite Elements Analysis.....</b>	<b>29</b>
<b>CHAPTER 3 .....</b>	<b>32</b>
<b>ANALYSIS USING MODELING SOFTWARE .....</b>	<b>32</b>
<b>3.1 Overview of Plaxis Software .....</b>	<b>32</b>
<b>3.2 Numerical Analysis for Appropriate Load and Geometry .....</b>	<b>34</b>
<b>3.2.1 General Information on the Model.....</b>	<b>34</b>
<b>3.2.2 Geotechnical Parameters and Design Methods.....</b>	<b>34</b>
<b>3.3 Numerical Analysis for Appropriate Geogrids Stiffness.....</b>	<b>39</b>
<b>3.3.1 General Information on the Model.....</b>	<b>39</b>
<b>3.3.2 Geotechnical Parameters and Design Methods.....</b>	<b>40</b>



<b>CHAPTER 4 .....</b>	<b>46</b>
<b>RESULTS AND DISCUSSION .....</b>	<b>46</b>
<b>4.1 Numerical Analysis for Appropriate Load and Geometry .....</b>	<b>46</b>
<b>4.1.1 The First Analysis .....</b>	<b>46</b>
<b>4.1.2 The Second Analysis .....</b>	<b>47</b>
<b>4.1.2.1 Load-Displacement Variation of Reinforced Soil Retaining Wall for Loose Sand .....</b>	<b>47</b>
<b>4.1.2.2 Load-Displacement Variation of Reinforced Soil Retaining Wall for Dense Sand .....</b>	<b>50</b>
<b>4.1.2.3 Load-Displacement Variation of Reinforced Soil Retaining Wall for Silty Sand .....</b>	<b>51</b>
<b>4.1.2.4 Load-Displacement Variation of Reinforced Soil Retaining Wall for Clayey Sand .....</b>	<b>52</b>
<b>4.1.2.5 Spacing Displacement Variation of Reinforced Soil Retaining Wall for Loose Sand .....</b>	<b>53</b>
<b>4.1.2.6 Spacing Displacement Variation of Reinforced Soil Retaining Wall for Dense Sand .....</b>	<b>54</b>
<b>4.1.2.7 Spacing Displacement Variation of Reinforced Soil Retaining Wall for Silty Sand .....</b>	<b>55</b>
<b>4.1.2.8 Spacing Displacement Variation of Reinforced Soil Retaining Wall for Clayey Sand .....</b>	<b>56</b>
<b>4.1.2.9 Comparison of Displacement for Different Soil Cases under the Same Arrangement of Geogrids Spacing 0.5m and Applied Load of 20KN/m .....</b>	<b>57</b>

<b>4.1.2.10 Displacement Variation of Displacement with the Length of Geogrids for Loose Sand .....</b>	<b>58</b>
<b>4.1.2.11 Displacement Variation of Displacement with the Length of Geogrids for Dense Sand.....</b>	<b>60</b>
<b>4.1.2.12 Displacement Variation of Displacement with the Length of Geogrids for Silty Sand .....</b>	<b>61</b>
<b>4.1.2.13 Displacement Variation of Displacement with the Length of Geogrids for Clayey Sand .....</b>	<b>62</b>
<b>4.2 Numerical Analysis for Appropriate Geogrids Fitness .....</b>	<b>62</b>
<b>4.2.1 The First Analysis .....</b>	<b>63</b>
<b>4.2.1.1 The Horizontal Displacement .....</b>	<b>63</b>
<b>4.2.1.2 The Axial Forces.....</b>	<b>64</b>
<b>4.2.1.3 The Bending Moments .....</b>	<b>65</b>
<b>4.2.2 The Second Analysis .....</b>	<b>66</b>
<b>4.2.2 The Static Analysis.....</b>	<b>66</b>
<b>4.2.2.1 Stiffness-Displacement Variation of a Reinforced Soil Retaining Wall..</b>	<b>66</b>
<b>4.2.3 The Dynamic Analysis .....</b>	<b>70</b>
<b>4.2.3.1 Stiffness-Displacement Variation of a Reinforced Soil Retaining Wall (Agio Earthquake).....</b>	<b>70</b>
<b>4.2.3.2 Stiffness-Displacement Variation of a Reinforced Soil Retaining Wall (Sepolia Earthquake) .....</b>	<b>74</b>
<b>4.2.4 Geogrids Stiffness Response and Construction Industry .....</b>	<b>77</b>

<b>CHAPTER 5 .....</b>	<b>80</b>
<b>CONCLUSION AND RECOMMENDATION .....</b>	<b>80</b>
<b>5.1 Conclusion.....</b>	<b>79</b>
<b>5.2 Recommendation.....</b>	<b>80</b>
<b>REFERENCES .....</b>	<b>82</b>
<b>APPENDICES .....</b>	<b>88</b>

# CHAPTER 1

## INTRODUCTION

### 1.1 General

Reinforced soil retaining walls or reinforced earth walls (commonly grouped as Mechanically Stabilized Embankments – MSE) represent an innovative method of resolving familiar as well as unfamiliar and challenging problems. Reinforced earth is a composite material constructed with artificial reinforcing formed by interaction between frictional soil and reinforcing strips. Instead of regarding soil as a mass to be contained by force, the earth itself is reinforced to become an integral part of the structure. The walls behave as gravity structures in an integral unit and provide structural flexibility. Welded wire mats, geosynthetics placed within layers of compacted backfill provide the necessary tensile strength. Native soils at the site or from excavation are often acceptable for backfill. The resulting structure is strong, yet resilient (Reinforced Earth Company, 2011).

The recent applications of reinforced earth structures are vast. MSE walls use metal strips, wire meshes or geosynthetics as reinforcement to retain soil mass. Since the advent of MSE walls using geosynthetics in 1970s, they are now constructed routinely as retaining wall structures for a variety of applications ranging from private properties to public facilities (Allen et al., 2002). They are used for retaining walls, bridges, abutments, ramps, mine dump walls, ore storage silos and reclaim bunkers, haul road overpasses, containment dykes, wharf and quay walls, dams and weirs, materials handling, blast barriers and landscaping.

Reinforced soil retaining wall have gained substantial acceptance as an alternative to conventional masonry and reinforced concrete cantilever retaining wall structures due to their simplicity, rapidity of construction, less site preparation and space requirement for construction operation. In addition to technical and performance advantages, another primary reason for the acceptance of reinforced earth retaining wall has been its inherent economy. According to the survey of earth retaining structure practice in the North America, geosynthetic-reinforced MSE walls

represented the lowest cost for all wall heights among all types of retaining walls (Yako and Christopher, 1988; Koerner and Soong, 2001). Besides the economic advantage, MSE walls possess other advantages such as easy construction, good tolerance to differential settlement, and excellent aesthetics (J. Huang et al., 2011).

It is reported that, in reinforced earth retaining structures, beside its outstanding performance, a cost saving of up to 30% to 50% below alternative solutions have been achieved (Reddy, 2003). Seismic loading, differential heave and settlement requirements make rigid masonry and concrete cantilever walls very difficult to achieve the desired safety factor. Whereas, reinforced earth system when subjected to seismic loads and differential earth movement has shown exceptional performance due to its flexibility and inherent energy absorption capacity.

Reinforced soil structures are both economically and technically vary advantageous over their conventional counterparts, especially under poor soil conditions when there are property line limitations. Moreover, reinforced soil structures provide numerous other indirect savings and conveniences, such as speedy construction time, ease in construction methods, graceful appearances, etc. (Zeynep, Durukan and Tezcan, 2003).

In his final report for Iowa Department of Transportation Iowa, United States in 1997, Jeff Bales observed that the linear cost of construction was raised by more than 50% per linear foot by reinforced concrete retaining wall for the same kind of construction of reinforced earth wall. He noted that in addition to the initial cost effectiveness of reinforced soil retaining wall, there has been little or no maintenance needed.

However, the increasing use of reinforced earth in geotechnical engineering requires the development of reliable and practical yield design methods for reinforced earth structures (Ochiai H. et al., 2001). Although comprehensive analytical and finite element studies of reinforced soil behaviour are necessary and important for a comprehensive analysis and design of reinforced soil structure, yet they are inevitably complicated by the fact that the precise geometry of the reinforcement and the elastic-plastic nature of the soil needs to be fully taken into account for optimum design of the reinforced earth wall. Examples of the analysis of reinforced soils using these types of approaches include those, among others, given by Rowe and Skinner, (2001); Saad, Mitri and Poorooshab (2006) Huang et al. (2010) and Yang (2010).

Extensive researches have been conducted to either investigate the reinforcement mechanisms or quantify a certain aspect of the reinforcement effects such as stress reduction for reinforced embankments and structure number increase for reinforced paved/unpaved roads, which include field and full-scale tests (e.g., Hatami and Bathurst 2005; Kwon et al. 2009b) as well as numerical modelling (e.g., Hatami and Bathurst 2005 and 2006; Huang 2007).

It is interesting to know that numerical modelling of reinforced earth retaining wall and other structures has been increasingly adopted in researches since in addition to their outstanding cost- and time-effectiveness, they possess the following preferable advantages as compared with the field and full-scale tests:

- *Flexibility*: Variables can be easily fixed or varied to assess their effects; parametric studies can be easily performed.
- *Comprehensive data*: The numerical modelling can provide a complete set of data, some of which are difficult or not able to be obtained from instrumentations such as shear stress/strain.
- *Efficiency for long-term behavior performance study*: The long-term performance is one of the interests for research and practice, e.g., consolidation of reinforced embankments and creep behaviour of MSE walls. Given the appearance of geosynthetic in 1970's, valid long-term monitoring data are rare. Numerical modelling can extend the time domain to the point of interest.
- *Exclusion of scale effect and external disturbance*: Full-scale laboratory tests tend to be influenced by scale, more or less and field tests are inevitably disturbed by external impacts. These scale effect and external disturbance can be easily excluded from or minimized in the numerical modelling.
- *Minimum measurement errors*: The experimental data intrinsically possess measurement errors, which is not a problem in numerical modelling.

Considering the above merits of the numerical modelling, numerical modelling plays an important, sometime irreplaceable, role in promoting the research and practice. This research work employs the use of Plaxis version 8, a finite element program and

EEAR Shake 91 for modelling and analysis of the model in each of the cases considered.

## **1.2 Objectives and Scope of Study**

Although reinforced earth is widely used in different parts of the world, it is still necessary to make further studies on the behaviour of the reinforced earth wall when the mechanical properties and geometry of its composite materials changes for optimum design of the wall. This dissertation aims at performing a parametric analysis on the behaviour of reinforced soil retaining walls under static and dynamic loadings. In order to achieve this aim, the followings objectives are set:

- To determine the influence of changes in the geometry on the performance of reinforced soil retaining walls.
- To determine the influence of changes in applied load on the performance of reinforced soil retaining walls.
- To determine the influence of changes in mechanical properties of geogrids on the performance of reinforced soil retaining walls.

In order to effectively determine the influence of geometry and mechanical properties of reinforced soil retaining walls, this research work will be divided into two different analytical cases with different case studies and these include:

- Numerical analysis of reinforced soil retaining wall for appropriate loads and geometry.
- Numerical analysis of reinforced soil retaining wall for appropriate geogrids stiffness selection.

### **1.2.1 Numerical Analysis of Reinforced Soil Retaining Walls for Appropriate Geometry and Load**

This part of my dissertation has to do with a comprehensive study of the effects of changes in geometry of reinforced earth's composite materials. The model used in this analysis was adapted from Wikipedia. It should be noted that Mr Gaurav Singhai in his M.Sc. thesis titled "Analysis of Reinforced Earth Wall" at Delhi University,

Delhi, has carried similar studies. In his studies, an attempt was made to determine the influence of changes in geometry and applied load in the responses of the reinforced soil retaining walls. There are four categories of soil types that he examined as case studies - loose sand, dense sand, silty sand and clayey sand. In addition, the soil parameters for both the wall and the foundation in his each case of study were assumed uniform (i.e. the same soil parameters were used for both the foundation and the fill).

However, my own study focused on the parametric analysis of the same wall and soil cases but with limestone as foundation material under static loading. Hence, there are three stages with two categories of analyses, involved in this part of my dissertation namely:

- Parametric analysis of the same wall with the same conditions of geometry and soil parameters like the case of Mr. Gaurav Singhai.
- Parametric analysis of the same wall but different foundation material.
- Analysis and comparison of the results obtained from the first two stages.

The idea is to determine the behaviour of the wall with underlying limestone as foundation material and any variation in the behaviour of the wall in each case (results of stages one and two). The geometry of soil layer and the reinforcement (geogrids) are varied in order to determine the response of the reinforced soil retaining wall and the results are analysed by comparing the horizontal and vertical displacements. Four different cases representing four different soil types with different geotechnical properties are considered in this analysis. The influence of changes in the applied load was also investigated. The response of the reinforced soil retaining walls (RRW) in each case is considered and compared for the optimum design of the (RRW).

### **1.2.2 Numerical Analysis of Reinforced Soil Retaining Walls for Appropriate Geogrids Stiffness Selection**

Nowadays geosynthetics have been used as a routine reinforcement in earth structures such as mechanically stabilized earth (MSE) walls, column-supported



embankments, soil slopes, and paved/unpaved roads. In those applications, reinforcement mechanisms of the geosynthetics are vaguely described as confinement, interlocking, and load shedding respectively but not fully understood. The uncertainties of the mechanisms have been reflected as over conservativeness, inconsistency and empiricism in current design methods of those applications (J. Huang, *et al.* 2011). This part of my dissertation involves a case study of reinforced soil retaining walls associated with the construction of the Egnatia Motorway in Greece. In order to determine the influence of geogrids stiffness on the stability of soil-reinforced wall, static and dynamic analyses were carried out using a model.

The numerical analysis was carried out using Plaxis. The soil model used in this analysis was adapted from a published journal of geotechnical engineering titled “Numerical Analysis of Reinforced Soil Retaining Walls” by V.N. Georgiannou et al. The soil parameters, model dimension and other design parameters were also adapted from the journal.

The journal titled “Numerical Analysis of Reinforced Soil Retaining Walls” by V.N. Georgiannou et al. focused on the analysis of soil retaining walls using the finite difference program FLAC and the finite element program PLAXIS. Convergence in the displacement calculations and forces in the reinforcement was observed for both numerical methods of analysis.

The analysis in this part of my dissertation is divided into two stages. In the first stage, analysis was carried out in line with the content of the journal from which the model is adapted and the results obtained are approximately the same with that obtained from the journal. In the second stage, two cases of analysis were considered. Static and dynamic analyses were performed in order to know the behaviour of the wall with or without the condition of earthquake. The results obtained from each analysis were examined independently and subsequently compared in order to determine the behaviour of the model as a whole.

The soil model used to characterize the site was the elasto-plastic Mohr-Coulomb model. The basic Mohr-Coulomb input parameters for the two layers of soil are fully

described in Chapter 3 of this dissertation. The soil-geogrids wall was modelled as an elasto-plastic material.

## CHAPTER 2

### DEVELOPMENT OF REINFORCED EARTH STRUCTURES AND THEIR UNDERLYING PRINCIPLES

#### 2.1 General

The Concept of reinforcing soil with tensile members is not new. Dikes constructed from earth and tree branches have been used in China for at least 100 years ago. Dikes have also been constructed in The Netherlands to avert the problem of flood from sea that is of higher level than most parts of the Country (Figure 2.1 and 2.2). In England, wooden pegs, bamboo and wire mesh have been used for erosion and landslide control (Reddy, 2003).



**Figure 2.1:** Map of the Netherlands showing Areas that are Extensively Protected by Dykes  
Source: Jan Arkesteijn at nl.wikipedia, 2004



**Figure 2.2:** Dykes in Netherlands  
Source: Marjonnabar, Holland-Behind the Dykes, Webshot Channel, 2002

In the modern context, reinforced soil began to be used during the 1970's where firstly steel strips reinforcement and later, geotextiles reinforcement were used in the construction of reinforced soil walls for slope stabilization. The present concept of systematic analysis and design of reinforced earth was first developed by a French Engineer, Henri Vidal in 1966 and later on, numerous works have been done by Darbin in 1970, Schlosser and Vidal in 1969 and Schlosser and Long in 1974, and Schlosser et al. in 1983 on the use of metallic strips as a reinforcing material. Reinforced earth retaining walls have been constructed around the world since Vidal started his work. Many hypotheses have been postulated in the past 25 years about the load transfer between the soil and reinforcement and their interaction. Many researchers have also carried out studies to find suitable method for the analysis and design of reinforced soil structures.

## **2.2 History and Development of Reinforcing Systems**

The development of the reinforced earth techniques was marked by the following timelines:

- The French architect and inventor Henri Vidal pioneered the development of modern earth reinforcement techniques; the system he developed, known as Reinforced Earth was patented in 1966 as Terre Armee in French and Reinforced Earth in English

- The first reinforced soil retaining wall was built in Pragneres France (1965).
- The first group of reinforced earth structures was constructed on the Roquebrune-Menton highway (1968-1969). Ten retaining walls on unstable slopes totalizing a facing area of  $5500m^2$  were constructed.
- The first wall supporting important concentrated walls at its upper surface (traveling gantry cranes) was built at the Dunkerque port (1970).
- The first highway bridge abutment (14m high) was built in Thionvile (1972) (James, 1987).
- The first reinforced soil retaining wall with metal strips as reinforcement was constructed in 1972 in USA in the San Gabriel Southern California (Das, 1995).
- The use of geotextiles in soil reinforcement started in 1971 in France after their beneficial effect noticed in the construction of embankments over weak sub grades.
- Stabilization of highway slopes was accomplished in France (1974) and in California (1977). Stabilization of railway slopes was accomplished for French Railroad Administration (1973); retaining structures were constructed (Stoccker et al, 1979; Shen et al, 1981; Cartier and Gigan, 1983; Guillou, 1983). Applications for tunnelling and other civil and industrial projects were realized (Juran, 1981).
- The fundamental researches on the mechanism and design of the reinforced earth, including, essentially, 15 full-scale experiments, were realized from 1967 to 1978 by the “Laboratoire Central des ponts et Chaussées” in Paris.
- Since 1972, the “Laboratoire Central des Ponts et Chaussées” and the “Reinforced Earth Company” have undertaken jointly the studies on the durability of the reinforcements and on the phenomenon of corrosion of metals buried in the backfill soil. Since then, an entire experience was acquired in this field due to the laboratory tests, to the experiences in the corrosion box, to full-scale experiments and to observations on actual structures constructed since 1968 (Mitchel, 1987).
- The use of geogrids was developed around 1980 (Reddy, 2003). By placing tensile reinforcing elements in the backfill soil of reinforced earth wall, the strength of the soil is improved. With the addition of facing system, very steep slopes and vertical walls as a composite construction material can be safely constructed (Figure 2.3).

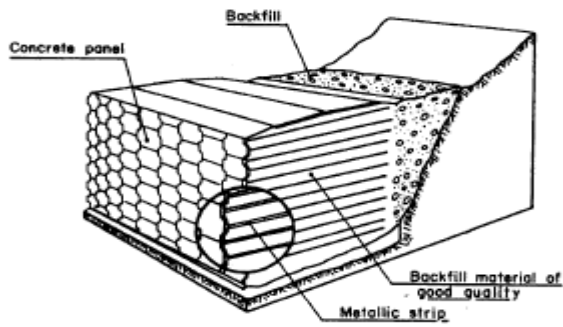


**Figure 2.3:** Typical Reinforced Earth System (Scholsser and Delage, 1987)

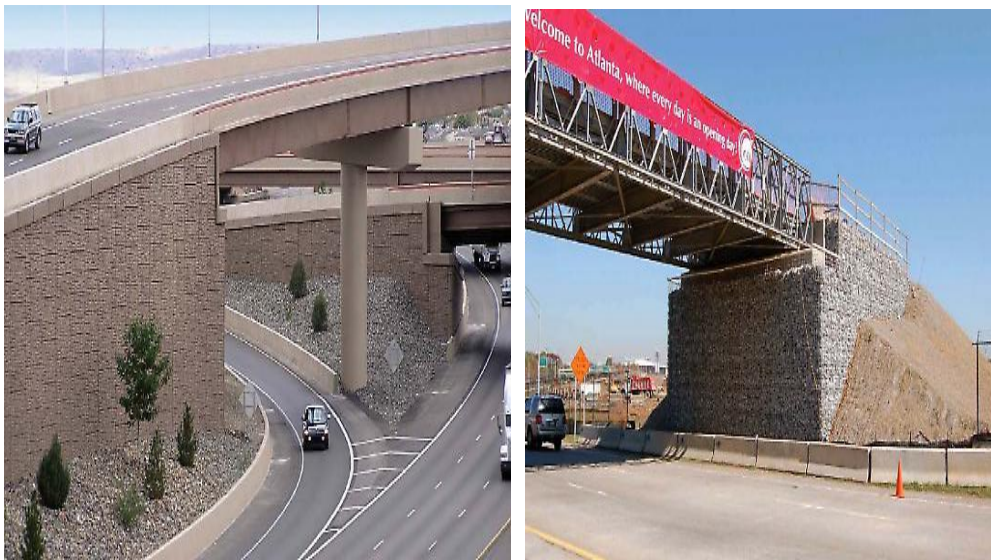
Two stages that marked the technological development of the reinforced earth are:

- The invention of the facing with concrete panels in 1971. Presently most of the structures are idealized with this type of facing.
- The development and the fabrication in 1975 of ribbed reinforcement strips for high adherence. These strips, 5mm thick, made of ordinary mild galvanized steel enable a large improvement of the soil-reinforcement friction

Therefore, since its invention in 1963, the reinforced earth technique has been quickly accepted on a worldwide basis as an economical and efficient solution and has been extensively used since then, in retaining walls and bridge abutments for highways, expressways and railroads lines as well as for other structures as industrial, civil, defence and water works projects. The reinforced earth is presently a well-known operating process generalized and accepted all over the world. Some applications of the techniques are shown in Figure 2.4. Structures were constructed in 32 countries and there are presently several specifications issued by state institutes on this technique (Germany, United States) (William and Bell, 1979).



(a)



(b)

**Figure 2.4:** Applications of Reinforced Earth as Retaining wall and Abutments (Reinforced Earth Company, 2011)

### 2.3 Types of Reinforcing Materials

The choices on the reinforcing material vary from inextensible reinforcements like steel, fiberglass to extensible polyester resins. In the literature, mainly two groups of reinforcements, extensible and inextensible, are discussed with respect to the stress-strain in response of soil mass. Stress-strain characteristics of typical inextensible and extensible reinforcing materials are illustrated in Fig. 2.5. Mc. Gown et al. (1978) originally defined inextensible and extensible reinforcements and Bonaparte et al. (1987) extended as follows:

(a) **Inextensible reinforcement** is reinforcement used in such a way that the tensile strain in the reinforcement is significantly less than the horizontal extension required to develop an active plastic state in the soil. An “absolutely” inextensible reinforcement is so stiff that equilibrium is achieved at virtually zero horizontal extension ( $k_0$  conditions prevail)

(b) **Extensible reinforcement** is reinforcement used in such a way that the tensile strain in the reinforcement is equal to or larger than the horizontal extension required to develop an active plastic state in the soil. An “absolutely” extensible reinforcement has such a low modulus that virtually no tensile forces are introduced to the soil mass at the strain required to develop an active plastic state ( $k_a$  conditions theoretically prevail).

Bonaparte (1987) considered steel reinforcement as an inextensible reinforcement and geosynthetic reinforcing materials as extensible reinforcements, for almost all practical applications. Thus, an inextensible metallic reinforcement makes the structure brittle and the extensible geosynthetic increases the ductility of the reinforced soil structure (Fig. 2.5).

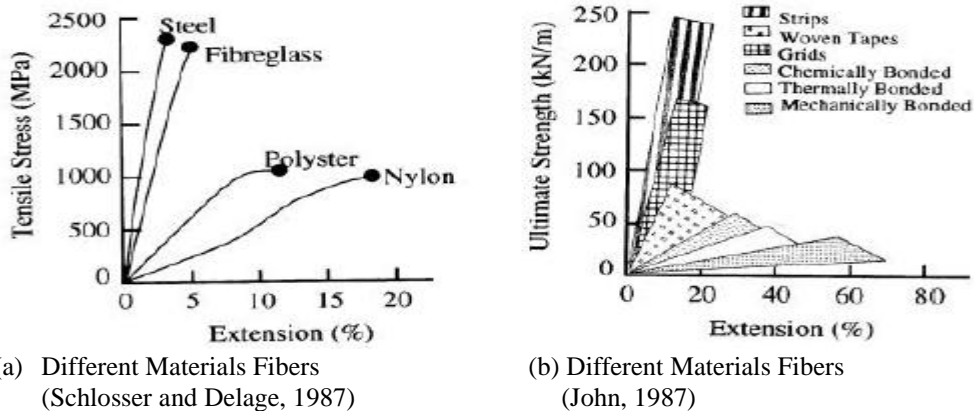


**Figure 2.5:** Stress-Strain Characteristics of Typical Reinforcing Material (Mc. Gown, Andrawes and Al-Hasani, 1978)

### 2.3.1 Inextensible Reinforcement

#### Steel Bar fibre glass reinforcements:

Galvanized steel has been used in wide variety of environments over very long periods, thus, its corrosion mechanism and the rate of corrosion have been known for long time. Similarly, polyester coated fiberglass, stainless steel and aluminium are



also used. The corrosion rate of these metals is faster than galvanized steel. Despite these drawbacks, the steel and fiberglass reinforcing materials have also gained popularity especially when the construction requires less post construction deformation such as in the case of bridge abutments, railway embankments, etc. The advantage of steel and fiberglass is due to their unique combination of elasticity, ductility/stiffness and favourable economics. Bonaparte et al. (1987) states that the tensile stiffness of steel reinforcements is stiff enough to keep the state of soil stress close to the at-rest ( $k_o$ ) condition.

### 2.3.2 Extensible Reinforcement

#### Geosynthetic and related products

Major geosynthetic materials currently used as reinforcements in soil structures are geogrids sheet (Fig.2.6), woven and non-woven geotextile sheet, coated fiber strips, rigid plastic strips, composites and three dimensional honeycomb type products. Geosynthetic materials have large ranges of deformation modulus and tensile strengths compared to metals (Fig. 2.3). Geosynthetic materials also exhibit creep behaviour. Bonaparte et al. (1987) has grouped geosynthetic reinforcements as extensible reinforcements, thus, the state of soil stress is far from at-rest ( $k_o$ ).

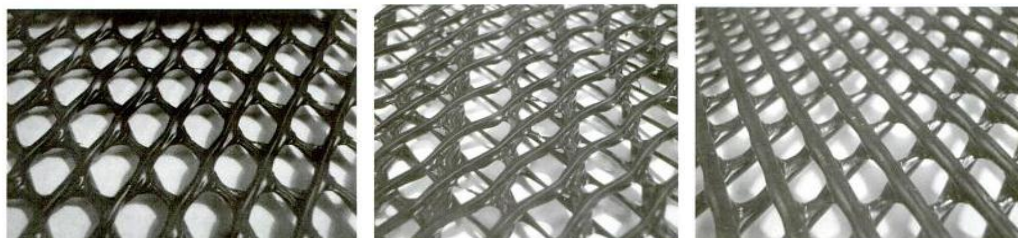


**Figure 2.6:** Samples of geogrids

Source: Geosynthetics in Civil and Environmental Engineering, Geosynthetics 2008, Proceedings of the 4<sup>th</sup> Asia Regional Conference in Geosynthetics in Shanghai, China

### 2.3.3 Miscellaneous

There are several other types of reinforcing materials used for particular purposes. Small inclusions (fibres, small plates) or continuous filaments (e.g. Texsol) are some typical reinforcing materials. Sometimes natural materials (e.g. bamboo, jute) are also used as reinforcing material. In the UK and the USA, redundant car tires have been used as reinforcement.

The failure mechanisms of both extensible and inextensible reinforcement have been studied. Their failure mechanism is shown in Figure 2.5.

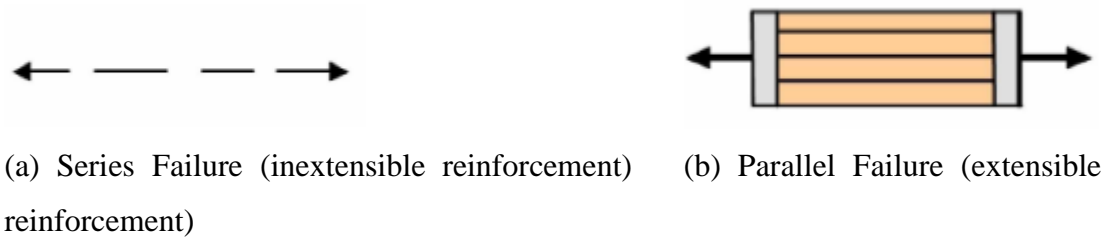


**Figure 2.7:** Analogy of Reinforced Soil Failure Mechanisms (Jones, 1985)

## 2.4 Concept and Mechanism of Reinforced Soils

Several experimental and theoretical investigations have been performed since the invention of Reinforced Earth wall (Vidal, 1963) to understand the concepts and mechanism of reinforced soil structure and interaction among its basic components, reinforcing elements, backfill soil and facing. H. Vidal, the pioneer of Reinforced Earth systems seems to be the first person to propose a general and realistic concept of reinforcing a soil.

### Anisotropic Cohesion Concept

Schlosser and Long (1972) indicated that the reinforced soil has higher shear strength than unreinforced plain samples (Fig. 2.6). Haussmann (1976) independently postulated a more unified anisotropic cohesion theory. They have shown that two failure modes can develop in such reinforced sand samples:

- (a) Failure by slippage of the reinforcement at low confining pressure leading to a curved yield line passing through the origin and
- (b) Failure by reinforcement breakage at higher confining pressure leading to a straight failure line which proves that the reinforced sand behaves as a cohesive material having the same frictional angle as the original sand and an anisotropic pseudo-cohesion due to reinforcements as shown in Fig. 2.8. This pseudo-cohesion is very rapidly mobilized at low axial deformations.

## Enhanced Cohesion Concept

Chapius (1972) independently presented *enhanced confining pressure concept* on the mechanism of reinforcing a soil mass. This concept is based on the assumption that the horizontal and vertical planes are no longer principal stress planes due to the shear stresses induced between the soil and reinforcements. Mohr's circle of stress is shifted due to reinforcing of the soil mass (Fig. 2.8b) while the slope of the failure envelope remained same for both reinforced and unreinforced samples. Such effect is called enhanced confining pressure effect.

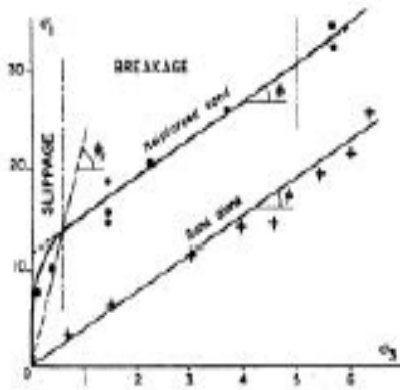


**Figure 2.8a:** Reinforced and Unreinforced Samples Triaxial Tests (Schlosser et al., 1972)

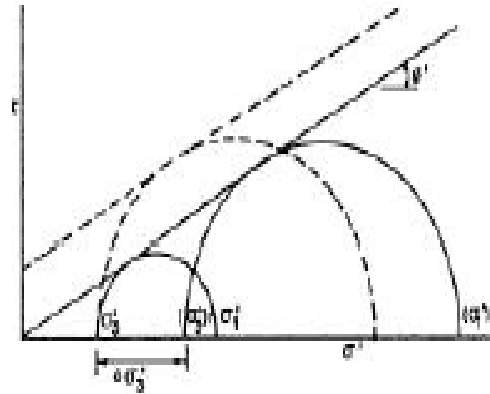


**Figure 2.8b:** Anisotropic Cohesion and Enhanced Cohesion Concepts (Ingold, 1982)

## 2.5 Behaviour of Reinforced Soil Structures

In the analysis and design of reinforced soil structure, stability and deformation are considered both critical and independent concerns for a soil structure and they are always dealt with separately. Past research reveals that major work was concentrated on stability analysis compared to the deformation problems. In deformation analysis, serviceability with respect to excessive differential settlement and horizontal deformation of the slope face are considered important. The stability analysis of reinforced soil structures is divided into internal and external stability analyses (Gourc, 1992; Rowe and Ho, 1992) as will be illustrated in later subsections.

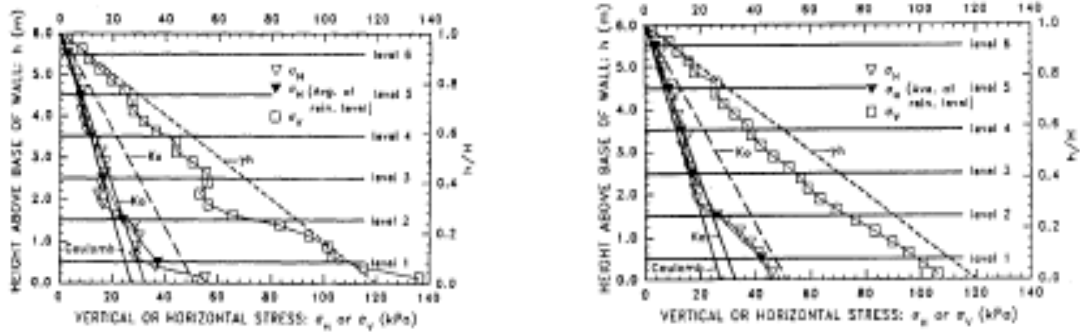
Rowe and Ho (1993) suggested that the overall behaviour of a reinforced soil structure may be considered known if one understands:

- State of stress within the reinforced soil mass
- State of strain in both the soil and the reinforcement

- Axial force distribution in the reinforcement
- Horizontal soil pressure acting at the back of the reinforced soil mass and the vertical soil pressure at the base
- Vertical soil stress on each reinforcement layer
- Horizontal soil pressure acting at the face
- Horizontal and vertical forces transferred to the wall face
- Horizontal deformation of the reinforced soil mass
- Effect of varying the design parameters (i.e. reinforcement stiffness, soil properties, reinforcement spacing, surcharge condition, construction procedures, etc.) on the response of the system

### **2.5.1 Vertical and Horizontal Soil Stress Distribution**

Several types of vertical stress distribution patterns are assumed in the analysis and design of reinforced soil mass. Uniform, trapezoidal, Meyerhof distributions and 2:1 stress dispersion method are typical examples. Maximum stress is attained within the reinforced zone. Close to the far end of reinforced zone, the vertical soil stress reaches a minimum. Further away into the unreinforced retained fill, the vertical soil stress attains the minimal value. The vertical soil stress close to the facing depends on the facing rigidity (Tatsuoka, 1992). Rigid facing decreases the vertical soil stress close to the facing due to load transfer from the soil to the facing. Such effect of the facing leads to higher reinforcement force and requires higher bearing capacity in the design of foundations. Horizontal soil stress primarily depends on the number of reinforcement layer, the stiffness and the creep of the reinforcement and the degree of yielding of the wall face as shown in Fig. 2.9. Relative deformation of the wall face and soil with the reinforcement results to increased transfer of horizontal stress to reinforcement rather than to facing. The horizontal soil stress increases as the number of reinforcement layers is increased. Rowe and Ho (1993) noted that there are no literatures giving any real observed information on the horizontal soil stress distribution further back into the reinforced soil.



(a) At Wall Face

(b) At Back of Reinforced Soil Block

**Figure 2.9:** Vertical and Horizontal Soil Stress Distributions from Numerical Analysis, (Ho and Rowe, 1992)

### 2.5.2 Forces in reinforcements

The magnitude of reinforcement force primarily depends on the shear strength mobilized in the backfill, the horizontal soil strain, the stiffness of the reinforced system, and the creep of reinforcement. Maximum tensile force close to toe is usually observed less than predicted by the Rankine active condition. Jewel (1988) and Ho-Rowe (1992) indicated that the maximum force in reinforcement becomes uniform with decreasing reinforcement stiffness and lower near the bottom due to the influence of foundation.

Variation in soil properties and construction methods results in shifting of the position of maximum tensile forces away from the failure plane. It also depends on the length and stiffness of reinforcements. Jewell (1988) stated that the locus of maximum tensile force ( $T$ ) would always be inclined to  $(45^\circ + \phi/2)$  the horizontal if the soil-reinforcement interface is sufficiently bonded, otherwise, the locus will move towards the facing. The maximum tensile force shifts towards the facing in the case of short reinforcements.

The force distribution in a reinforcement layer is most influenced by the construction method, the existence of facing, the lateral restraint of facing during construction and the facing- reinforcement connections. There are two general types of axial force distributions as shown in Fig.2.10 (a) & (b).

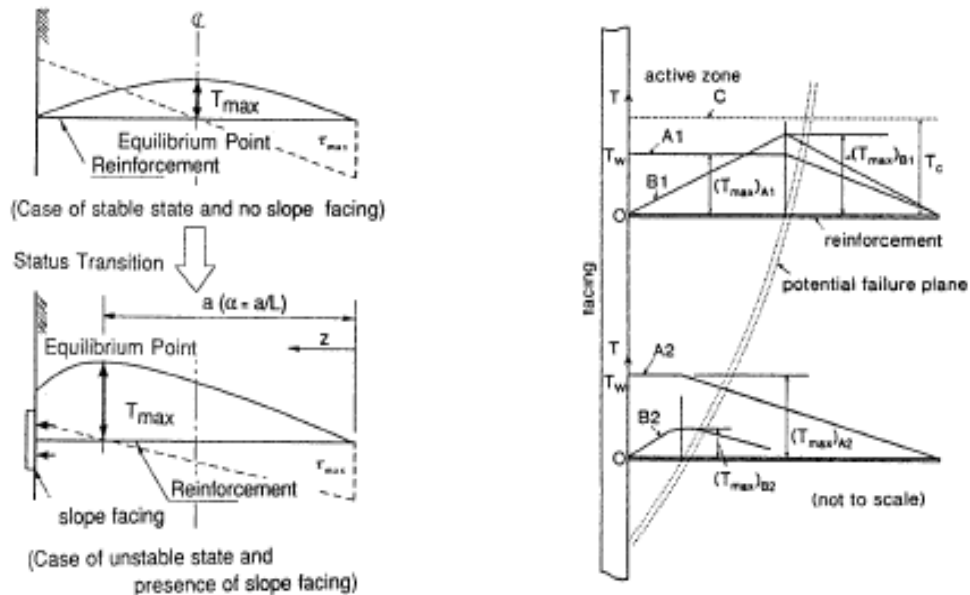


Figure 2.10: General Tensile Force Distribution Patterns along Reinforcement

Type A: This pattern is observed when lateral deformation of the wall face is restrained until the end of construction, e.g., ideal pull-out test. In this situation, the maximum tensile force is induced at the back of the facing, remains more or less constant up to the potential failure plane, and decreases to zero close to inner end of the reinforcement. When perfect lateral restraining of facing during construction is not possible, the tensile force in the reinforcement at the back of facing may be much smaller than its maximum value attained near the potential failure surface.

Type B: The parabolic tensile force distribution is observed when facing provides little or no lateral restraint against deformation e.g. wrapped back facing, slope face without any facing. The maximum force in the reinforcement is assumed to occur at the potential failure plane as shown in Figure 2.8 (b).

### 2.5.3 Horizontal Displacement

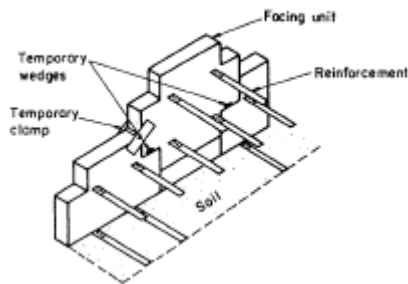
Magnitude of horizontal movement depends on the interaction between various components of reinforced soil structure and construction methods. Higher reinforcement density and stiffness reduce the strain in the soil, and larger shear strength of fill results in less force in the reinforcement, being required to maintain equilibrium and hence less deformation. The soil movement behind the reinforced zone depends on the strain level of the unreinforced zone above the stable slope.

### 2.5.4 The Role of Face Rigidity

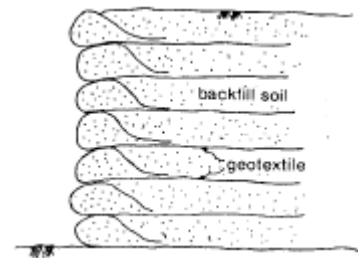
Currently, facing material ranges from rigid full-faced concrete facing to flexible wrapped around geosynthetic facing as shown in Fig. 2.11 (a-f). Most of the soil reinforced stabilization techniques assume that facing does not play a significant structural role; they are rather used for aesthetic reasons. However, Tatsuoka (1992) has demonstrated the roles of the facing in improving the stability of reinforced soil structures based on extensive literature review. Horizontal movement of the wall face and subsequent earth pressure development within the reinforced zone as well as the reinforcement force are significantly affected by the facing rigidity.

Tatsuoka (1992) has classified various types of facing according to the degree of facing rigidity. The facing rigidity increases the stability of wall in the following three ways:

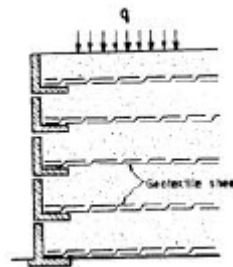
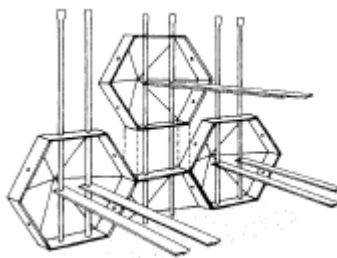
1. Rigid facings (Types D and E) support the combination of earth pressure and tensile force in reinforcement.
2. Weight of backfill is partly transmitted to the facing through the frictional force on the back face.
3. Due to high confining pressure behind rigid facing, the location of the overall reaction force becomes closer to the facing.



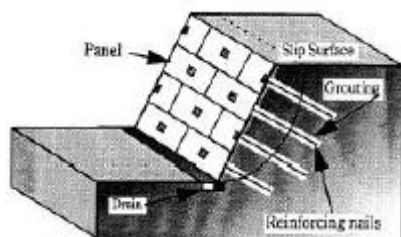
(a) Concrete Panel Facing (*Reinforced Earth system*)



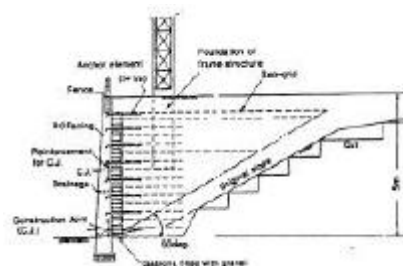
(b) Wrapped around Facing



(c) York Wall Facing (Jones, 1994)



(d) L-shaped Concrete Facing (Broms, 1988)



(e) Reinforced Concrete Panel (Japanese System)

(f) Full Height Reinforced Concrete Facing

**Figure 2.11:** Currently Used Typical Facings in Reinforced Soil Structures (Jones, 1994)

Tatsuoka et al. (1992) studied the effect of facing rigidity in a set of GRS-RWs model tests having facing Types A, D. The test result reveals that the location of failure surface moved from an intermediate elevation to the bottom of the facing depending on the facing rigidity. The tensile force just behind the facing is greatly influenced by the facing rigidity. Location of  $T_{max}$  (Fig. 2.10) approaches back of the facing with increasing facing rigidity. Thus, the contribution of the facing rigidity on the stability of the reinforced soil structure was clearly demonstrated and several other researchers (e.g., Juran-Schlosser, 1979, Bolton-Pang, 1982, and Koga et al., 1992) report similar conclusions.

## 2.6 Typical Current Design Methods

For the analysis and design of reinforced soil structures numerous approaches have been developed. All methods are either empirical in nature or based on limit equilibrium analysis. These methods do not consider either the stress-deformation characteristics of the structure or the interactions between the wall components e.g. the soil, the reinforcement, the facing and the foundation. Their main purpose is to compute the factor of safety against several modes of failure. In general, the design methods use the allowable strengths (corresponding to each component) which are significantly lower than the ultimate strengths and further partial safety factors are applied to account for the uncertainties in the behaviour of the reinforcement and soil/reinforcement interaction mechanism. Consequently, these methods are lagging in adequately describing the real behaviour of the reinforced soil structures. Hence,



their application typically introduces an extra level of conservatism. Rimoldi (1988) based on eight case histories reported that current design methods are conservative.

Most of the current design methods can be divided into two main categories. The first category use simple force equilibrium analysis where the horizontal forces developed in the reinforcement balance the destabilizing horizontal force from the soil. The forces considered in these methods are:

- The vertical soil stress,
- The horizontal soil stress,
- The stress in the reinforcement and
- The horizontal resistance to pull-out of the reinforcement behind the potential failure plane.

Two independent factors of safety, for reinforcement rupture and pull-out resistance are calculated for each layer of reinforcement. The methods in the second category evaluate the force and or moment equilibrium on an assumed failure surface similar to conventional slope stability analysis but with the inclusion of the balancing force/moment developed in the reinforcement.

### **2.6.1 Force Equilibrium Methods**

Some of the widely used force equilibrium methods for the design of numerous reinforced soil structures are as follows:

**1. Jewell Method (1987)** - This method was proposed and applied first to predict the performance of Royal Military College trial wall in 1987. In this method, the reinforced soil structure is divided into 3 zones based on the reinforcement force as shown in Figure 2.12.

Zone-1: The zone between the wall face and the most critical surface where the reinforcement force required for maintaining equilibrium is constant (i.e. between the surface and wall face). Thus, the most critical surface was defined as a surface through the toe that requires the greatest total reinforcement force to maintain equilibrium on this surface. The surface in vertical wall case is inclined at an angle  $\theta = (45 + \phi/2)$  to the horizontal as shown in Fig.2.12.

Zone-2: This zone is confined between the previously mentioned most critical surface and the locus of zero required force as shown in Fig.2. 12. A surface beyond which no additional stresses are required from the reinforcement to maintain equilibrium is called the locus of zero required force. Ideally, beyond this zone, the reinforcement can be truncated and equilibrium can be maintained by soil itself, such length of the reinforcement is called the ideal reinforcement length.

Zone-3: The zone beyond the locus of zero required force is in equilibrium without requiring any reinforcements.

Jewell (1988) proposed uniform spacing and ideal spacing pattern for reinforcement spacing. He further explained a truncated length concept and consequences of the truncation in the design. He also provided several design charts.

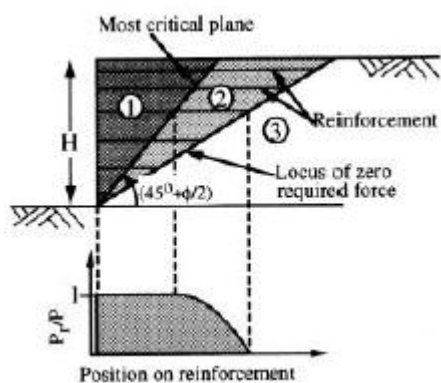


Figure 2.12: Reinforcement Layout and Force Distribution for Ideal Length Case (Jewell, 1988)

**2. Bonaparte et al. Method (1987)** - In this design method, the extensible and inextensible reinforcements are clearly distinguished. Then, the influence of reinforcement extensions is evaluated by defining hyperbolic relations between  $k \sim \epsilon_h$ . Detailed explanation about the method may be referred to Bonaparte et al. (1987).

**3. Tie Back Design Method (1978)** - Tie back method was originally developed by the U.K. Department of Transport (1978) and is based upon limit equilibrium methods. It is independent of the reinforcement material and it is used with both inextensible and extensible reinforcement and with anchors.

## 2.6.2 Slope Stability Methods

Many basic methods have been derived from the conventional slope stability studies; the most widely used (Rowe and Ho, 1992; Smith, 1992) being the Fellenius or Bishop methods or the Wedges methods. There are three noticeable differences among these methods as follow:

- (a) The shape of the failure surface
- (b) The distribution of force in the reinforcement and
- (c) The means by which a surcharge is considered

Typical slope stability methods are as follows:

### **Fellenius Method:**

In this method, it is assumed that for each slice the resultant of the interslice forces is zero. Taga et al. (1992) have summarized all the possible combinations of various forces based on the Fellenius (simplified) method used in the analysis and design of reinforced soil structures where the basic computational formula used is as follows:

*Sliding & Safety Factor,*

$$F_s = \frac{\text{Force resisting sliding}}{\text{Force inducing sliding}} \\ = \frac{\sum [cb + W \cos \alpha \cdot \tan \phi]}{\sum W \sin \alpha} \dots \dots \dots (2.1)$$

Where,

$W$  - The weight of sliced blocks

$b$  -The length of sliding plane in sliced block

$\phi$  - The angle of internal friction of sliding surface

$c$  - The cohesion of sliding surface

$\alpha$  – Inclination of sliding surface with horizontal

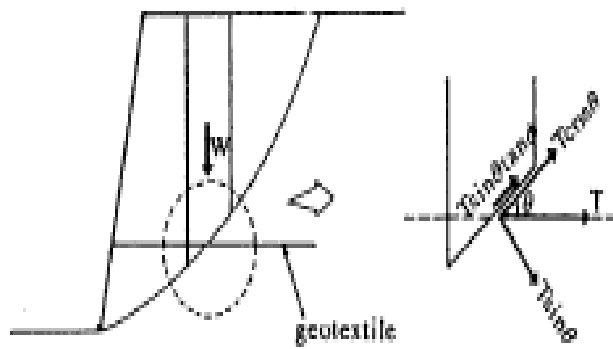


Figure 2.13: Fellenius Method of Analysing Reinforced Soil Structures

There are two reinforcement effects of the tensile force generated in the reinforcements in the sliding surface (see Fig. 2.13).

(1) Anchoring effect,  $T \cos \alpha$

(2) Confining effect,  $T \cos \alpha \cdot \tan \phi$

Regarding the confining effect (2), involves the equation, Eq. (2.1), and regarding the anchoring effect (1), two possible conditions arise, it may be considered as a resisting force (numerator) and as a sliding force (denominator). Sometimes, both effects are considered simultaneously together depending on the problem. Thus following five combinations can be derived by coupling these two effects with the Eq. (2. 1).

Formula (a):

$$F_s = \frac{\sum [cb + W \cos \alpha \cdot \tan \phi + T \cos \alpha]}{\sum W \sin \alpha} \dots \dots \dots (2.2)$$

Formula (b):

$$F_s = \frac{\sum [cb + W \cos \alpha \cdot \tan \phi]}{\sum (W \sin \alpha - T \cos \alpha)} \dots \dots \dots (2.3)$$

Formula (c):

$$F_s = \frac{\sum [cb + W \cos \alpha \cdot \tan \phi + T \sin \alpha \cdot \tan \phi]}{\sum W \sin \alpha} \dots \dots \dots (2.4)$$

Formula (d):

$$F_s = \frac{\sum [cb + W \cos \alpha \cdot \tan \phi + T \cos \alpha + T \sin \alpha \cdot \tan \phi]}{\sum W \sin \alpha} \dots \dots \dots (2.5)$$

Formula (e):

$$F_s = \frac{\sum [cb + W \cos \alpha \cdot \tan \phi + T \sin \alpha \cdot \tan \phi]}{\sum (W \sin \alpha - T \cos \alpha)} \dots \dots \dots (2.6)$$

**Bishop Method:**

In this method, it is assumed that the resultant forces on the sides of the slices are horizontal. Thus, moment equilibrium is checked in this method as follows (refer Figure 2.14):

$$F_s = (M_R + \Delta M_R) / M_D \dots \dots \dots (2.7)$$

Where  $M_D$  = sliding moment,  $M_R$  = resisting moment of soil,  
 $\Delta M_R$  = resisting moment of geogrids,  $\Delta M_R = R \cdot T_i$   
 $R$  = radius of slip circle, and  $T_i$  = sum of tensile strengths of geogrids.

A typical formula for computing the factor of safety based on Bishop's Method is:

$$F_s = \frac{\sum [cb + (W - ub + P + T \sin \gamma) \tan \phi]}{\sum [W \sin \alpha + P \sin \alpha - T \cos (\alpha + \gamma)]} \dots \dots \dots (2.8)$$

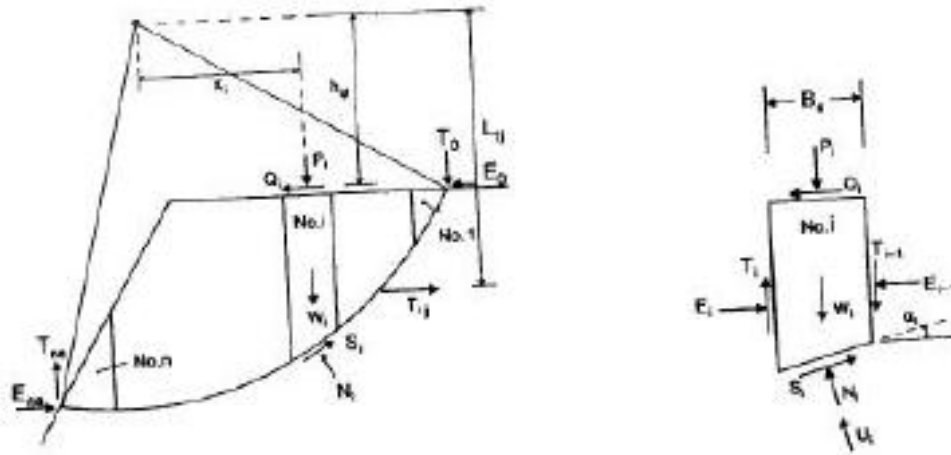


**Figure 2.14:** Bishop's Simplified Method of Analysing Soil Structures (Alan Mc. Gown, Khen Yeo and Andrawes, 1990)

**Trial Wedges Method:**

Slip surfaces in the trail wedge method can be assumed as two straight-line slips caused by the horizontal earth pressure, similar to the experimental data.

$$F_s = \frac{\sum T_i}{P_H} \dots \dots \dots (2.9)$$

In this equation,

$P_H$  = horizontal earth pressure and

$\sum T_i$  = sum of tensile strengths of the geogrids.

Total horizontal earth pressure components of the two straight- line slips, divided into two areas, Zone-1 and Zone-2, as shown in Figure 2.15, can be obtained based on the concept of force polygons. It can be determined that the embankment is stable when the external force of retaining wall acting is larger than  $P_H$ .

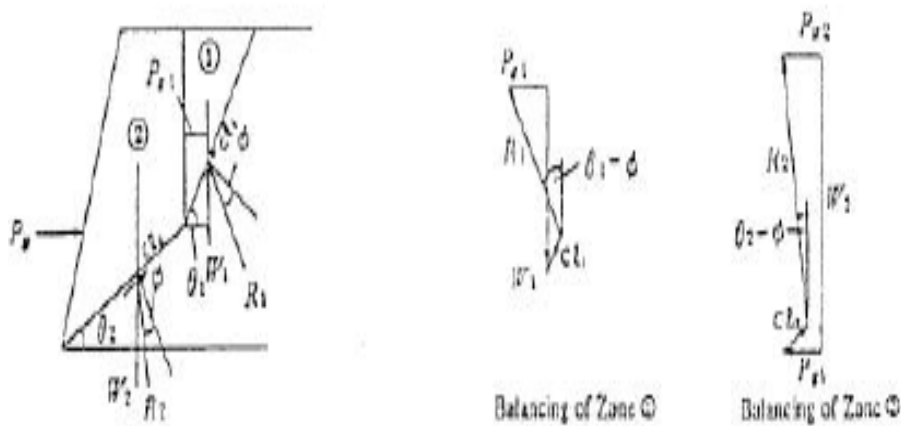


**Figure 2.15:** Trial Wedge Method of Analysing Reinforced Soil Structures (Taga et al., 1992)

### **2.6.3 Failure Modes**

Sometimes several possible failure modes are checked in reinforced soil walls depending on type of the structure itself and the field conditions. Generally, four independent types of failure modes (see Figure 2.16) are suggested sufficient enough for most of the geotechnical design problems (Bolton, 1989). These failure modes are grouped into two (external and internal) stability criteria. Typical failure modes that are checked (Jones, 1994) in the design of reinforced soil structures are mentioned below:

#### **External Stability**

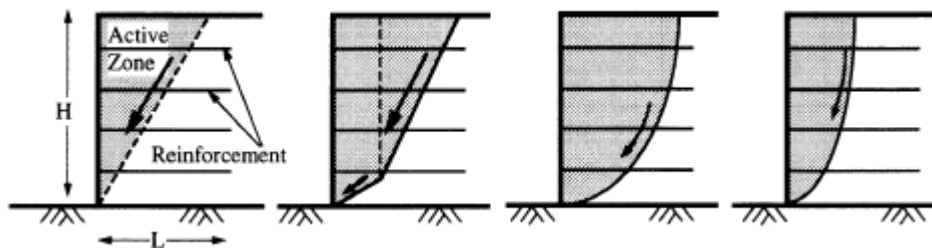
- (a) Vertical and horizontal deformations resulting into unacceptable differential settlement.
- (b) Lateral sliding of reinforced soil
- (c) Overturning failure due to rotation about toe of the wall
- (d) Bearing capacity failure (punching) of the foundation soil under the reinforced soil
- (e) Overall collapse of the reinforced wall or embankment or nailed slope

#### **Internal Stability**

- (a) Rupture failure of reinforcement
- (b) Pull-out failure of reinforcement

Sliding	Overturning	Bearing capacity	Stability against sliding
$F_s = \frac{\mu (W - P_v)}{P_H} \geq 1.5$ <p><math>\mu</math>: Frictional coefficient at the bottom of the dam or retaining wall</p>	$d = \frac{\Sigma M_r - \Sigma M_o}{\Sigma V}$ $e = \frac{L}{2} - d \leq \frac{L}{8}$ <p>L: Length of the geotextile  <math>\Sigma M_r</math>: Resistance moment around the toe  <math>\Sigma M_o</math>: Overturning moment around the toe</p>	$\frac{q_1}{q_2} \leq q_u = \frac{q_s}{3.0}$ <p><math>q_s</math>: Allowable bearing capacity  <math>q_u</math>: Ultimate bearing capacity</p>	$F_s = \frac{R \Sigma (c + W \cos \theta \tan \phi)}{R \Sigma W \sin \theta} \geq 1.2$

**Figure 2.16a:** Typical Failure Modes to be examined in the Design of Reinforced Soil Walls (Onodera et al., 1992)



(a) Straight Edge (b) Two-Part Wedge (c) Circular Arc (d) Logarithmic Spiral  
**Figure 2.16b:** Common Shapes for Potential Failure Surfaces for Limit Equilibrium Analysis Techniques

## 2.7 Finite Elements Analysis

Finite element method (FEM) is a vigorous well-known method of numerically solving boundary value problems, which can accommodate highly non-linear stress-strain relations of materials including even creep, any geometrical configuration with complex boundaries, construction sequence, etc. FEM has been used as the standard tool for the design and analysis (e.g. prediction of safety factor and settlement analysis) of many geotechnical structures. Similarly, it is becoming a design and analysis tool for the reinforced soil structures. These features of FEM can be achieved only when material parameters, constitutive equations and boundaries are appropriately defined or modelled.



## **General Philosophy of FEM**

Finite element method is the representation of a body or a structure by an assemblage of subdivisions called finite elements, these elements are considered to be interconnected at points, which are called nodes. This method is a numerical procedure for analysing structures and continua. FEM is a powerful tool in structural analysis of simple to complicated geometries.

## **Steps in FEM**

Following steps are followed in finite element method:

1. Divide the structure or continuum in finite elements
2. Formulate the properties of each element
3. Assemble the elements to obtain the finite element model of the structure
4. Apply the known loads: nodal force or/and moments in stress analysis
5. Impose boundary conditions
6. Calculate the displacement vector
7. Calculate strain, and finally calculate stress from strain

## **Modelling of Components: *soil, reinforcement and facing***

The incorporation of mechanism of soil-reinforcement- facing interaction in the FEM are greatly influenced by the construction method, compaction, propping of facing during construction and its release later including the boundary conditions (loading on top, etc.), thus, making it difficult to model the problem.

**Soil:** most researchers as pointed out by Gourc, 1993, have adopted nonlinear elastic or elasto- plastic models. The initial deformation is sometimes calculated using linear elastic constitutive models and failure load is calculated using limiting equilibrium methods employing appropriate constitutive models e.g. Mises or Mohr- Coulomb, Drucker-Prager etc.

**Reinforcement:** Reinforcement is generally modelled by linear bar element capable of taking only axial tensile forces. Behaviour of extensible geosynthetic materials is generally nonlinear. Sometimes metallic reinforcements are also modelled as continuous beam element and the bending moment is calculated in addition to the axial force.

## **Modelling of Soil Reinforcement Interface**

Several authors have proposed various types of inter face elements to model the interface behaviour. Most of the interface elements, originally developed in rock

mechanics, are used in the analysis of reinforced soils. Interface elements can be classified (Gens et al., 1989) into the following categories:

- a. Standard finite elements of small thickness
- b. Quasi-continuum elements possessing a weakness plane in the direction of the interface
- c. Linkage elements in which only the connections between opposite nodes are considered
- d. Interface elements in which relative displacement between opposite nodes are the primary deformation variables. They can have finite or zero thickness.

Several differences exist among these methods and the main argument concerns the physical existence of shearing band of soil around reinforcement. FEM methods are based on continuity of soils except the contact plane between soils and reinforcing materials. Goodman element (1968) originally introduced interface element concept in the geotechnical contact problems. This type of interface element is extensively used in the reinforced soil problems. A typical interface element is illustrated in Figure 2.17 below.

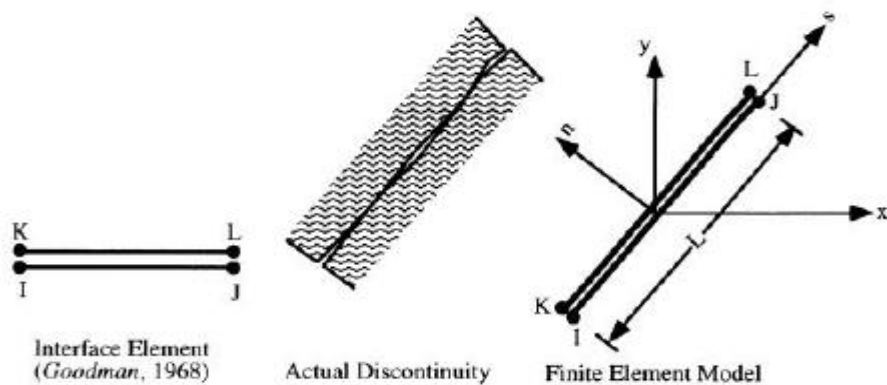


**Figure 2.17:** A Typical Interface Element used in the Modelling of the Soil-Reinforcement Interfaces (Goodman et al., 1968)

## CHAPTER 3

### ANALYSIS USING MODELLING SOFTWARE

#### 3.1 Overview of Plaxis Software

“Plaxis version 8” is a finite element software program developed in the Netherlands for two and three-dimensional analysis of geo-structures and geotechnical engineering problems. It includes from the most basic to the most advanced constitutive models for the simulation of the linear or non-linear, time-dependent and anisotropic behaviour of soil and/or rock. Plaxis is also equipped with features to deal with various aspects of complex structures and study the soil-structure interaction effect. In addition to static loads, the dynamic module of Plaxis also provides a powerful tool for modelling the dynamic response of a soil structure during an earthquake. The analysis is carried out in the sequence indicated below:

#### **Input Program**

To carry out finite element analysis using Plaxis, the user has to create a finite element model and specify the material properties and boundary condition(s). This is done in the input program to set up a finite element model. The user must create a two dimensional geometry model composed of points, lines and other components in the x-y plane. The Plaxis mesh generator based on the input of the geometry model automatically performs the generation of a mesh at an element level. User may also customize the finite element mesh in water pressure and initial stresses to the initial stage.

#### **Prepare Mode using Plaxis Tools**

In principle, first draw the geometry contour, and then add the soil layers, then structural objects, then construction layers, then boundary conditions and then loadings. Using the geometry line option, the user may draw points and lines in the draw area. Plates are structural objects used to model slender structures in the ground with a significant flexural rigidity or normal stiffness. Plates can be used to simulate the walls, shells or linings extending in z-direction. Geogrids are slender structures

with their normal stiffness generally used to model reinforcement. To model the interaction between the wall and the soil, interfaces are used which are intermediate between smooth and fully rough.

### **Modelling of Soil Behaviour**

In Plaxis, soil properties and material properties of structure are stored in material data sets. The database sets of properties are assigned to the soil clusters or to the corresponding structural objects in the geometry model. Plaxis supports various models to simulate the behaviour of soil and other continua such as the linear elastic model, Mohr-Coulomb model, jointed rock model, hardening soil model, soft soil model, soft soil creep model and other user define models. Once the geometry has been created and finite element mesh has been generated, the initial stress state and the initial configuration must be specified. This is done by the initial conditions part of the input program.

### **Calculations**

After this, the actual finite element calculations must be executed. Here, it is necessary to define which types of calculations are to be performed; and which type of loadings or construction stages are to be activated during the calculations. Plaxis allows for different types of finite element calculations in engineering practice and a project is usually divided into calculation phases. Examples of calculation phases are the activation of a particular loading at a certain time, the simulation of a construction stage, the introduction of a consolidation period, the calculation of safety factors etc.

### **Output program**

The main output quantities of a finite element calculation are the displacement at the nodes and the stresses at the stress points. In addition, when a finite element model involves structural elements, structural forces are calculated in these elements. Extensive ranges of facilities exist within Plaxis to display the results of a finite analysis. The curves program can be used to draw load-displacement curves, stress-strain curves and stress or strain paths of pre-selected points in the geometry. These curves visualize and give an insight into the global and local behaviour of the soil.

When subsequently clicking on the output button the results of all construction phases are displayed on separate windows in the output program. In this way, results of phases can be obtained.

### 3.2 Numerical Analysis for Appropriate Load and Geometry

#### 3.2.1 General Information on the Model

**Table 3.1:** Units

Type	Unit
Length	m
Force	kN
Time	day

**Table 3.2:** Model Dimensions

	Min.	Max.
X	0	21
Y	0	11

**Table 3.3:** The Model

Model	Plane strain
Element	15-Noded

#### 3.2.2 Geotechnical Parameters and Design Methods

As described previously in chapter 1, two categories of analyses will be performed which are the analysis of the wall and analysis of the same wall with different foundation material. The idea is to determine the behaviour of the wall under static loading and any variation(s) in the observed behaviour in each case.

##### The First Analysis

The Plaxis input model is shown in Figure 3.1 while the design sections for these different cases of models are shown in Figures 3.2 to 3.5. The design parameters for the different soil cases are shown in Table 3.4. The diaphragm wall and geogrids parameters are shown in Table 3.5 and 3.6 respectively. The model was prepared as retaining wall proving support for a 4.5m width motor park.

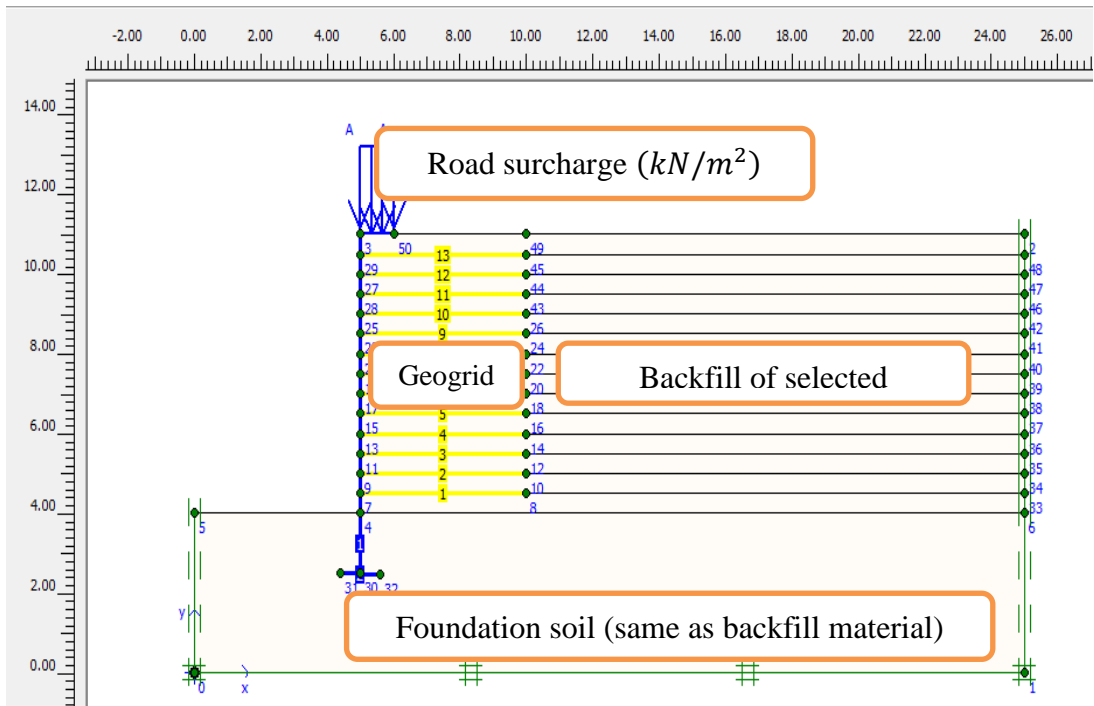


Figure 3.1: Plaxis Input Model

### Model-1

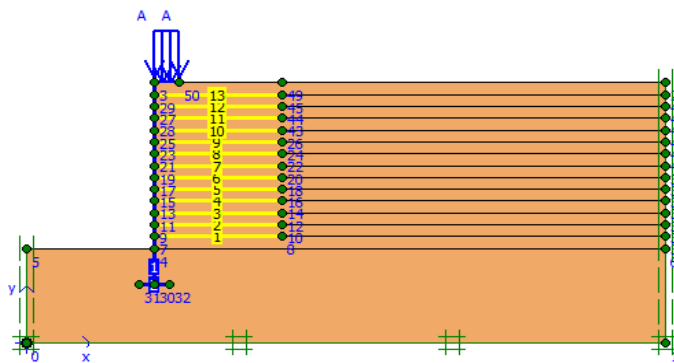


Figure 3.2: Reinforced Earth Retaining Wall with Loose Sand used as a Backfill Material

### Model-2

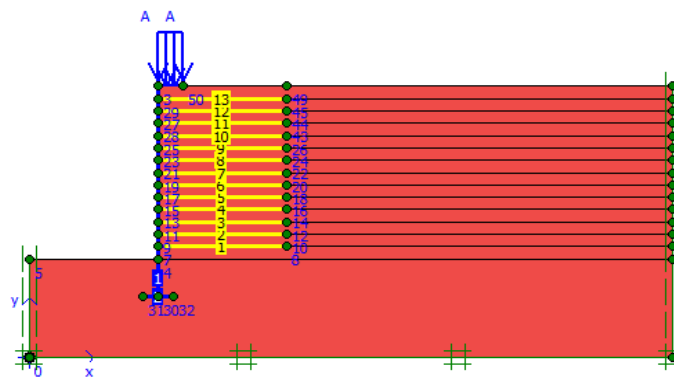


Figure 3.3: Reinforced Earth Retaining Wall with Dense Sand used as a Backfill Material

### Model-3

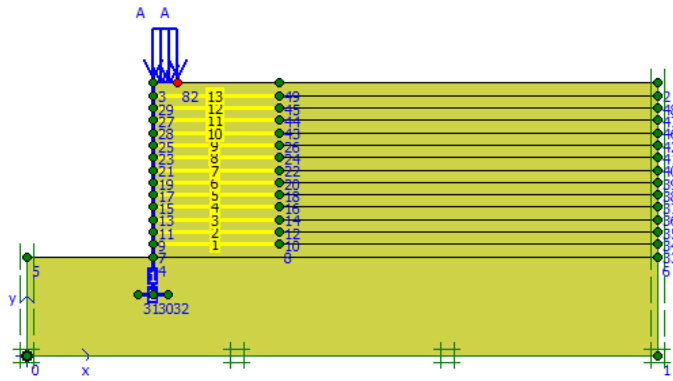


Figure 3.4: Reinforced Earth Retaining Wall with Silty Sand used as a Backfill Material

### Model-4

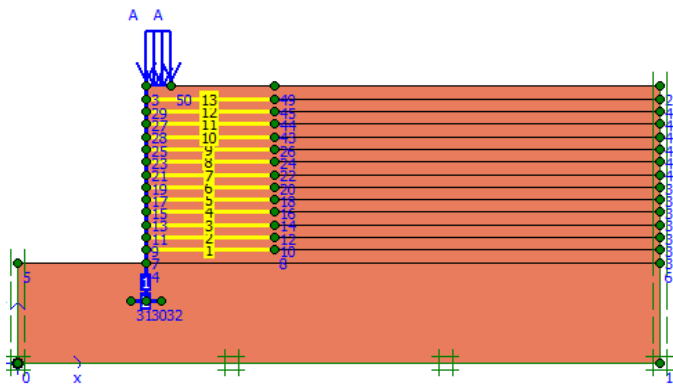


Figure 3.5: Reinforced Earth Retaining Wall with Clayey Sand used as a Backfill Material

Table 3.4: Soil Data Parameters

<i>Mohr-Coulomb</i>		1	2	3	4
		Loose Sand	Dense Sand	Silty sand	Clayey sand
Type		Drained	Drained	Drained	Drained
$\gamma_{unsat}$	[kN/m <sup>3</sup> ]	16.5	18	17	19
$\gamma_{sat}$	[kN/m <sup>3</sup> ]	18	20	19	21
$k_x$	[m/day]	1	1	1	1
$k_y$	[m/day]	1	1	1	1
$E_{ref}$	[kN/m <sup>2</sup> ]	20000	65000	15000	40000
$\nu$	[-]	0.25	0.3	0.35	0.3
$c_{ref}$	[kN/m <sup>2</sup> ]	0	0	0	10
$\phi$	[°]	34	40	32	40
$\psi$	[°]	0	10	4	2
$R_{inter.}$	[-]	0.67	0.8	0.8	0.85
Interface permeability		Neutral	Neutral	Neutral	Neutral

**Table 3.5:** Beam Data Parameters

No.	Identification	EA [kN/m]	EI [kNm <sup>2</sup> /m]	w [kN/m/m]	n [-]	Mp [kNm/m]	Np [kN/m]
1	Diaphragm wall	7.50E+06	1.00E+06	10	0	1.00E+15	1.00E+15
2	Footing	5.00E+06	8.50E+03	10	0	1.00E+15	1.00E+15

**Table 3.6:** Geotextiles Data Parameters

No.	Identification	EA [kN/m]	v [-]
1	Geogrid	2500	0

### The Second Analysis

In this case, analyses were performed with different geometric properties of the wall and the applied load and limestone was considered as the foundation material. The Plaxis input model is shown in Figure 3.6 while the design sections for these different cases of models are shown in Figures 3.7 to 3.10. The diaphragm wall and geogrids parameters are the same as in the first analysis. The design parameters for the different soil cases including the foundation soil are shown in Table 3.7.

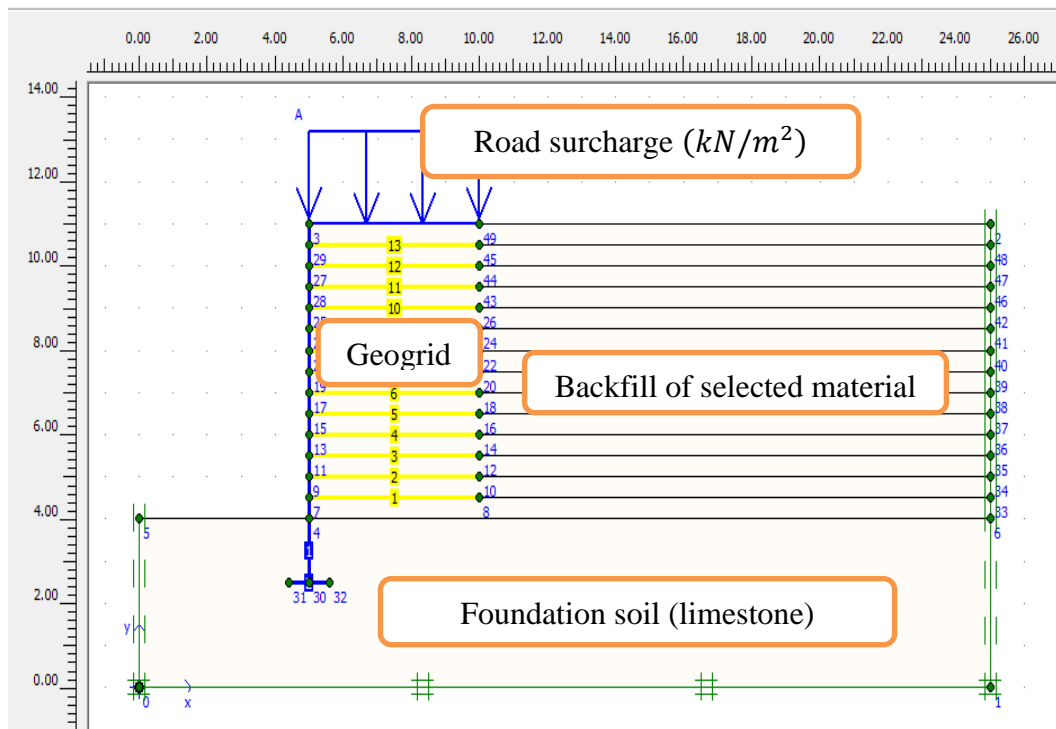


**Figure 3.6:** Plaxis Input Model



### Model-1

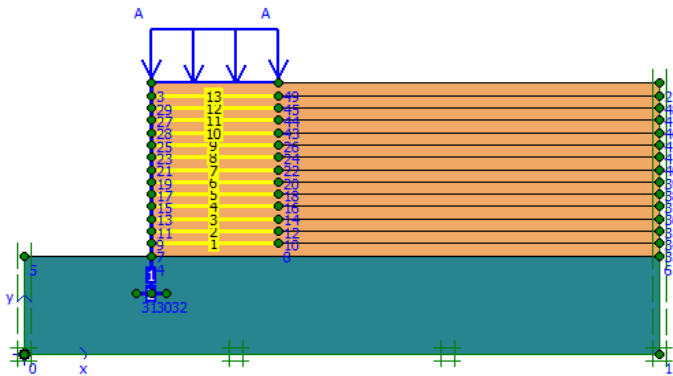


Figure 3.7: Reinforced Earth Retaining Wall with Loose Sand used as a Backfill Material

### Model-2

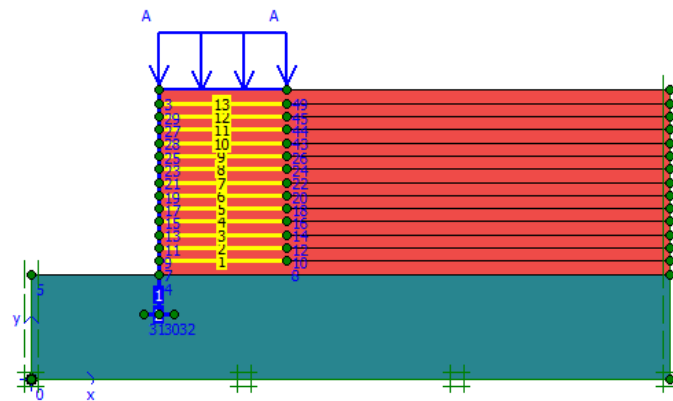


Figure 3.8: Reinforced Earth Retaining Wall with Dense Sand used as a Backfill Material

### Model-3

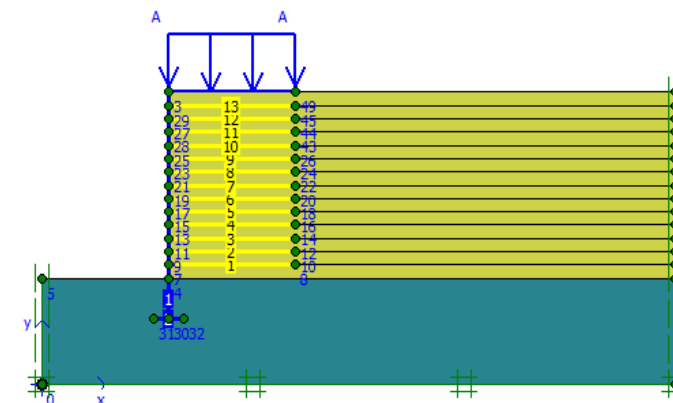


Figure 3.9: Reinforced Earth Retaining Wall with Silty Sand used as a Backfill Material

## Model-4

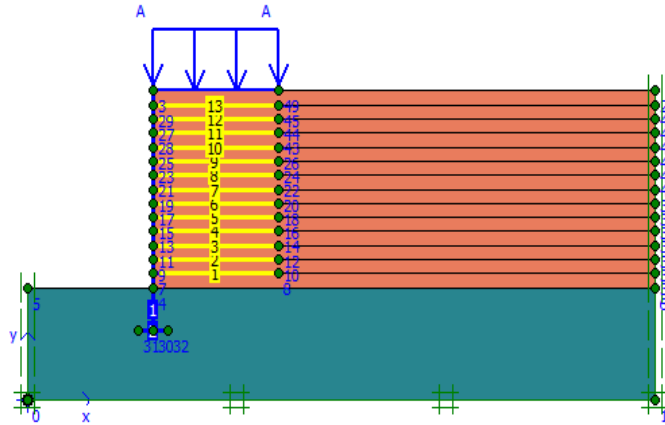


Figure 3.10: Reinforced Earth Retaining Wall with Clayey Sand used as a Backfill Material

Table 3.7: Soil Data Parameters

<i>Mohr-Coulomb</i>		1	2	3	4	5
		Foundation soil	Loose Sand	Dense Sand	Silty sand	Clayey sand
Type		Drained	Drained	Drained	Drained	Drained
$\gamma_{\text{unsat}}$	[kN/m <sup>3</sup> ]	22	16.5	18	17	19
$\gamma_{\text{sat}}$	[kN/m <sup>3</sup> ]	24	18	20	19	21
$k_x$	[m/day]	1	1	1	1	1
$k_y$	[m/day]	1	1	1	1	1
$E_{\text{ref}}$	[kN/m <sup>2</sup> ]	60000	20000	65000	15000	40000
$\nu$	[-]	0.25	0.25	0.3	0.35	0.3
$c_{\text{ref}}$	[kN/m <sup>2</sup> ]	1	0	0	0	10
$\phi$	[°]	45	34	40	32	40
$\psi$	[°]	0	0	10	4	2
$R_{\text{inter.}}$	[-]	0.65	0.67	0.8	0.8	0.85
Interface permeability		Neutral	Neutral	Neutral	Neutral	Neutral

## 3.3 Numerical Analysis for Appropriate Geogrids Stiffness

### 3.3.1 General Information on the Model

Table 3.8: Units

Type	Unit
Length	m
Force	kN
Time	day

**Table 3.9:** Model Dimensions

	Min.	Max.
X	0	40
Y	0	15

**Table 3.10:** The Model

Model	Plane strain
Element	15-Noded

### 3.3.2 Geotechnical Parameters and Design Methods

The reinforced soil wall provides support to the lower side of the Egnatia motor park. The topography and ground conditions vary along the wall length. The existing ground slope in front of the wall also varies along the length. There are two analyses considered in this part of my thesis as described previously in chapter one.

#### The First Analysis

The model used for this analysis was prepared in accordance to the design specifications obtained from the published journal on geotechnical engineering titled “Numerical Analysis of Reinforced Soil Wall” by V.N Georgiannou et al.

A road surcharge of  $20kN/m^2$  was assumed in the calculations. The wall foundation is the main within limestone. The soil model used to characterize the site was the elasto-plastic Mohr-Coulomb model. The design section (Plaxis input model) for this analysis is shown in Figure 3.11. The soil data parameters are shown in Table 3.11. The diaphragm wall and geogrids parameters are shown in Table 3.12 and 3.13 respectively.

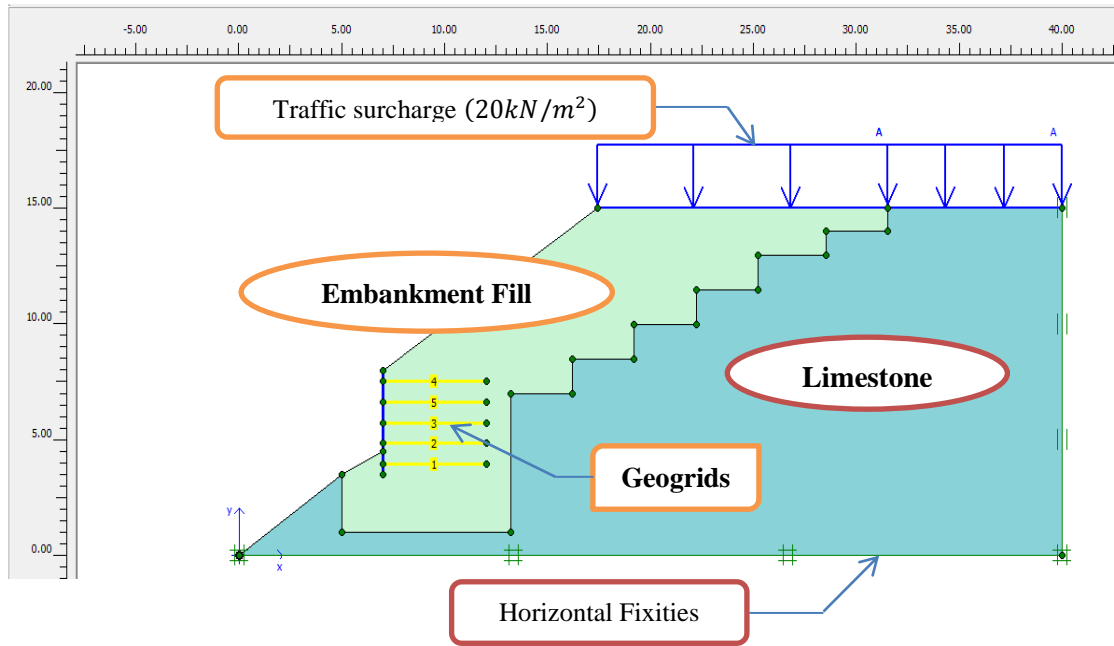


Figure 3.11: Plaxis Input Model

Table 3.11: Soil Data Parameters

Mohr-Coulomb		Limestone	Embankment Fill
Type		Drained	Drained
$\gamma$	[kN/m <sup>3</sup> ]	24	22
$K_x$	[m/day]	1	1
$k_y$	[m/day]	1	1
$E_{ref}$	[kN/m <sup>2</sup> ]	8000	8000
$\nu$	[-]	0.3	0.3
$c$	[kN/m <sup>2</sup> ]	300	5
$\phi$	[°]	28	37
$\Psi$	[°]	0	0
$R_{inter.}$	[-]	0.65	0.65
Interface Permeability		Neutral	Neutral

Table 3.12: Beam Data Parameters

No.	Identification	EA [kN/m]	EI [kNm <sup>2</sup> /m]	w [kNm/m]	v [-]	Mp [kNm/m]	Np [kN/m]
1	Diaphragm wall	7.50E+06	1.00E+06	10.00	0.00	1.00E+15	1.00E+15

**Table 3.13:** Geotextiles Data Parameters

No.	Identification	EA [kN/m]	v [-]
0	Geogrid	varies	0

### The Second Analysis

The model used for this analysis is the same as the one used for the first analysis. The design sections are shown in Figures 3.12 and 3.14 for both static and dynamic analyses. Table 3.11, 3.12 and 3.13 show the initial values of the basic Mohr-Coulomb input design parameters for the two layers of soil, diaphragm wall and the geogrids. In the numerical analyses, the reinforcements are modelled as flexible elastic elements that can sustain only tensile forces (no compression). The only property to redefine is the axial stiffness (EA), which is the ratio of the axial force per unit width. Different values of the axial stiffness were set while the analysis was performed for both static and dynamic loading conditions. Two cases are considered for the wall- *static and dynamic*.

### Static Analysis

This analysis was carried out by considering four intermediate phases to simulate the staged construction of the reinforced earth wall in the field. In each phase, simulation of the excavation lifts was performed and structural elements were activated to simulate the installation of the soil geogrids along with application of the diaphragm wall facing. A uniformly distributed surcharge of  $20 \text{ kN/m}^2$  was applied on the retaining side to simulate the traffic surcharge. The design section (Plaxis input model) for this analysis is shown in Figure 3.12.

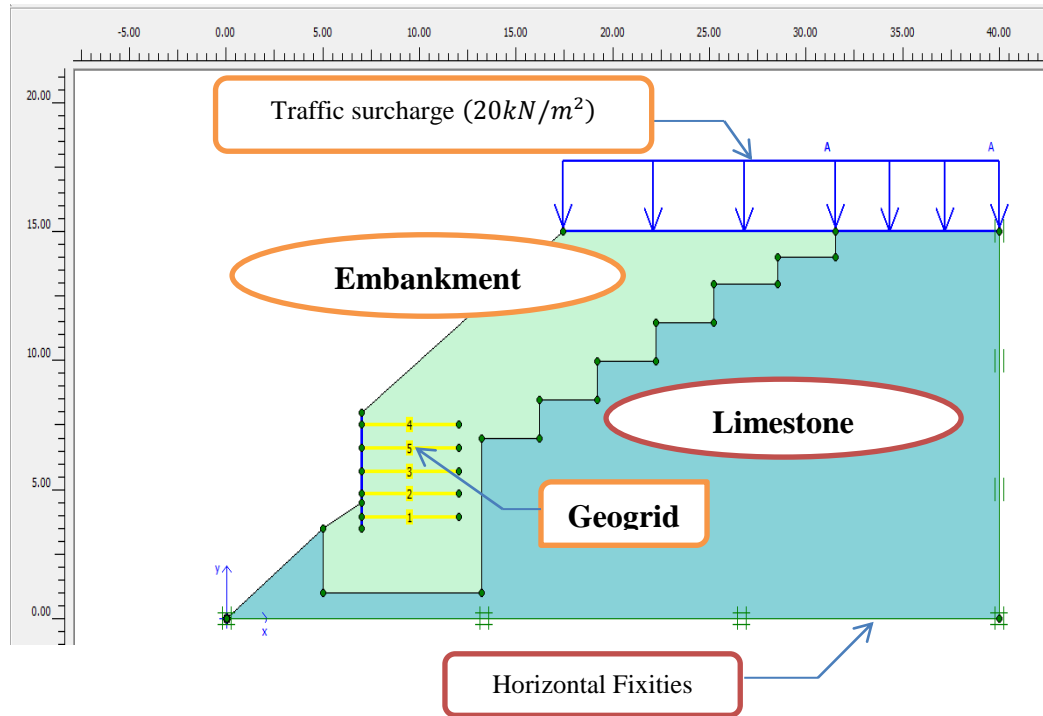


Figure 3.12: Plaxis Input Model for Static Analysis

### Dynamic Analysis

There are five intermediate stages involved in this analysis to simulate the staged construction and the action of seismic acceleration input on the wall as a whole. A uniformly distributed surcharge of  $20 \text{ kN/m}^2$  was also applied on the retaining side to simulate the traffic surcharge.

A design basis earthquake (DBE) of peak horizontal acceleration of  $0.12g$  for 10% probability of exceedance in 50 years, which translates to a return period of 475 years, was assumed for this analysis.

Two sets of times histories were used for the analysis. Database are references based on the closet similarity of seismological and geological features: *Agio (1995)*, recorded during the earthquake in the Corinthian Gulf (15-6-1995) and *Sepolia (1999)*, recorded during the main earthquake of Athens, Greece (7-9-1999). The above selected horizontal motions were spectrally matched to the targeted horizontal uniform hazard spectral (UHS), and the vertical motions spectrally matched to the target vertical UHS.

It should be noted that these spectrum-matched acceleration time histories are corresponding to an outcropping condition. To obtain the input motion at the bottom of the Plaxis model, I have used “*EERA-SHAKE91*” (Idriss et al., 1991) to perform the deconvolution process. “*EERA-SHAKE91*” is a widely used computer program developed for the one-dimensional ground response analysis of layered sites with the equivalent linear approach. The assumed layers of soil (soil profile) below the reinforced wall section is shown in Figure 3.13 below.

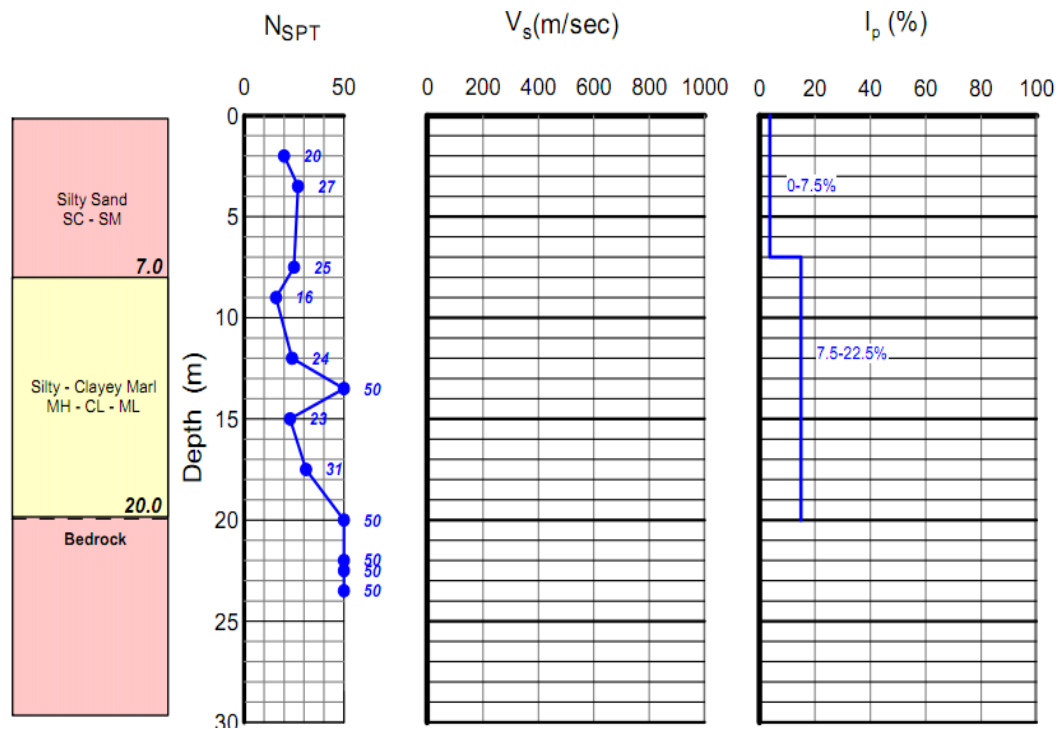
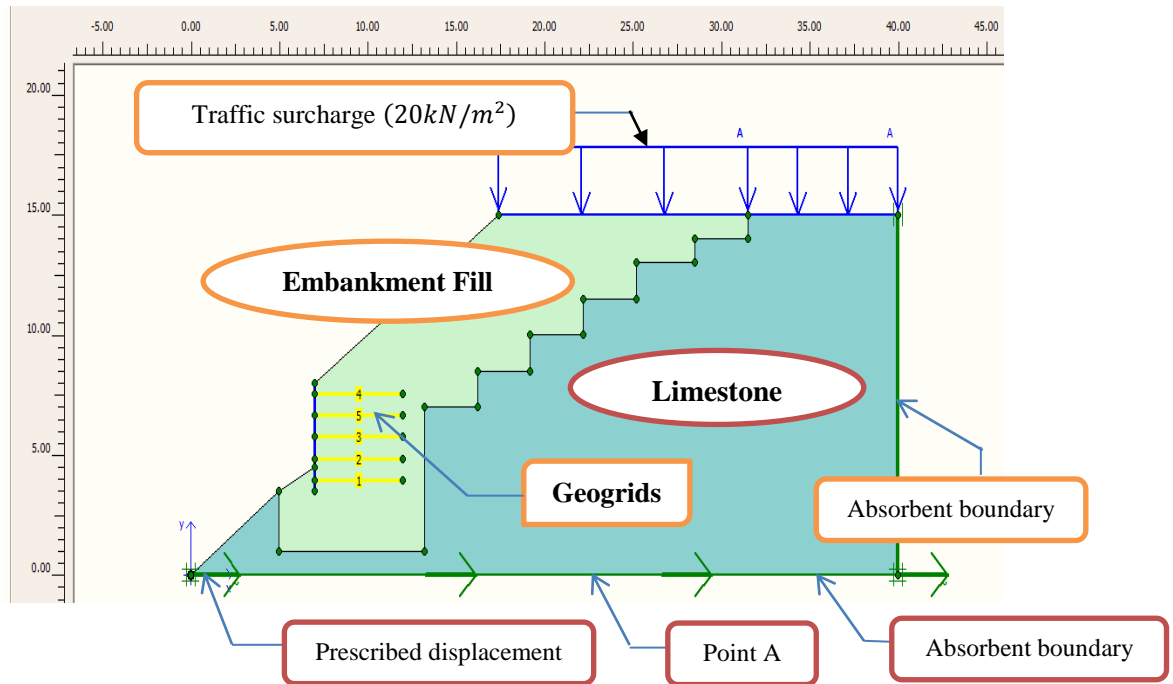


Figure 3.13: The Assumed Soil Profile below the Reinforced Wall Section

The output accelerations in the two earthquakes from Point A, which is recorded at the bottom of the mesh, match the input motions. The output spectrum-matched accelerations obtained from EERA-SHAKE91 and one published by Plaxis are essentially the same for both Agio and Sepolia Acceleration-time histories (See Figures 2.1 and 2.2 for Agio earthquake; Figure 2.3 and 2.4 for Sepolia earthquake in Appendix-2).

The input ground motions at appropriate depths are defined by means of the dynamic multipliers. These multipliers are a set of scaling factors on the prescribed unit displacement, applied on the bottom of model, to produce the actual dynamic load magnitudes such as displacements, velocities and accelerations. In the dynamic

calculation, the time-acceleration curve is generated at the bottom of the mesh (Point A) to verify the input motions. See Figure 3.7 shown below for the exact location of the point.



**Figure 3.14:** Plaxis Input Model for Dynamic Analysis



## CHAPTER 4

### RESULTS AND DISCUSSION

#### 4.1 Numerical Analysis for Appropriate Load and Geometry

Finite element analysis was carried out using commercial software PLAXIS version 8 for the four types of problems mentioned in the previous chapter. The results are compared and reported in this chapter. Behaviours of reinforced soil retaining walls under different conditions are investigated using PLAXIS version 8. Effect of the changes in the surcharged load (UDL) is shown through the relationship between load and deformation. The effect(s) of spacing of reinforcement on the soil is explained through the displacements developed. Effects of the geogrids length are also considered.

##### 4.1.1 The First Analysis

This analysis was carried out like the case of Mr Gaurav Singhai and the results obtained are essentially the same. For example, in the case of load-displacement variation of reinforced soil retaining wall for loose sand, the results obtained are shown below in Table 4.1 while the load-displacement curves from my analysis and that obtained from Mr Gaurav Singhai are shown in Figures 4.1 and 4.2.

**Table 4.1:** Displacements under Different Loadings for Loose Sand

Loads ( $\text{kN/m}^2$ )	Horizontal displacement (mm)	Vertical displacement (mm)
10	-78.90	-79.85
20	-85.50	-86.30
30	-92.50	-91.90
40	-98.00	-95.00
50	-103.70	-99.00
60	-109.60	-107.10
70	-115.30	-115.70
80	-121.40	-124.60
90	-125.80	-133.80
100	-130.40	-134.10

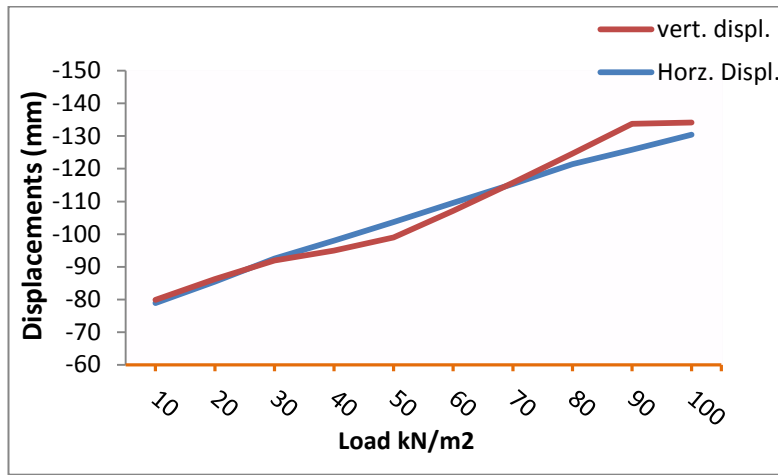


Figure 4.1: Load Displacement Relationship for Loose Sand

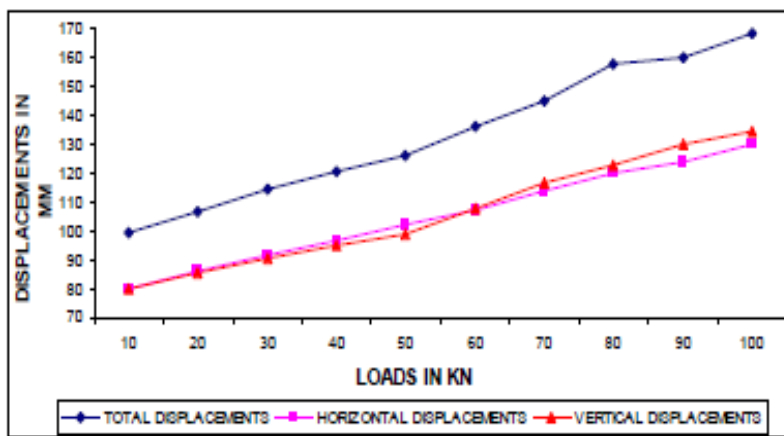


Figure-G1 Load displacement relationship for loose sand

Figure 4.2: Load-Displacement Relationship for Loose Sand Curve obtained by Mr Gaurav Singhai

In each case, the displacements of the soil increased steadily when the applied load is increased. Both horizontal and vertical displacements are almost the same in magnitude.

#### 4.1.2 The Second Analysis

##### 4.1.2.1 Load-Displacement Variation of Reinforced Soil Retaining Wall for Loose Sand

The detailed displacements observed in the finite element analysis for the wall section with an applied load of  $10 \text{ kN/m}^2$  are shown in Figures 4.3 and 4.4 below.

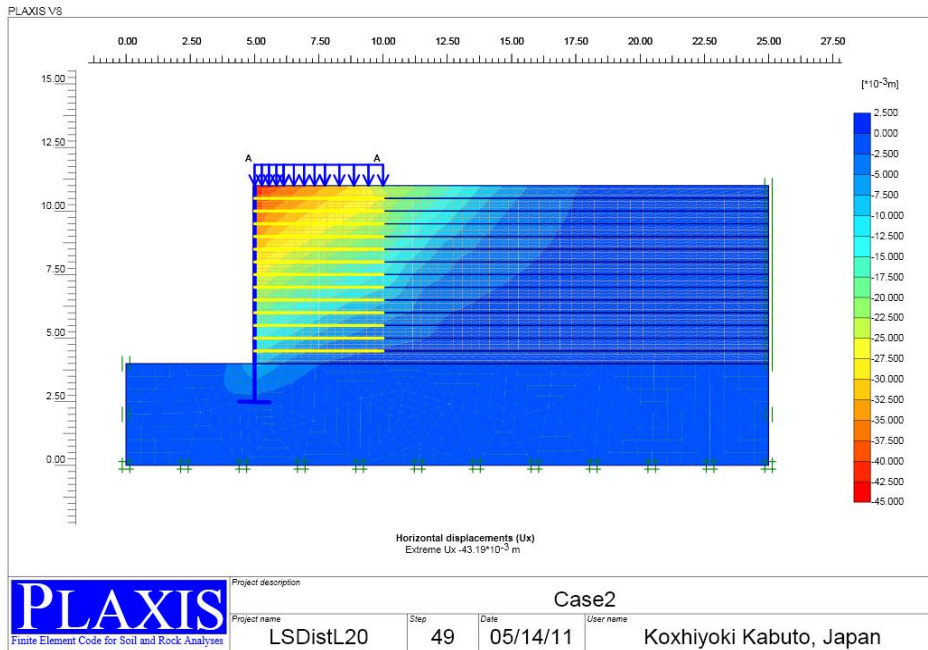


Figure 4.3: Horizontal Displacements (max. hor. dipl. = 43.19mm)

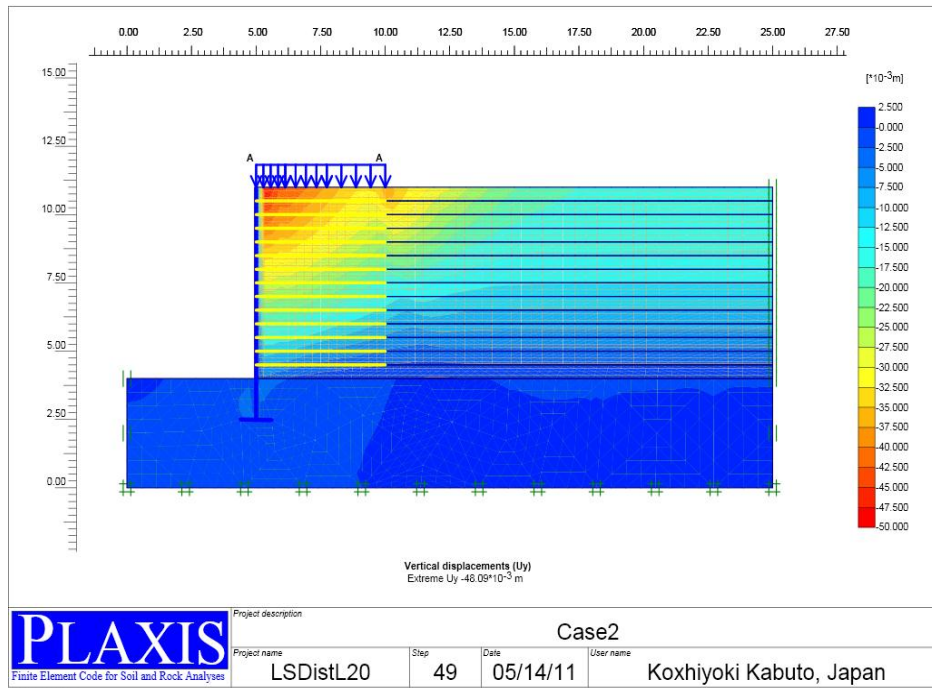


Figure 4.4: Vertical Displacements (max. vert. dipl. = 48.09mm)

The deformed mesh of this section is shown in Figure 1.1 in Appendix 1. In addition, the effective stress contours and plastic stress contours of this section are shown in Figure 1.2 and 1.3 in Appendix 1.

The detailed results of displacements obtained from the numerical analysis with different values of applied loads are shown below in Table 4.2 while Figure 4.5 shows the load-displacement curve.

**Table 4.2:** Displacements under Different Loadings for Loose Sand

Loads ( $kN/m^2$ )	Horizontal displacement (mm)	Vertical displacement (mm)
10	-43	-48.1
20	-45	-50.0
30	-50	-56.0
40	-56	-64.0
50	-64	-74.0
60	-68	-80.0
70	-72	-85.0
80	-80	-95.0
90	-85	-100.0
100	-90	-110.0

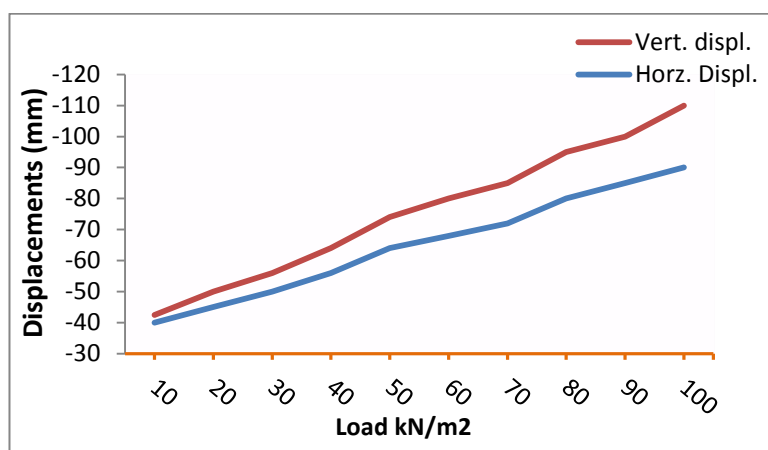


**Figure 4.5:** Load Displacement Relationship for Loose Sand

**Remarks:**

This Figure shows that with an increase of load there is rapid increase in the value of both vertical and horizontal displacements. Both horizontal and vertical displacements are almost of the same magnitude at the beginning of the curve under an applied surcharge of  $10kN/m^2$  while a divergence of displacement occurs as the curve advances (as the applied load increases). The rate of increase in the vertical displacement exceeds that of horizontal displacement. This result is different from

the one obtained earlier in Figure 4.1 where there is no divergence of the resulted displacements.

#### 4.1.2.2 Load-Displacement Variation of Reinforced Soil Retaining Wall for Dense Sand

**Table 4.3:** Displacements under Different Loadings for Dense Sand

Loads (kN/m <sup>2</sup> )	Horizontal displacement (mm)	Vertical displacement (mm)
10	-24.0	-13.0
20	-26.0	-15.0
30	-28.0	-17.0
40	-32.0	-20.0
50	-34.0	-22.0
60	-38.0	-26.0
70	-40.0	-28.0
80	-42.5	-30.0
90	-47.5	-32.0
100	-50.0	-36.0

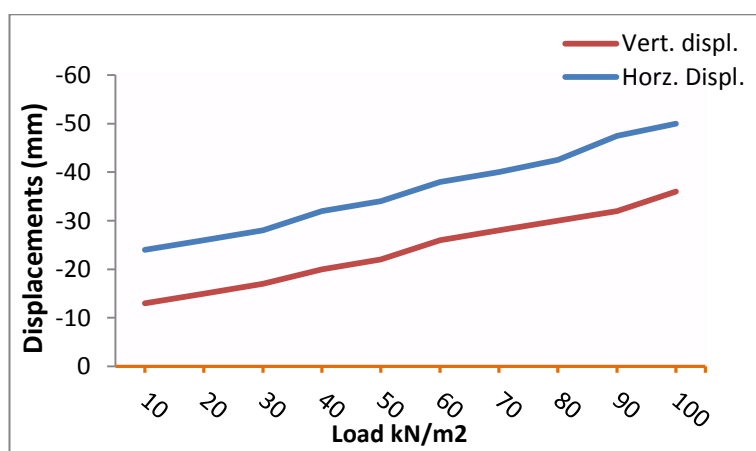


**Figure 4.6:** Load Displacement Relationship for Dense Sand

#### Remarks:

This Figure shows that with an increase of load there is a steady increase of both vertical and horizontal displacements. The rate of increment in both cases is approximately the same. However, the value of horizontal displacement is almost twice that of vertical displacement.

### 4.1.2.3 Load-Displacement Variation of Reinforced Soil Retaining Wall for Silty Sand

**Table 4.4:** Displacements under Different Loadings for Silty Sand

Loads ( $kN/m^2$ )	Horizontal displacement (mm)	Vertical displacement (mm)
10	-38.0	-32.0
20	-42.5	-38.0
30	-47.5	-42.5
40	-52.0	-47.5
50	-60.0	-56.0
60	-64.0	-60.0
70	-68.0	-68.0
80	-76.0	-72.0
90	-80.0	-76.0
100	-85.0	-78.0

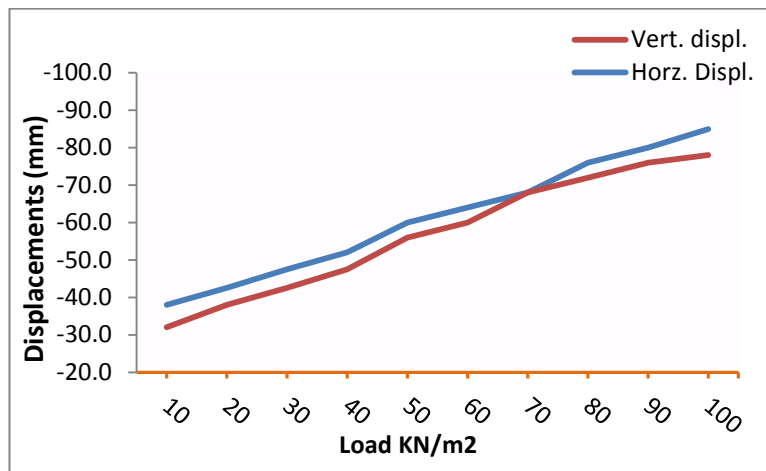


**Figure 4.7:** Load Displacement Relationship for Silty Sand

**Remarks:**

This Figure shows that with the increase of load there is sharp increase in the values of both vertical and horizontal displacements. The variation of displacements in this case is less when compared to both loose and dense sand cases. Horizontal displacement is higher than vertical displacement except for the displacement corresponding to an applied load of  $70kN/m^2$  where both of them have a displacement value equal  $-68mm$

#### 4.1.2.4 Load-Displacement Variation of Reinforced Soil Retaining Wall for Clayey Sand

Table 4.5: Displacements under Different Loadings for Clayey Sand

Loads ( $kN/m^2$ )	Horizontal displacement (mm)	Vertical displacement (mm)
10	-19	-12
20	-20	-13
30	-22	-15
40	-24	-17
50	-26	-19
60	-28	-22
70	-30	-26
80	-32	-28
90	-34	-32
100	-36	-34

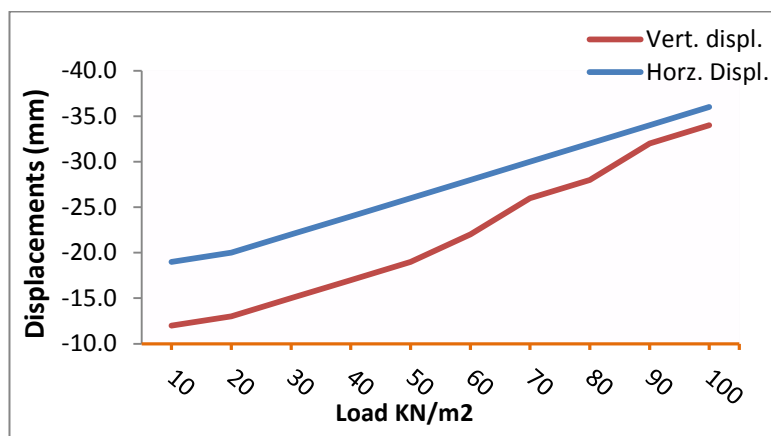


Figure 4.8: Load Displacement Relationship for Clayey Sand

#### Remarks:

This Figure shows that in clayey sand case minimum values of both horizontal and vertical displacements are observed. In contrary to loose sand case, at initial load, horizontal and vertical displacements are of different values while a convergence of both displacements occurred as the load increases and at an applied load of  $100kN/m^2$ , horizontal and vertical displacements are almost of the same magnitude.

### 4.1.2.5 Spacing Displacement Variation of Reinforced Soil Retaining Wall for Loose Sand

The detailed displacements observed in the finite element analysis for the wall section with geogrids spacing of 0.5m are shown in Figure 4.9 and 4.10 below.

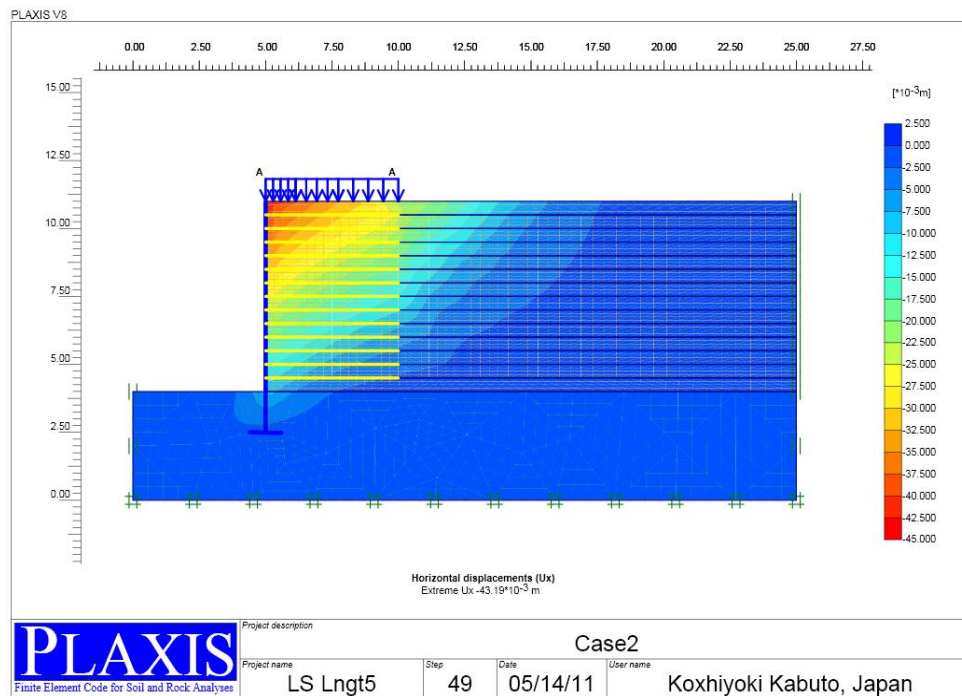


Figure 4.9: Horizontal Displacements (max. hor. displ. = 43.19mm, PLAXIS)

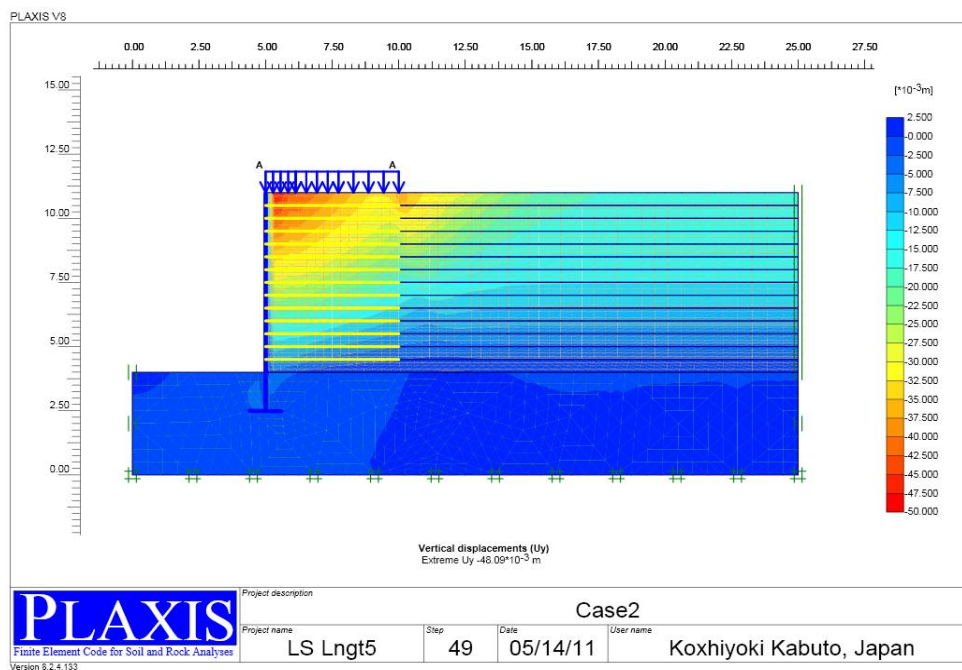


Figure 4.10: Vertical Displacements (max. vert. displ. = 48.09mm, PLAXIS)



The detailed results of displacements obtained from the numerical analysis with different spacing of geogrids are shown in Table 4.6 while the spacing-displacement curve is shown in Figure 4.11.

**Table 4.6:** Displacements under Different Spacing for Loose Sand

Spacing (m)	Horizontal displacement (mm)	Vertical displacement (mm)
0.3	-36	-40
0.5	-43	-48
0.8	-60	-64

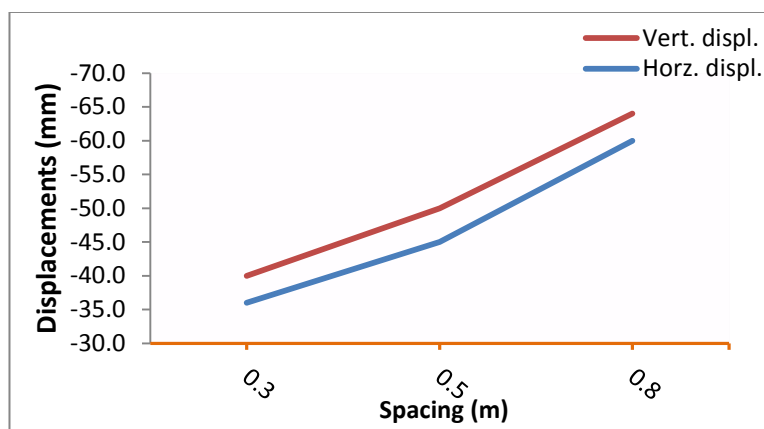


**Figure 4.11:** Spacing Displacement Relationship for Loose Sand

**Remarks:**

This Figure shows that both displacements increase by nearly 70% if we increase the spacing of geogrids from 0.3 m to 0.8 m. In addition to this observed behaviour, the reinforced soil body collapses when the spacing is increased beyond 0.8 m.

**4.1.2.6 Spacing Displacement Variation of Reinforced Soil Retaining Wall for Dense Sand**

**Table 4.7:** Displacements under Different Spacing for Dense Sand

Spacing (m)	Horizontal displacement (mm)	Vertical displacement (mm)
0.3	-22	-12
0.5	-26	-15
0.8	-32	-19

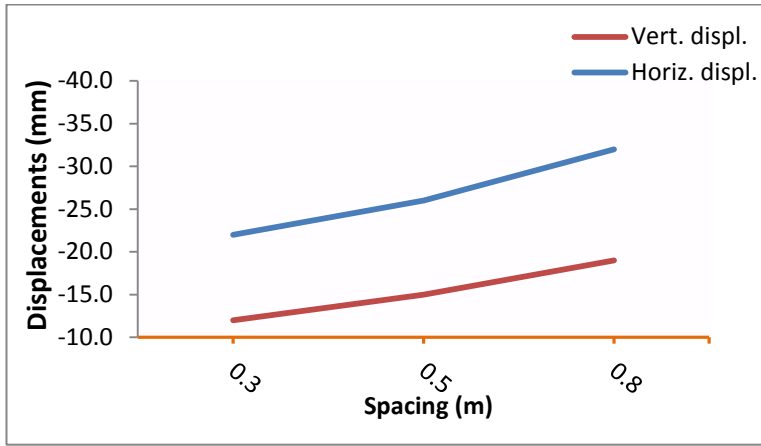


Figure 4.12: Spacing Displacement Relationship for Dense Sand

**Remarks:**

This Figure shows a gradual increase in the value of both vertical and horizontal displacements when the spacing of geogrids is increased from 0.3 to 0.8 m. It is also observed that the reinforced soil body collapses when the geogrids spacing is increased beyond 0.8 m.

**4.1.2.7 Spacing Displacement Variation of Reinforced Soil Retaining Wall for Silty Sand**

Table 4.8: Displacements under Different Spacing for Silty Sand

Spacing (m)	Horizontal displacement (mm)	Vertical displacement (mm)
0.3	-34.0	-32.0
0.5	-42.0	-38.0
0.8	-56.0	-47.5

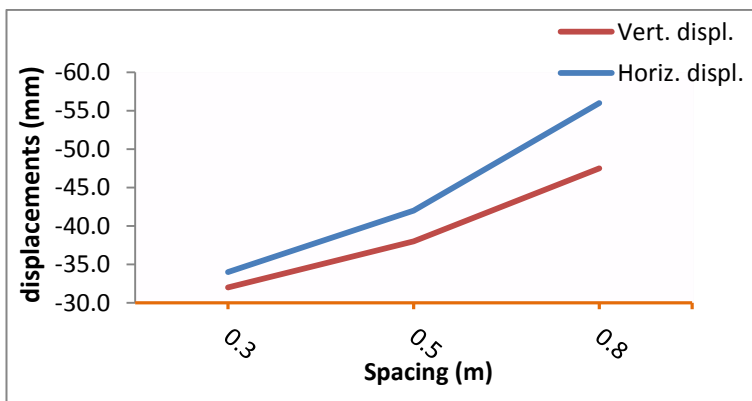


Figure 4.13: Spacing Displacement Relationship for Silty Sand

**Remarks:**

This Figure shows that both vertical and horizontal displacements increase rapidly with increase in spacing of geogrids. A variation in the rate of both displacements is observed, the horizontal displacement increased at a rate higher than vertical displacement.

**4.1.2.8 Spacing Displacement Variation of Reinforced Soil Retaining Wall for Clayey Sand**

**Table 4.9:** Displacements under Different Spacing for Clayey Sand

Spacing (m)	Horizontal displacement (mm)	Vertical displacement (mm)
0.3	-18	-13
0.5	-20	-13
0.8	-22	-13

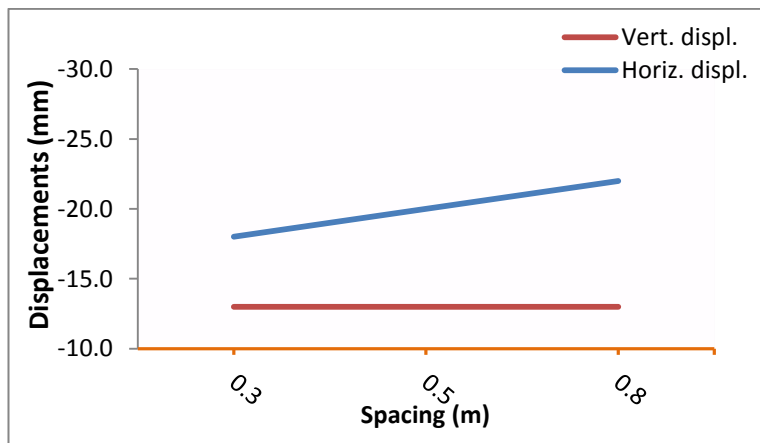


**Figure 4.14:** Spacing Displacement Relationship for Clayey Sand

**Remarks:**

This Figure shows that the value of horizontal displacement increases steadily with an increase in spacing of geogrids while the value of vertical displacement remains constant at -13mm. This observed behaviour is due to cohesive property of clayey sand. The effect of geogrids spacing is different from the effect of applied load. If we compare Fig. 4.12 with Fig. 4.6, the curve tends to converge in the case of applied load while divergence of the curve is observed in the case of geogrids spacing.

#### 4.1.2.9 Comparison of Displacement for Different Soil Cases under the Same Arrangement of Geogrids Spacing 0.5m and Applied Load of $20kN/m^2$

**Table 4.10:** Displacements for Different Soil Cases under Same Spacing of Geogrid and Same Applied Load

Serial no.	Type of soil	Horizontal Displacement (mm)	Vertical Displacement (mm)
1	Loose sand	-45	-50
2	Dense sand	-26	-15
3	Silty sand	-42	-38
3	Clayey sand	-20	-13

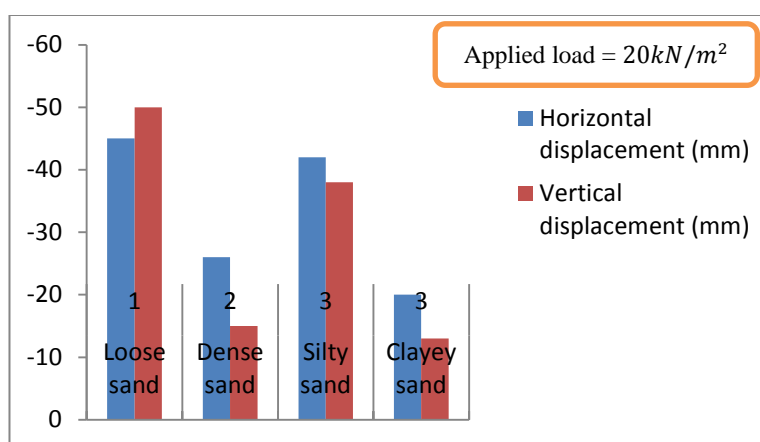


**Figure 4.15:** Displacements of the Four Cases of Sand under Same Spacing of Geogrid and applied Load

#### Remarks:

This Figure shows that the horizontal displacement is generally higher than vertical displacement except the case of loose sand. This result further corroborates the observed behaviour of loose sand with its vertical component of displacement higher than horizontal displacement. In addition, the behaviour of loose sand in terms of displacement is similar to that of silty sand while the responses of both dense and clayey sands are also comparable. In general, clayey sand is most stable with the lowest value of both vertical and horizontal displacements.

### 4.1.2.10 Displacement Variation of Displacement with the Length of Geogrids for Loose Sand

The detailed displacements observed in the finite element analysis for the wall section are shown in Figure 4.16 and 4.17 below for geogrids length of 6m.

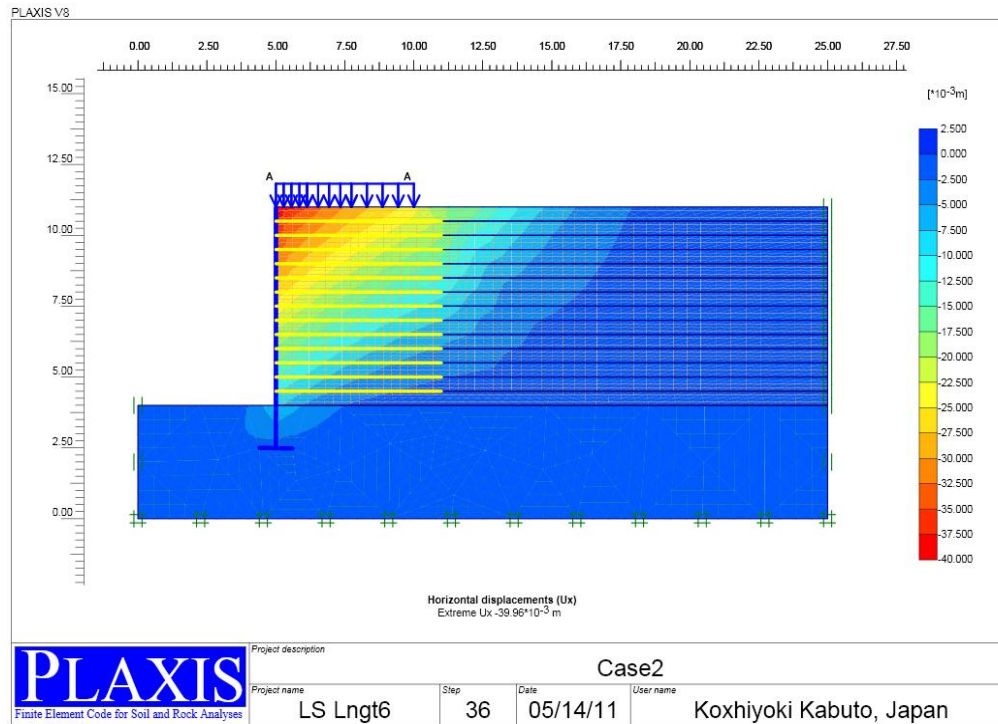


Figure 4.16: Horizontal Displacements (max. vert. dipl. = 39.96mm)

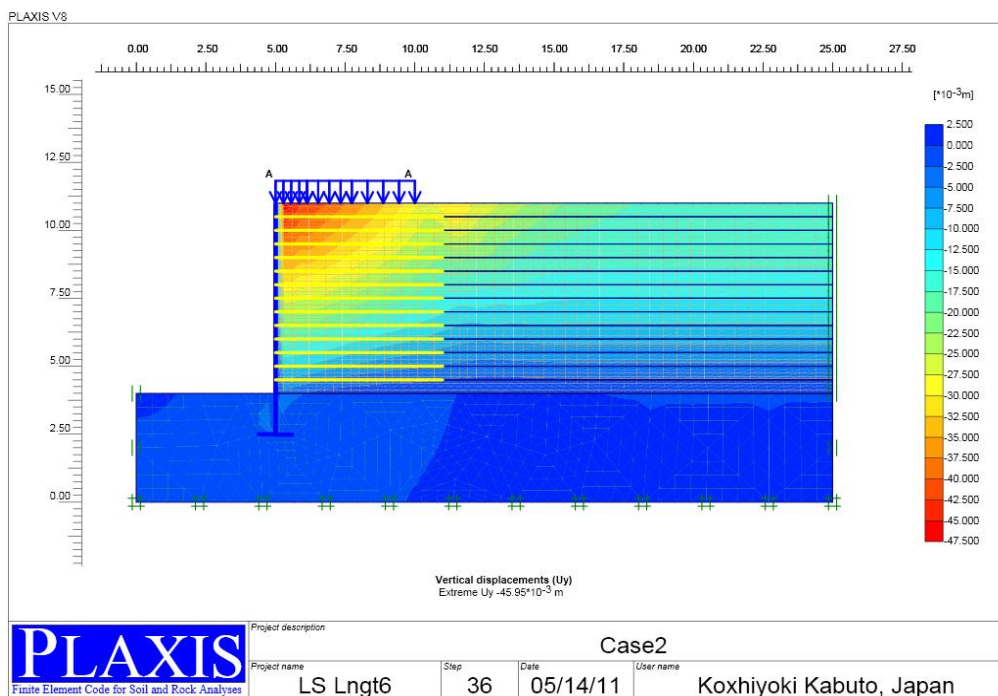
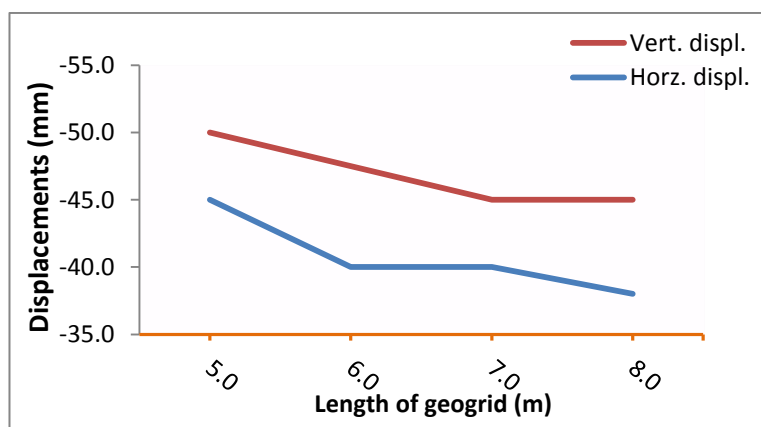


Figure 4.17: Vertical Displacements (max. vert. displ. = 45.96mm)

The detailed results of displacements obtained from the numerical analysis with different spacing of geogrids are shown in Table 4.11 while the geogrids length-displacement curve is shown in Figure 4.18.

**Table 4.11:** Displacements Variation with the Length of Geogrids of Loose Sand

Length of geogrid (m)	Horizontal displacement (mm)	Vertical displacement (mm)
5	-45	-50
6	-40	-46
7	-40	-45
8	-38	-45



**Figure 4.18:** Displacements Variation with the Length of Geogrids for Loose Sand

**Remarks:**

This Figure shows that with the increase of length of geogrids, both vertical and horizontal displacements decrease. The horizontal displacement remained steady when the length of geogrids is increased from 6m to 7m while a steady state of vertical displacements is observed when the length of geogrids is increased from 7m to 8m.

#### 4.1.2.11 Displacement Variation of Displacement with the Length of Geogrids for Dense Sand

Table 4.12: Displacements Variation with the Length of Geogrids of Dense Sand

Length of geogrid (m)	Horizontal displacement (mm)	Vertical displacement (mm)
5	-26	-15
6	-26	-15
7	-26	-15
8	-26	-15

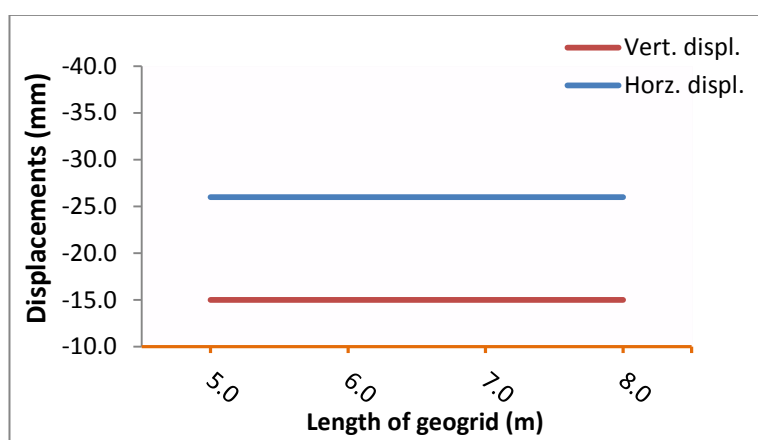


Figure 4.19: Displacements Variation with the Length of Geogrids for Dense Sand

#### Remarks:

This Figure shows that an increase in the length of geogrids has no effect on both vertical and horizontal displacement. The displacements neither increase nor decrease and this shows that the soil has reached its state of equilibrium. This implies that a minimum length of reinforcement (<5m) is deemed sufficient to provide stability for the wall.

#### 4.1.2.12 Displacement Variation of Displacement with the Length of Geogrids for Silty Sand

Table 4.13: Displacements Variation with the Length of Geogrids for Silty Sand

Length of geogrid (m)	Horizontal displacement (mm)	Vertical displacement (mm)
5	-42.5	-38
6	-40.0	-36
7	-40.0	-36
8	-38.0	-36

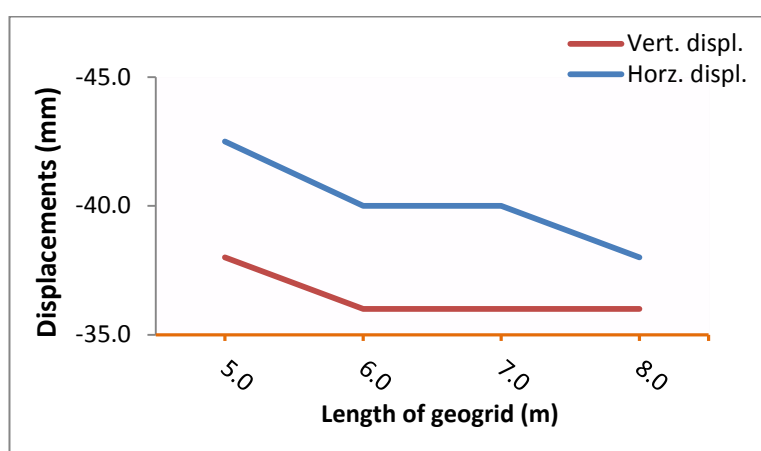


Figure 4.20: Displacement Variation with the Length of Geogrids for Silty Sand

#### Remarks:

This Figure shows that both vertical and horizontal displacements decrease at the same rate when the length of geogrids is increased from 5m to 6m. The vertical displacement remains constant for the rest of geogrids length increment while the horizontal displacement only remains constant between 6m and 7m and decreases thereafter.



#### 4.1.2.13 Displacement Variation of Displacement with the Length of Geogrids for Clayey Sand

Table 4.14: Displacements Variation with the Length of Geogrids for Clayey Sand

Length of geogrid (m)	Horizontal displacement (mm)	Vertical displacement (mm)
5	-20	-13
6	-20	-13
7	-20	-13
8	-20	-13

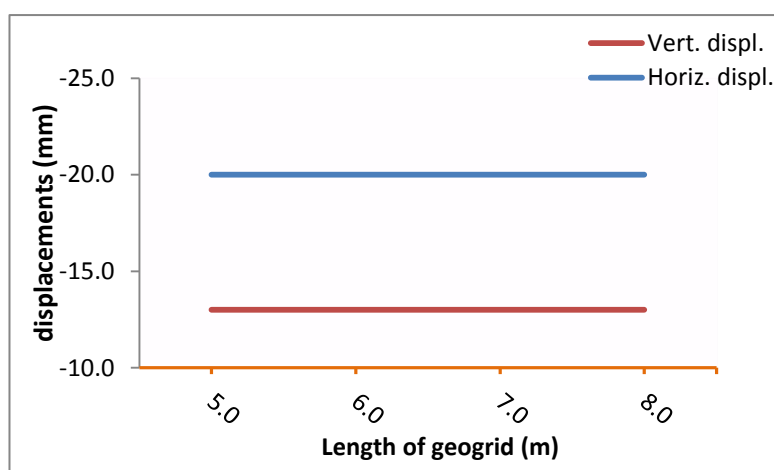


Figure 4.21: Displacement Variation with the Length of Geogrids for Clayey Sand

#### Remarks:

This Figure shows that there is no effect of geogrids length on displacements in case of clayey sand. This observed behaviour is due to the cohesive nature of clayey soils. This implies that a minimum length of reinforcement (<5m) is deemed sufficient to provide stability for the wall.

#### 4.2 Numerical Analysis for Appropriate Geogrids Stiffness

Finite element analysis is carried out using commercial software PLAXIS version 8 for both types of analysis mentioned in the previous chapter. The results are compared and reported in this chapter. The results obtained from the first and second analyses are examined and analysed here. Behaviours of the reinforced soil retaining walls under different values of axial stiffness of geogrids are investigated using PLAXIS version 8. Effects of the soil reinforcement's stiffness are shown through the relationships between stiffness (EA) and deformation.

## 4.2.1 The First Analysis

### 4.2.1.1 The Horizontal Displacement

The detailed horizontal displacements observed in the finite element analysis for the wall section are shown below in Figure 4.22.

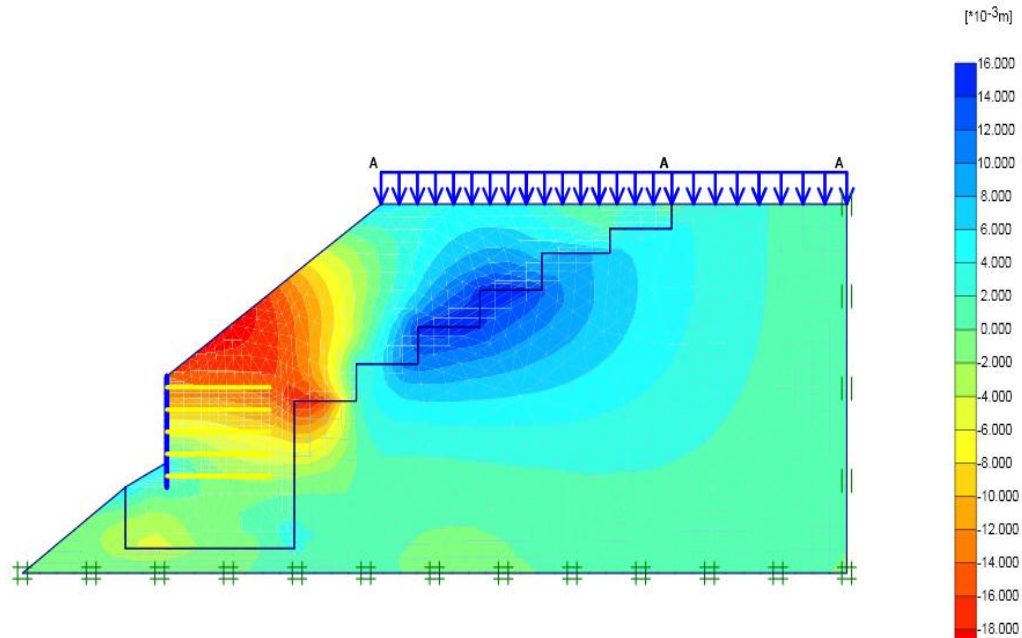


**Figure 4.22:** Horizontal displacements (max. hor. dipl. = 17.97mm, PLAXIS)

The detailed values of the horizontal and vertical displacements published as results from PLAXIS are shown in Table 2.1 in appendix 2.

This maximum value of horizontal displacement is approximately the same as the one obtained from the analysis carried out in the journal. The maximum value of horizontal displacement obtained from the journal is 16.57mm.

The detailed horizontal displacements observed in the finite element analysis for the same wall section as obtained from the journal are shown in Figure 4.23 below.

The detailed horizontal displacements observed in the finite element analysis for wall section 1 are shown in detail in Figure 4.

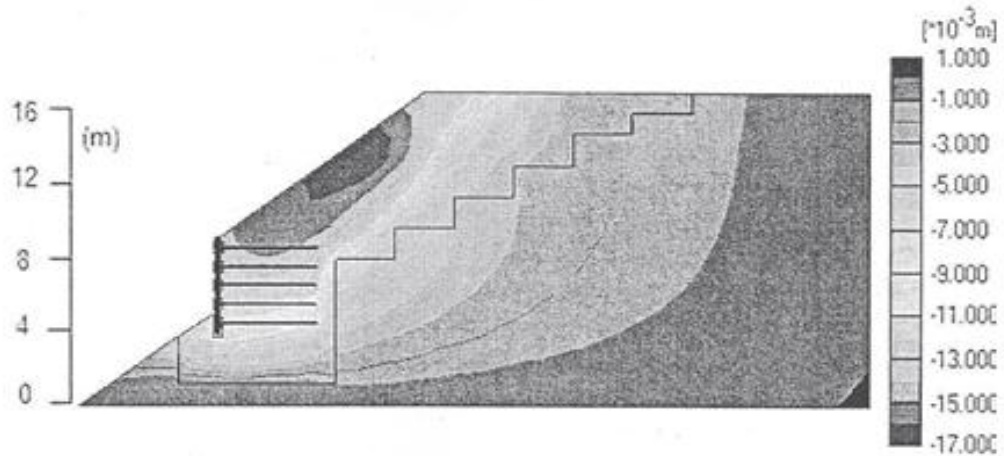


Figure 4: Horizontal displacements (section 1, max hor. displ.=16.57mm, PLAXIS)

**Figure 4.23:** Horizontal displacements

Source: Published journal of geotechnical engineering titled “Numerical Analysis of Reinforced Soil Retaining Walls” by V.N. Georgiannou et al.

#### 4.2.1.2 The Axial Forces

The values of the axial forces in each geogrids are approximately the same as those observed in the journal. For example, at reinforcement level of +3.95m the maximum value of the axial force observed is 26.56kN while the corresponding value of the axial force at the same level of reinforcement as obtained from the journal is 28.68kN (See Table 4.15).

Figure 4.24 shows the axial force diagram obtained from the PLAXIS at reinforcement level +3.95m.

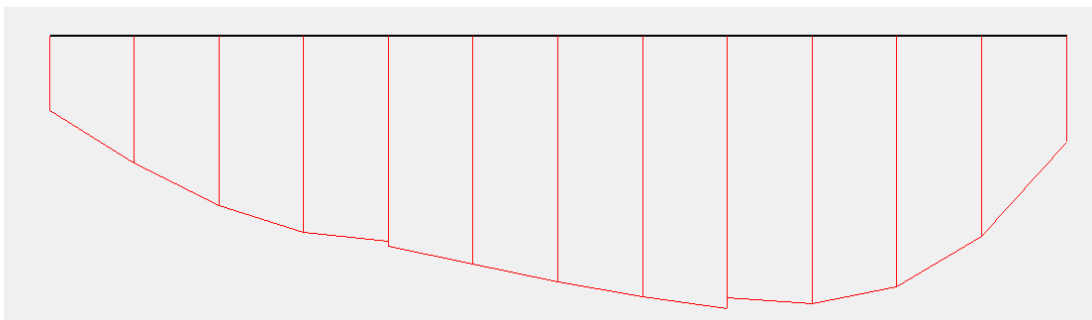


**Figure 4.24:** Axial Force Diagram (max. axial force = 26.56kN, PLAXIS)

The detailed values of the axial force are shown in Table 2.2 in appendix 2.

Table 4.15 below shows the various values of axial forces observed in FLAC and PLAXIS for wall sections 1 and 2 at various reinforcement layers as obtained from journal.

**Table 4.15:** Axial forces

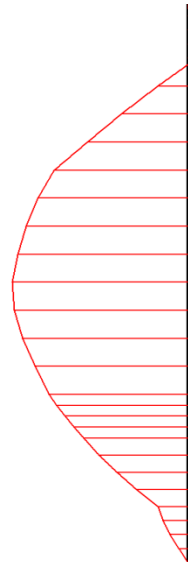
Section 1			Section 2		
Reinforce- ment layers (m)	FLAC Axial force (kN)	PLAXIS Axial force (kN)	Reinforce- ment layers (m)	FLAC Axial force (kN)	PLAXIS Axial force (kN)
+7.55	19.61	7.99	+7.55	25.27	4.61
+6.65	17.45	9.11	+6.65	17.92	16.22
+5.75	18.73	13.62	+5.75	20.08	20.46
+4.85	23.63	19.02	+4.85	26.87	23.26
+3.95	24.04	28.68	+3.95	33.07	26.18
-			+3.05	36.09	26.14
-			+2.15	36.79	26.24

Table 3: Tensile forces developed at each level of reinforcement for wall sections 1 & 2

Source: Published journal of geotechnical engineering titled “Numerical Analysis of Reinforced Soil Retaining Walls” by V.N. Georgiannou et al.

#### 4.2.1.3 The Bending Moments

The bending moment diagram as obtained from the Plaxis is shown in Figure 4.25 below.



**Figure 4.25:** Bending Moment Diagram (max. bending moment = 24.361KNm/m, PLAXIS)

The detailed values of the bending moments along the wall section are shown in Table 2.3 in appendix 2.

The values of the bending moments obtained from the numerical analysis carried out in the journal are approximately the same. The values of the bending moments obtained from the journal using PLAXIS and FLAC are within a range of 25KNm to 50KNm (See Figure 4.25).

Figure 4.25 shows the bending moment diagrams from FLAC and PLAXIS as obtained from the journal.

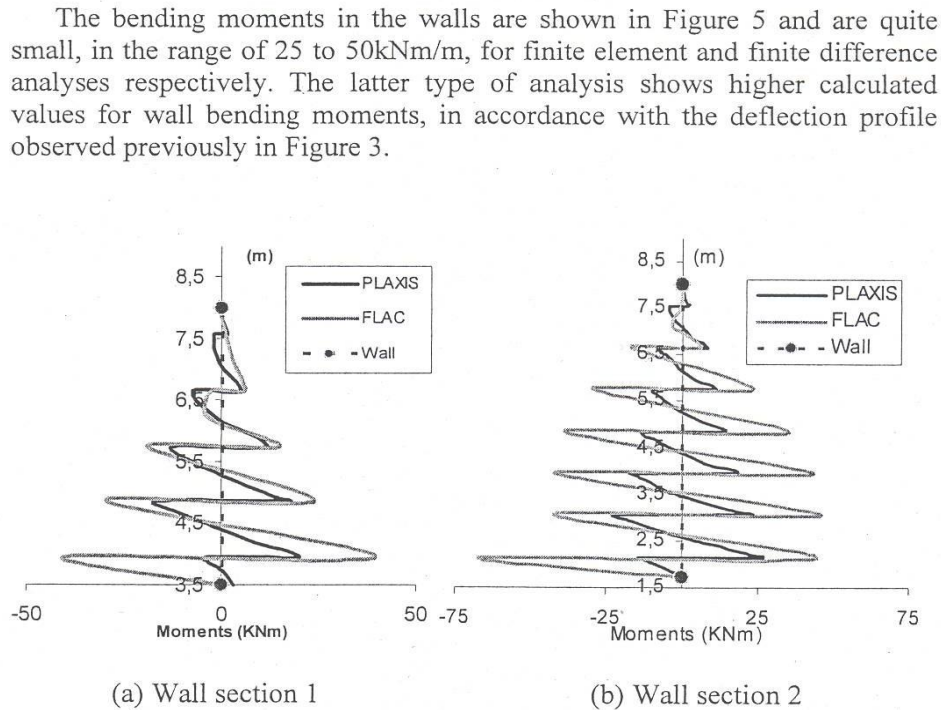


Figure 5: Bending moments calculated on (a) wall section 1; (b) wall section 2

**Figure 4.26: Bending Moments**

Source: Published journal of geotechnical engineering titled “Numerical Analysis of Reinforced Soil Retaining Walls”

**4.2.2 The Second Analysis**

As previously explained, this analysis is divided into two parts-*static and dynamic analyses*

**4.2.2 The Static Analysis**

**4.2.2.1 Stiffness-Displacement Variation of a Reinforced Soil Wall**

Figure 4.27 and 4.28 show the detailed displacements (with geogrids stiffness value of 100kN/m) observed in the finite element analysis.

The detailed values of the horizontal and vertical displacements published as results from PLAXIS are shown in Table 2.4 in appendix 2.

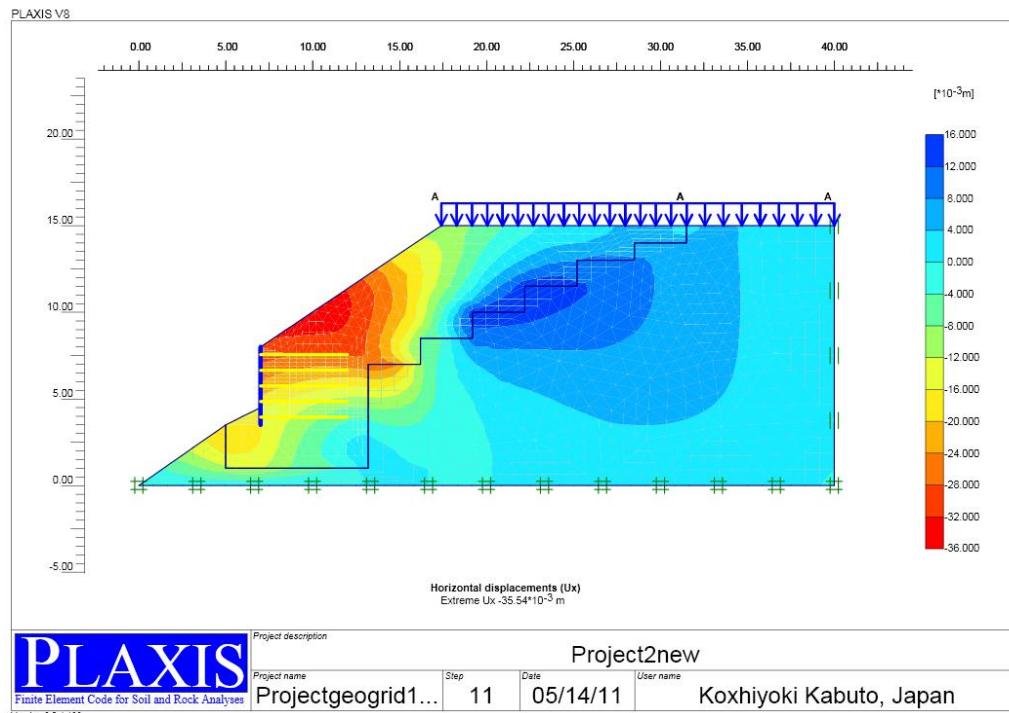


Figure 4.27: Horizontal Displacements (max. hor. displ. = 35.54mm)

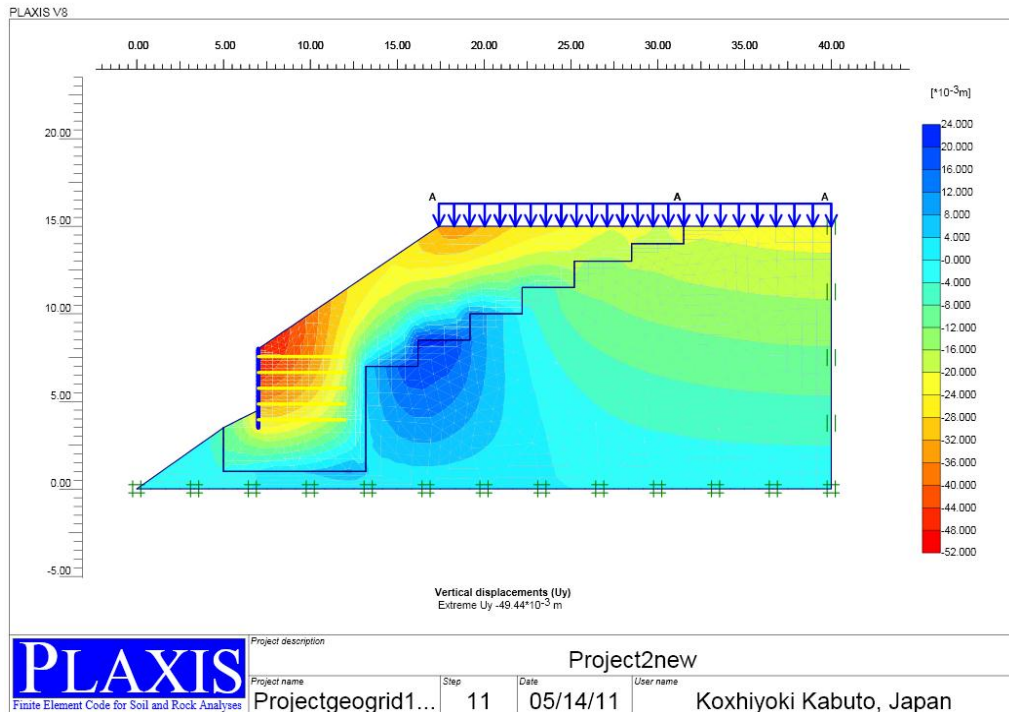
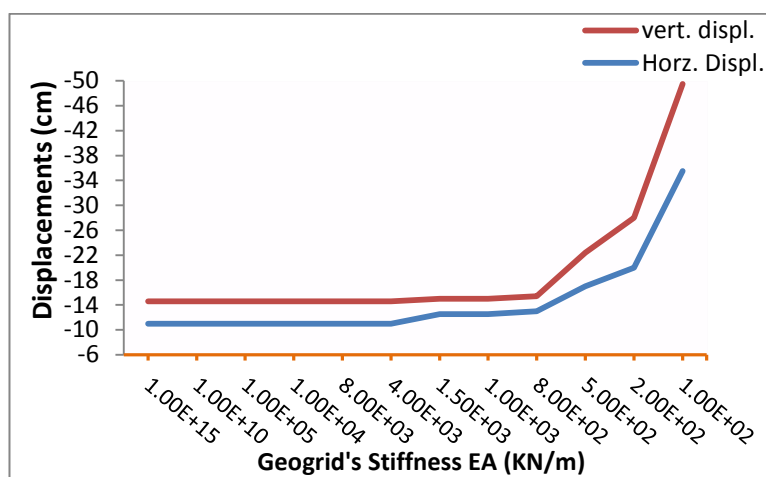


Figure 4.28: Vertical Displacements (max. vert. displ. = 49.44mm)

The detailed results of displacements obtained from the numerical analysis with different values of geogrids stiffness are shown in Table 4.16.

**Table 4.16:** Displacements under Different Stiffness of the Geogrids

Axial stiffness of geogrids (kN/m)	Displacement	
	Horizontal	Vertical
	(mm)	
1.00E+15	-11.00	-14.60
1.00E+10	-11.00	-14.60
1.00E+05	-11.00	-14.60
1.00E+04	-11.00	-14.60
8.00E+03	-11.00	-14.60
4.00E+03	-11.00	-14.60
1.50E+03	-12.50	-15.00
1.00E+03	-12.50	-15.00
8.00E+02	-13.00	-15.40
5.00E+02	-17.00	-22.40
2.00E+02	-20.00	-28.00
1.00E+02	-35.50	-49.50



**Figure 4.29:** Stiffness-Displacement Relationship

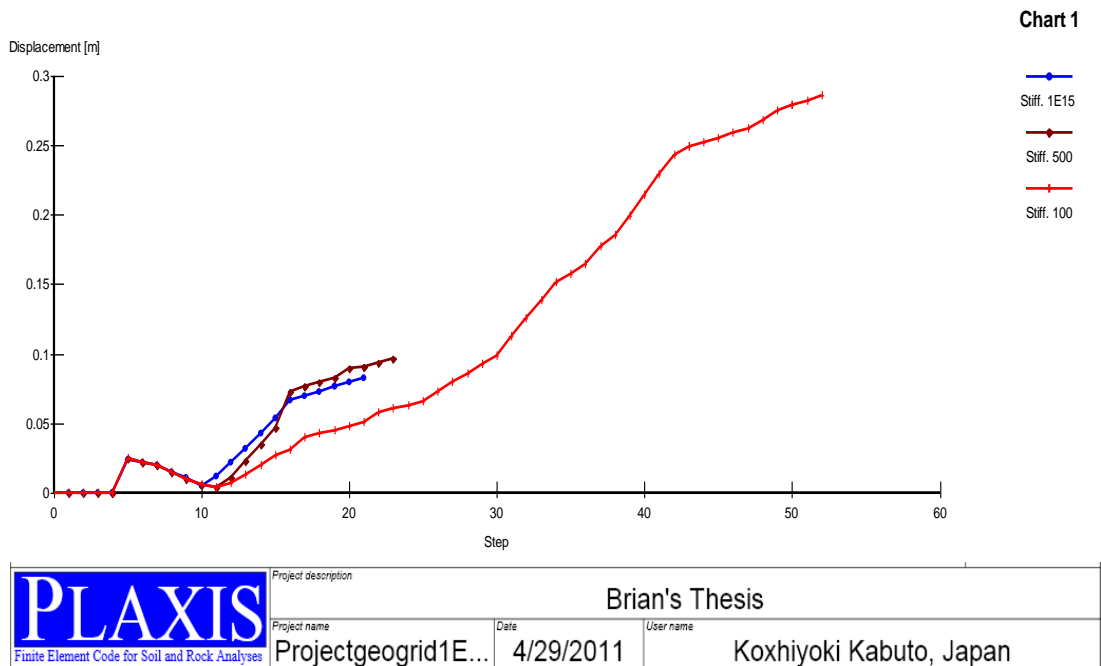


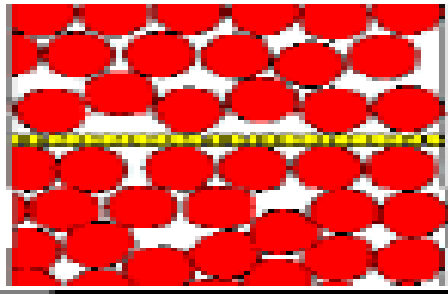
**Figure 4.30:** Step-Displacement Relationship for Selected Cases of Geogrids Stiffness

**Remarks:**

These figures (Figures 4.29 and 4.30) show that the displacement of the reinforced wall is approximately the same within a wide range of geogrids stiffness ( $(1.00E15 - 8.00E02)kN/m$ ) for both vertical and horizontal displacements (see Figures 2.5, 2.7a and 2.8 in Appendix-2 for the deformed mesh, effective stress contours and plastic points contours of the wall with geogrids stiffness of  $1.00E15kN/m$ ). However, the displacement changes rapidly for both horizontal and vertical displacements immediately upon further reduction in the stiffness of the geogrids even though the rate of change is smaller compared to the preceding rate of change in the stiffness of the geogrids. This result shows a wide range of values of geogrids stiffness for steady and stable displacements of the reinforced wall. This observed behaviour of the wall can be explained from the soil-geogrids interaction point of view.

As far as soil-geogrids-interaction is concerned, around the reinforcements, a set of interfaces (suited to model bond mechanisms) and refinement has to be applied. The interface strength (analogous to an “efficiency” parameter) can be defined according to soil and geogrids characteristics, as outlined by Jewell (1992).





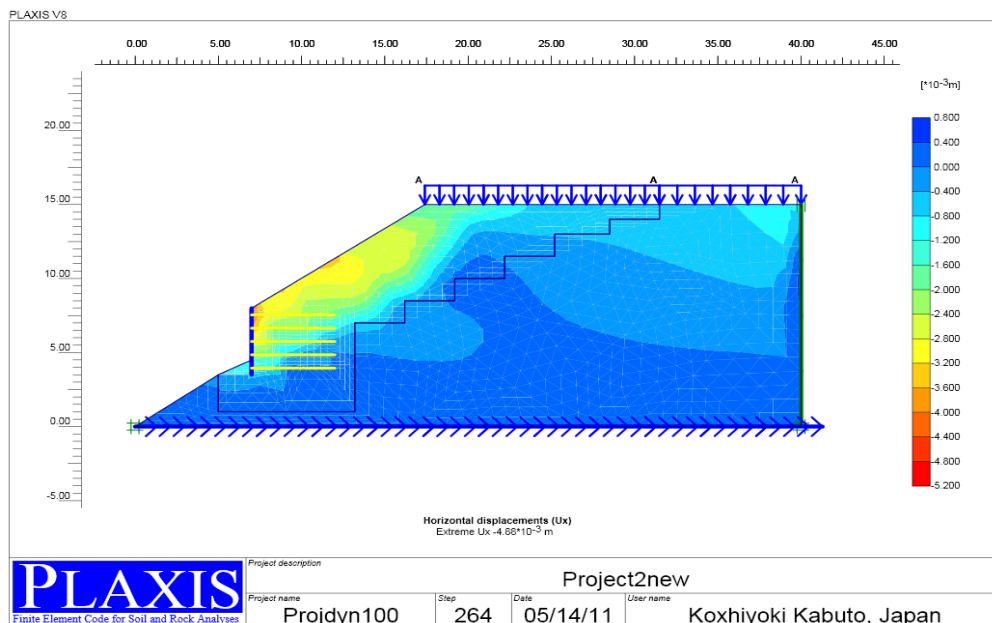
**Figure 4.31:** DEM Model (Bhandari and Han, 2010)

Figure 4.31 shows the DEM model of APA test simulation, it essentially represents soil-reinforcements interface relationship. Failure along the soil-geogrids interface will only occur when the limiting values of bonding and tensile internal frictional force are reached. However, this value of internal frictional force is dependent on the stiffness of the geogrids. It therefore becomes necessary for a Civil Engineer designing reinforced earth wall to fully examine this behaviour of the wall for optimum design and increased efficiency of the wall.

### 4.2.3 The Dynamic Analysis

#### 4.2.3.1 Stiffness-Displacement Variation of a Reinforced Soil Retaining Wall (Agio Earthquake)

Figure 4.32 and 4.33 show the detailed displacements (with geogrids stiffness value of  $100\text{kN/m}$ ) observed in the finite element analysis.



**Table 4.32:** Horizontal Displacements (max. hor. displ. = 4.88mm)

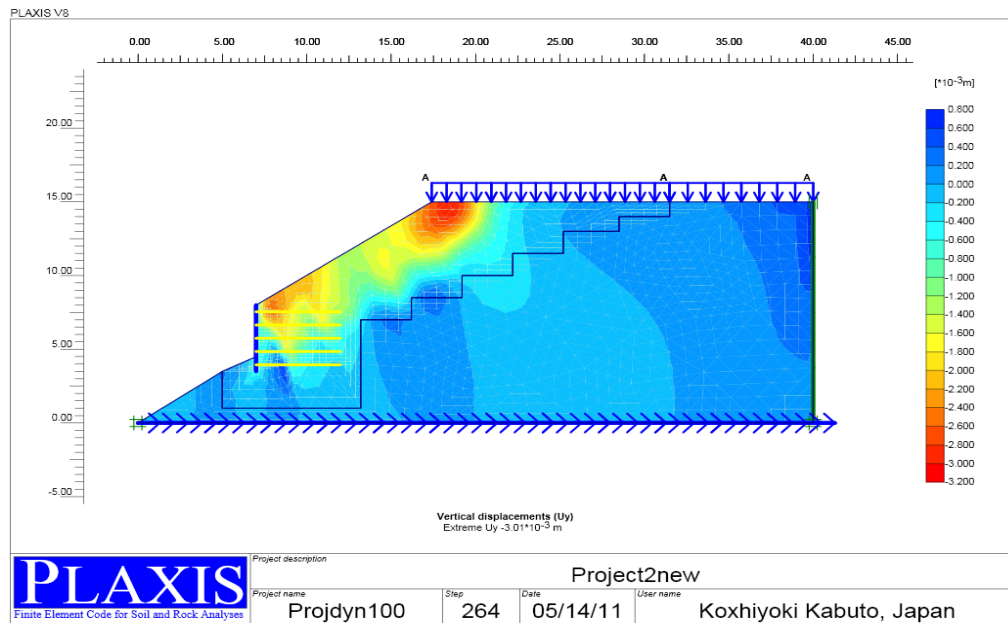


**Table 4.33:** Vertical Displacements (max. vert. displ. = 3.01mm)

The detailed results of displacements obtained from the numerical analysis with different values of geogrids stiffness are shown in Table 4.17.

**Table 4.17:** Displacements under Different Stiffness of the Geogrids

Axial stiffness of geogrids (kN/m)	Displacement	
	Horizontal	Vertical
	(mm)	
1.00E+15	-	-
1.00E+10	-	-
1.00E+05	-2.30	-1.80
1.00E+04	-2.30	-1.80
8.00E+03	-2.30	-1.81
4.00E+03	-2.30	-1.80
1.50E+03	-2.30	-1.80
1.00E+03	-2.30	-1.82
8.00E+02	-2.50	-1.80
5.00E+02	-2.70	-2.10
2.00E+02	-3.20	-2.50
1.00E+02	-4.80	-3.01

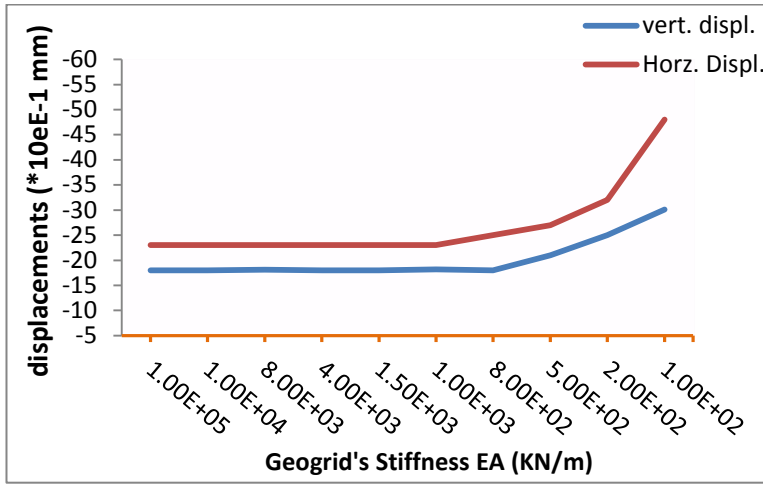


Figure 4.34: Stiffness-Displacement Relationship

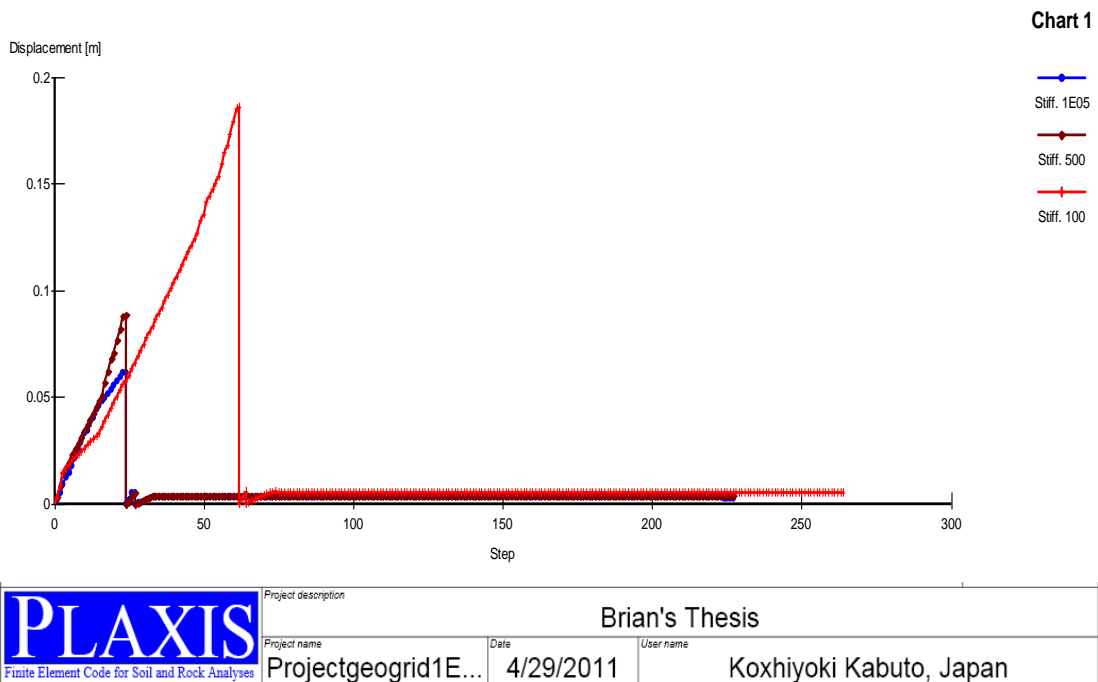
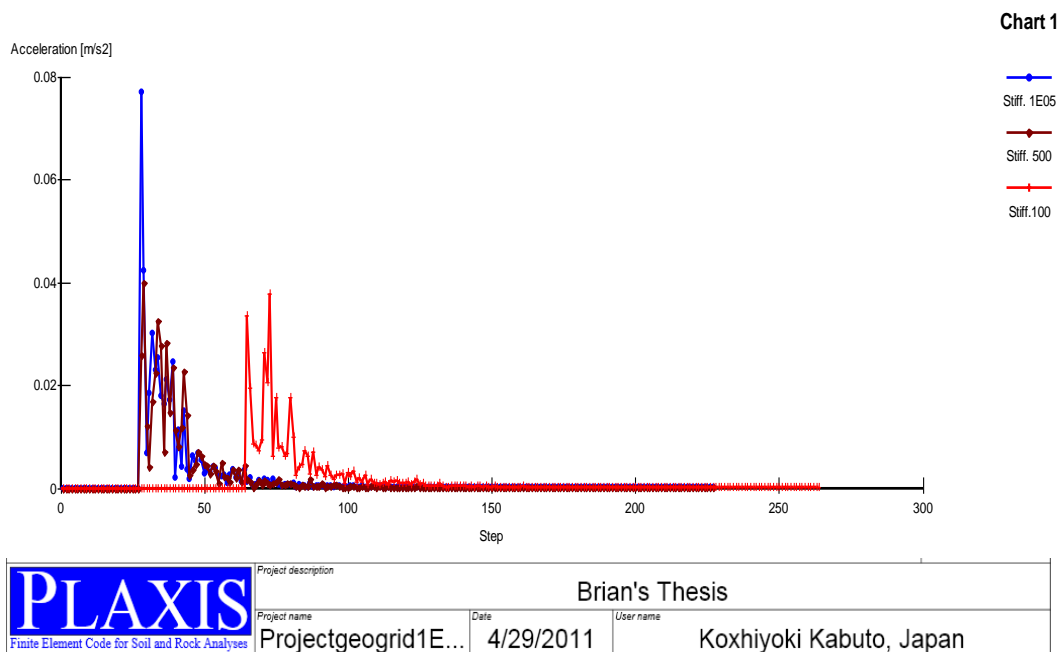


Figure 4.35: Step-Displacement Relationship for Selected Cases of Geogrids Stiffness

**Remarks:**

These figures also show that the displacement of the reinforced wall is approximately the same with a wide range of geogrids stiffness ( $(1.00E5 - 8.00E02)kN/m$ ) for both vertical and horizontal displacements (see Figure 2.6 and 2.7b for the deformed mesh and effective stress contours corresponding to the stiffness of  $1.00E5kN/m$  in Appendix 2). However, the displacement changes rapidly for both horizontal and vertical displacements immediately upon further reduction in the stiffness of the geogrids. This result shows a wide range of values of geogrids stiffness for steady and stable displacements of the reinforced wall. It is interesting to note that the wall

failed during the analysis for geogrids stiffness of  $1.00E15kN/m$  and  $1.00E10kN/m$  respectively. This observed behaviour of the wall can be explained in terms of the compatibility condition and relation(s) between reinforcement (geogrids) and the soil as well as the soil-structure interface of structure for seismic stability. The stability of a structure to seismic actions and loads depends heavily on the stiffness of the structure, and it has been proved that the higher the stiffness of a structure, the better the ability of a structure to resist seismic loads. However, the case of geogrids is not different from this general philosophy. In addition to this established load theory, the behaviour of soil-reinforced wall with geogrids under the influence of seismic loads depends on the compatibility between the stiffness of the geogrids and the angle of internal friction of the soil being reinforced. A state of equilibrium between the geogrids stiffness and the soil's angle of internal friction has to be reached for the reinforced wall to be stable, once this state of equilibrium is reached; an additional stiffness becomes unnecessary and uneconomical.



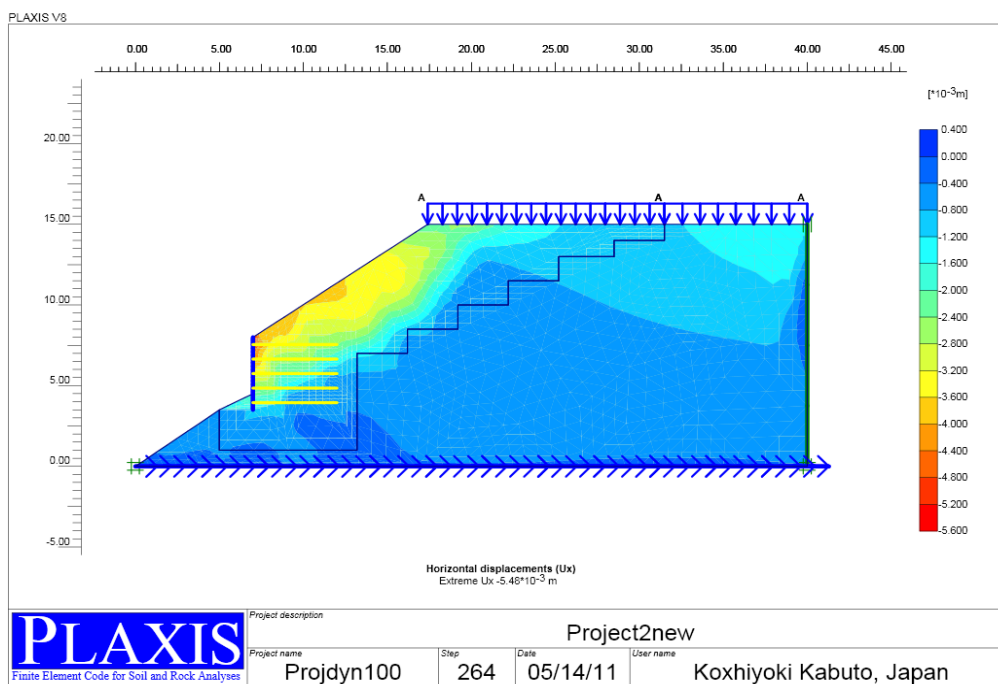
**Figure 4.36:** Step-Acceleration Relationship for Selected Cases of Geogrids stiffness

Figure 4.36 shows the Step-acceleration relationship for selected stiffness of geogrids investigated. This figure shows that the acceleration spectrums for the cases of the geogrids with stiffness of  $1.00E05kN/m$ ,  $500kN/m$  and  $100kN/m$ . The acceleration spectrums for the soil reinforced wall with stiffness values between  $1.00E05kN/m$  and  $500kN/m$  are essentially similar with approximately the same

fundamental period of vibration while the spectrum for the case of stiffness  $100kN/m$  changed with higher value of fundamental period of vibration. Structures with higher natural frequencies, and a short natural period, tend to suffer higher accelerations but smaller displacement while structures with lower natural frequencies, and a long natural period show reverse response with lower accelerations but larger displacements (Pankaj, A. and Manish, S. (2006)). Thus, the wall with the lowest stiffness of  $100kN/m$  has the largest natural period of vibration with the highest observed displacements.

#### 4.2.3.2 Stiffness-Displacement Variation of a Reinforced Soil Retaining Wall (Sepolia Earthquake)

Figures 4.37 and 4.38 show detailed displacements (with geogrids stiffness value of  $100kN/m$ ) observed in the finite element analysis (PLAXIS).



**Figure 4.37:** Horizontal Displacements (max. hor. displ. = 5.48mm)

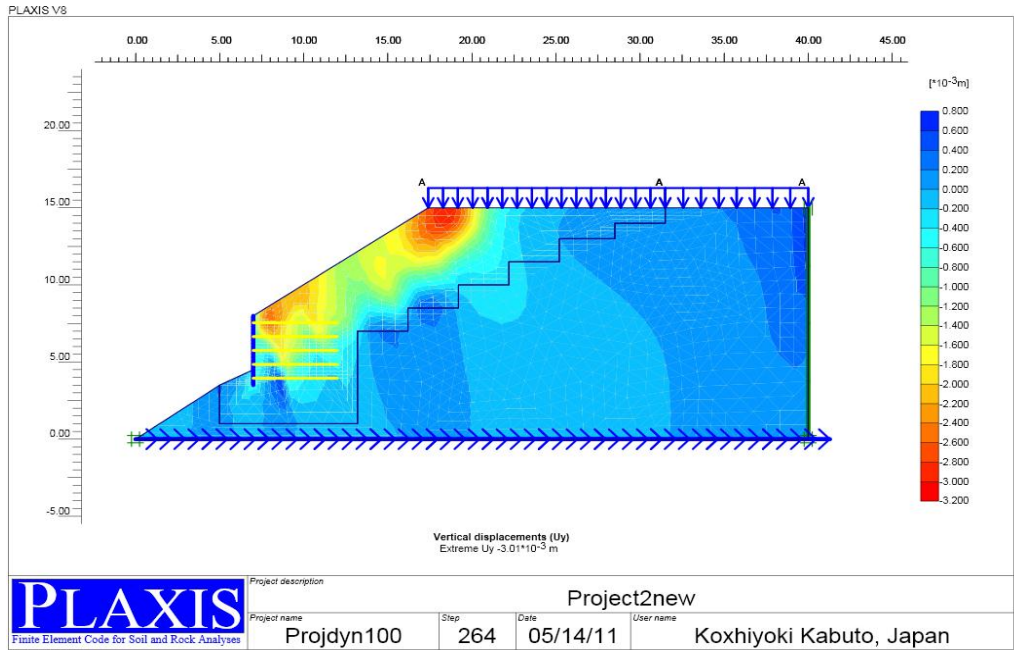


**Table 4.38:** Vertical Displacements (max. vert. displ. = 3.01mm)

The detailed results of displacements obtained from the numerical analysis with different values of geogrids stiffness are shown in Table 4.18.

**Table 4.18:** Displacements under Different Stiffness of the Geogrids

Axial stiffness of geogrid (kN/m)	Displacement	
	Horizontal	Vertical
	(mm)	
1.00E+15	-	-
1.00E+10	-	-
1.00E+05	-2.52	-1.01
1.00E+04	-2.52	-1.02
8.00E+03	-2.42	-0.98
4.00E+03	-2.51	-1.01
1.50E+03	-2.48	-1.00
1.00E+03	-2.50	-0.98
8.00E+02	-3.01	-1.81
5.00E+02	-3.20	-2.05
2.00E+02	-3.61	-2.52
1.00E+02	-5.50	-3.01

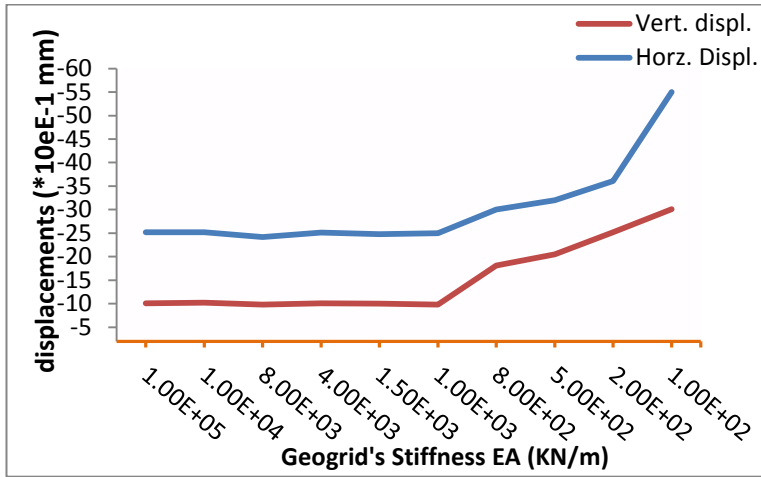
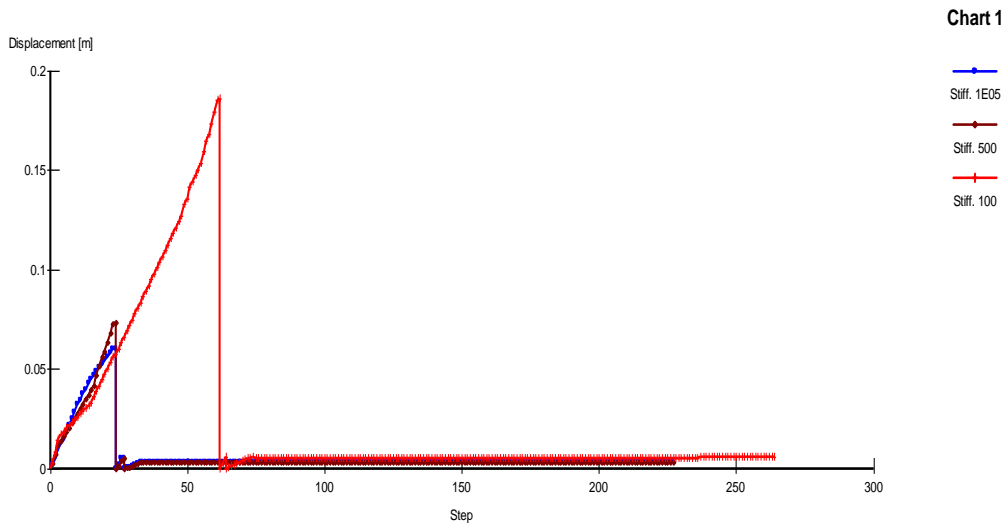


Figure 4.39: Stiffness-Displacement Relationship



	Project description		
	Brian's Thesis		
Project name	Date	User name	
Projectgeogrid1E...	4/29/2011	Koxhiyoki Kabuto, Japan	

Figure 4.40: Step-Displacement Relationship for Selected Cases of Geogrids Stiffness

**Remarks:**

Just like the case of Agio earthquake, these figures also show that the displacements of the reinforced wall are approximately the same with a wide range of geogrids stiffness ( $1.00E5 - 1.00E03$ ) for both vertical and horizontal displacements. However, the displacement changes rapidly for both horizontal and vertical displacements immediately upon further reduction in the stiffness of the geogrids. This result shows a wide range of values of geogrids stiffness for steady and stable displacements of the reinforced wall. It is interesting to note that the wall also failed during the analysis for geogrids stiffness of  $1E15kN/m^2$  and  $1E10kN/m^2$

respectively and the reason for this observed behaviour of the wall is the same as in the case of Agio earthquake.

Figure 4.41 shows the Step-acceleration relationship for selected stiffness of geogrids investigated. The reason for this observed behaviour is the same as the case of Agio earthquake explained earlier.

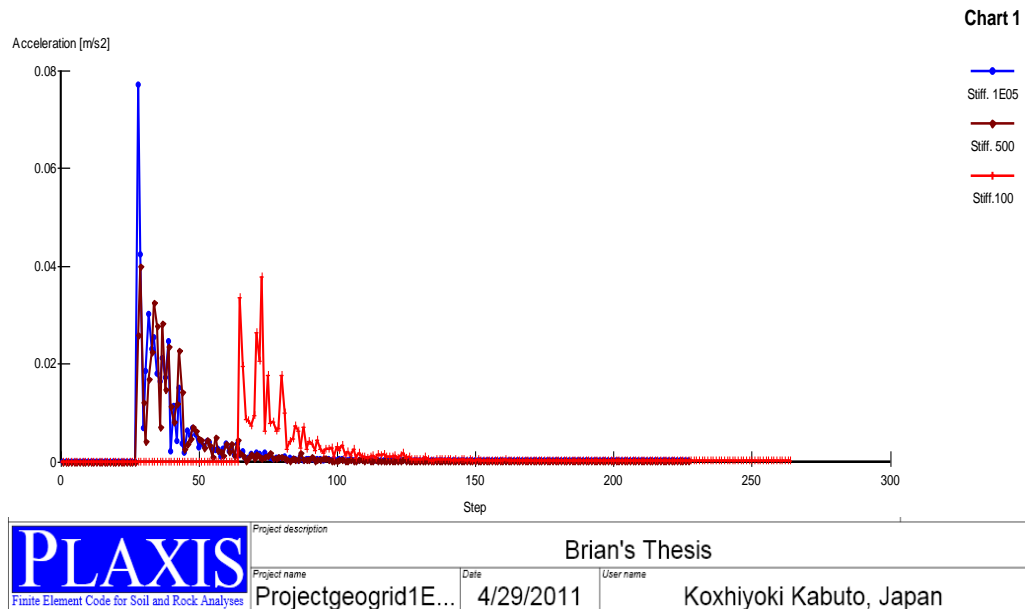


**Figure 4.41:** Step-Acceleration Relationship for Selected Cases of Geogrids Stiffness

In general, these results show a unique behaviour of the reinforced soil retaining wall under different conditions of geogrids stiffness. This is a condition that the structural engineers have to examine when designing reinforced soil retaining wall for both static and dynamic loading conditions in order to make a more economical and wise choice of the geogrids stiffness based on the allowable and safe level of displacement.

#### 4.2.4 Geogrids Stiffness Response and Construction Industry

After the analysis and design for an appropriate and required value of the geogrids stiffness, the designer can proceed to order for the appropriate geogrids required for the reinforced soil retaining wall. It should be noted that most geogrids are extensible and are sold based on the required stiffness (axial stiffness). Figure 4.42 shows a web page of a geogrids supplier company with the geogrids price expressed in terms of axial stiffness (EA).



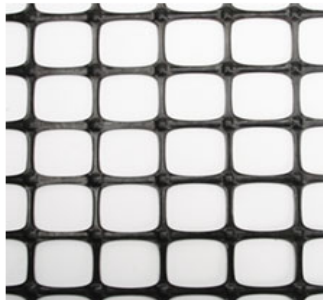
Geogrids prices obtained from other companies are based on tensile strength of the geogrids. The price of the geogrids varies with its tensile strength, the higher the tensile strength the higher the price its price per unit length. Another specifications data of geogrids, as obtained from the official website of one of the famous world's geogrids supplier is shown in Table 4.19.

Home > [Pest, Deer & Rabbit Control](#) > [Deer & Rabbit Control](#) > [Fencing & Netting](#)

### Black Poly Geogrid

This unique Poly Geogrid, with superior tensile strength and UV-resistance, is ideal for both fencing and stabilization applications.

- Manufactured from a unique, black, biaxially orientated polymer material that is lightweight, flexible and easy to handle, yet extremely durable.
- Superior UV resistance.
- Offers an attractive, long-lasting and easy-to-install fencing solution. Ask your knowledgeable National Account Manager for installation recommendations.
- Excellent long-term strength of this environmentally safe and friendly polymer material makes it ideal for stabilization, separation, reinforcement and filtration.



Item #	Description	Price
<a href="#">109750</a>	Black Poly Geogrid 4'x164'	\$175.00 /EA <a href="#">More Info</a>
<a href="#">109751</a>	Black Poly Geogrid 5'x164'	\$205.00 /EA <a href="#">More Info</a>
<a href="#">109752</a>	Black Poly Geogrid 6'x164'	\$255.00 /EA <a href="#">More Info</a>
<a href="#">109753</a>	Black Poly Geogrid 7'x164'	\$295.00 /EA <a href="#">More Info</a>
<a href="#">109754</a>	Black Poly Geogrid 8'x164'	\$339.00 /EA <a href="#">More Info</a>
<a href="#">109749</a>	Black Poly Geogrid 13'x164'	\$479.00 /EA <a href="#">More Info</a>

**Search**

Product Search  [Go](#)

Catalog Item #  [Go](#)

[Advanced Search](#)

**Shop Our Products**




- ▶ New Products
- ▶ High Tunnels & Cold Frames
- ▶ Greenhouse Kits
- ▶ Commercial Greenhouses
- ▶ Greenhouse Cooling & Fans
- ▶ Seed-Starting Supplies
- ▶ Pots, Trays & Containers
- ▶ Greenhouse Film & Covering
- ▶ Hydroponic Systems
- ▶ Shade Houses & Shade Cloth
- ▶ Canopies & Party Tents
- ▶ Greenhouse Lighting
- ▶ Greenhouse Irrigation
- ▶ Greenhouse Building Materials
- ▶ Hobby Greenhouses
- ▶ Greenhouse Accessories
- ▶ Temporary Storage Buildings
- ▶ Thermostats & Controllers
- ▶ Soil Testing & Meters
- ▶ Nursery Handtrucks
- ▶ Nursery Carts & Wagons
- ▶ Shelving & Benches
- ▶ Patio Growhouses
- ▶ AquaCool Systems
- ▶ EZ-Grow Greenhouses
- ▶ Greenhouse Heaters
- ▶ Ground Cover, Liners & Tarps
- ▶ TekFoil Reflective Insulation
- ▶ Nursery Display Racks & Units
- ▶ Pest, Deer & Rabbit Control
- ▶ Garden Fences
- ▶ Safety & Protection
- ▶ Lawn & Garden
- ▶ Monthly Specials
- ▶ Steals & Deals


**Shopping Help**

- ▶ Instruction Manuals
- ▶ Video Help Library
- ▶ Customer Service
- ▶ Contact Us
- ▶ Live Help
- ▶ Site Map

**Resources**

- ▶ Request a Catalog
- ▶ Email Promotions
- ▶ Payment Options
- ▶ Customer Testimonials
- ▶ Careers
- ▶ Press Releases



1.800.476.9715 | [Contact Us](#) | [Live Help](#)

[Cold Frames](#) - [Shelves & Benches](#) - [Greenhouse Film](#) - [Greenhouse Materials](#) - [Pots, Trays, Flats & Containers](#)  
[Customer Service](#) - [Privacy Policy](#) - [Terms & Conditions](#) - [Site Map](#) - [Careers](#) - [Home](#)

Copyright © 2011 Growers Supply 1440 Field of Dreams Way, Dyersville, IA 52040

**Figure 4.42:** Geogrids Specifications

Source: FarmTek-Grower Supply Web Page

[http://www.growerssupply.com/farm/supplies/prod1;gs1\\_garden\\_fences;pg109750.html](http://www.growerssupply.com/farm/supplies/prod1;gs1_garden_fences;pg109750.html)

**Table 4.19:** Size & Specification of Geogrids (PP Biaxial Geogrids)

Item	TGSG15-15	TGSG20-20	TGSG45-45	TGSG30-30	TGSG40-40
Longitudinal Tensile Strength, kN/m	15	20	45	30	40
Transverse Tensile Strength, kN/m	15	20	45	30	40
Longitudinal Yield Elongation,%	15				
Transverse Yield Elongation,%	13				
Longitudinal Yield Strength at 2% Elongation, kN/m	5	7	17	11	14
Transverse Yield Strength at 2% Elongation, kN/m	5	7	17	11	14
Longitudinal Yield Strength at 5% Elongation, kN/m	7	14	33	21	30
Transverse Yield Strength at 5% Elongation, kN/m	7	14	33	21	30
Product Length/roll, m	50				40
Product width, m	2/3.9/3.95/4/4.5/5				

Source: Feichang Lianyi Engineering Plastics Co. Ltd.

<http://www.chinageogrid.com/en/products.asp?qclid=COzdya3L6qcCFcJP4OodNXhgaO>

## CHAPTER 5

### CONCLUSION AND RECOMMENDATION

#### 5.1 Conclusion

Following the results obtained from both static and dynamic analyses carried out on the two case studies presented in this research work, the following concluding remarks can be made:

- The behaviour of the reinforced soil retaining wall is dependent on some factors which can positively or negatively influence the general performance of the wall. These factors include the value and dimension of the surcharge load (imposed load), length of the geogrid(s), stiffness of the geogrids, spacing of the geogrids among others.
- The behaviour of loose sand in terms of displacement is similar to that of silty sand while the responses of both dense and clayey sands are also comparable.
- Loose and silty sands showed higher degrees of instability as a backfill and foundation material in reinforced soil retaining wall.
- Dense and clayey sands are more stable and suitable as a backfill and foundation materials in reinforced soil retaining wall.
- Dense and clayey sands require minimum length of reinforcement while an increase in the length of reinforcement can result to a decrease in the values of the wall's deformations when loose or silty sand is used as backfill material.
- In general, clayey sand is most stable with the lowest value of both vertical and horizontal displacements.
- The stiffness of geogrid plays a vital role in the stability of reinforced soil retaining wall. The maximum tensile force shifts towards the facing or the failure plane in the case of short reinforcements or lower stiffness of the reinforcement.
- The exact degree of contribution of the soil reinforcement (geogrids) to the stability of the wall can be best determined by analysis.
- There exists a wide range of values of geogrids stiffness by which the wall analyzed remained stable after which rapid changes in the displacements of the wall become evident.

- The behaviour of the wall in both static and dynamic conditions is similar.
- The behaviour of reinforced soil retaining wall with geogrids under the influence of seismic loads depends on the compatibility condition between the stiffness of the geogrids and the angle of internal friction of the soil being reinforced. A state of equilibrium between the geogrids stiffness and the soil's angle of internal friction has to be reached for the reinforced wall to be stable, once this state of equilibrium is reached; an additional stiffness becomes unnecessary and uneconomical.
- When the stiffness of the geogrid is increased beyond certain limit, brittle mode of failure of the reinforced soil retaining wall will occur.
- Failure along the soil-geogrids interface will only occur when the limiting values of bonding and tensile internal frictional force are reached. However, this value of internal frictional force is dependent on the stiffness of the geogrids. It therefore becomes necessary for a civil engineer designing reinforced earth wall to fully examine this behaviour of the wall for optimum design and increased efficiency of the wall.

## **5.2 Recommendations**

The following are the possible ways of improving this research work:

- By studying the effect(s) of changes in the geometry (shape) of the wall in the general stability of the wall.
- By studying the effect(s) of changes in the position of the wall's imposed load in the stability of the wall.

## REFERENCES

- Allen, T.M., Bathurst, R. J., and Berg, R. R. (2002) “Global Level of Safety and Performance of Geosynthetics Walls” An Historical Perspective” *Geosynthet. Int.*, 9\_5–6\_, 395–450.
- Bhandari, A. and Han, J. (2010) “Investigation of Geotextile-Soil Interaction under a Cyclic Vertical Load using the Discrete Element Method” *Geotextiles and Geomembranes*, 28(1), pp. 33-43.
- Bolton, M.D. and P.L.R. Pang (1982) “Collapse Limits of Reinforced Earth Walls” *Geotechnique*, Vol. 32(4), pp. 349-367.
- Bolton, M. D. (1989) “Reinforced Soil Laboratory Testing and Modelling. Performance of Reinforced Soil Structures” *Proc. of Intl. Reinforced Soil Conference*, Editors: McGown et al., 1989, Thomas Telford.
- Bonaparte, R. and Schmertmann, G.R. (1987) “Reinforcement Extensibility in Reinforced Soil Wall Design” *The Application of Polymeric Reinforcement in Soil Retaining Structures*, pp. 409–457.
- Broms, B.B. (1988) “Fabric Reinforced Retaining Walls” *Proc. of Intl. Geotechnical Synp. On Theory and Practice of Reinforcing Earth*, Is Kyushu, Japan, Balkema, pp. 3-31.
- Chapius (1972), “Rapport de recherché de DEA”, Institut de Mécanique de Grenoble. (Unpublished)
- Das B. (1995) “*Principles of Foundation Engineering*” Pws Publishing Company.

Guangxin Li, Yunmin Chen and Xiaowu Tang (2008) “Geosynthetics in Civil and Environmental Engineering, Geosynthetics” *Proceedings of the 4<sup>th</sup> Asia Regional Conference in Geosynthetics* Shanghai, China.

Goodman, R.E., R.L. Taylor and T. L. Berkke (1968) “A model for the Mechanics of Jointed Rock” *J. Soil Mech. Found. Div.*, ASCE, Vol. 94(3), pp. 637-659.

Gourc, J.P. (1993) “Keynote Lecture: Geosynthetic in Embankments, Review of theory” *Proc. of the Intl. Symp. on Earth Reinforcement Practice*. Nov. 11-13, 1992)

Hatami, K. and Bathurst R. (2005) “Development and Verification of Numerical Model for the Analysis of Geosynthetic-reinforced soil Segmental Walls under Working Stress Conditions” *Can. Geotech. J.*, 42, pp. 1066-1085.

Hatami, K. and Barturst, R. J. (2006) “Numerical Model for Reinforced Soil Segmental Walls under Surcharge Loading” *Journal of Geotechnical and Geoenvironmental Engineering*, 132 (6), pp. 673-684.

Hausmann, M.R. (1976) “Strength of Reinforced Soil” *Australian Road Research Board Proceedings*, (8), 1-8, Session 13, 1976.

Huang, J., (2007) “*Coupled Mechanical and Hydraulic Modelling of Geosynthetic-Reinforced Column Supported Embankments*” Ph.D. Dissertation, the University of Kansas, p. 394.

Ingold, T.S. (1982) “Reinforced Earth”, Thomas Telford Limited, London, England.

James, K. and Mitchel, (1987) “*Reinforcement of Earth Slopes and Embankments*”, National Cooperative Highway Research Board, Washington D.C., June 1987.

Jeff B. (1997) “Reinforced Slope with Geogrids” Greenhill Road Bikeway Waterloo, Iowa Project, IX-6585(9)--79-07, USA.

Jewell, R.A. (1988) "Reinforced Soil Wall Analysis and Behaviour" *Proceedings of the NATO Advance Research Workshop on the 'Application of Polymeric Reinforcement in Soil Retaining Structures'*, Kingston, Ontario, Canada June 8-12, 1987, Eds. Jarret and McGown, pp. 365-407.

Jewell, R.A. (1992) "Keynote Lecture: Links between the Testing, Modelling and Design of Reinforced soil" *Proc. of the Intl. Symp. on Earth Reinforcement Practice*, Nov. 11-13, 1992 (Editors: Ochiai, H., S. Hayashi & J. Otani); A. A. Balkema, Vol. 2, pp. 755-772.

Jones, C.J.F.P. "*Reinforced Earth and Soil Structures*" Butterworth, 1985.

Jones, C.J.F.P. (1994) "Economic Construction of Reinforced Soil Structures" *Proc. of the Intl. Symp. on Recent Case Histories of Permanent Geosynthetic-Reinforced soil Retaining Wall*, Tokyo, Nov. 6-7, 1992 (Editors: Tatsuoka, H. Leshchinsky, D.); A.A. Balkema, pp. 103-106.

Juran, Dr. Deputy Director-Soil Mechanics Research Centre- Ecole Nationale des Ponts et Chaussées, Paris, France, 1981 "Reinforced Soil Systems-applications in Retaining Structures"

J. Huang, A. Bhandari, and X. Yang, (2011) "Numerical Modelling of Geosynthetic-Reinforced Earth Structures and Geosynthetic-Soil Interactions", *Geotechnical Engineering Journal of the SEGS & AGSSEA* Vol. 42.

Koerner, R.M. and Soong, T. Y. (2001) "Geosynthetic Reinforced Segmental Retaining Walls", *Geotextiles and Geomembranes*, 19 (2001), pp. 359-386.

Kwon, J., Tutumluer, E. and M. Kim (2009b) "Development of a Mechanistic Model for Geosynthetic-Reinforced Flexible Pavements" *Geosynthetics International*, 12(6), pp. 310-320.

McGown, A., K.Z. Andrawes and M.M. Al-Hasani (1978) "Effect of Inclusion Properties in the Behaviour of Sand" *Geotechnique*, Vol. 28(3). Pp. 327-346.

McGown, A., K.Z. Andrawes, and K.C. Yeo (Eds.) (1990), *Proc. of the Intl. Reinforced soil Conference*, Sept. 10-12, 1990, Glasgow Scotland, Thomas Telford Ltd.

Muramatsu, M, K.Nagura, T. Sueoka, K. Suami and Kitamura (1992) “Stability Analysis for Reinforced Cut Slopes with a Rigid Facing”, *Proc. of the Intl. Symp. on Earth Reinforcement Practice*, Nov. 11-13, 1992 (Editors: Ochai, H., S. Hayashi & J. Otani); A.A. Balkema, Vol. 1. Pp. 503-508.

Ochiai H. et al. (2001) “Landmarks in Earth Reinforcement” Proceedings of the 3<sup>rd</sup> International Symposium on Earth Reinforcement, Fukuoka, Kyushu, Japan.

Onodera, S., S. Naemura, A. Nakane and S. Maruo (1992) “A design Method for Steep Reinforced Embankment with Geotextiles” *Proc. of the Intl. Symposium on Earth Reinforcement Practice*, Nov. 11-13, 1992 (Editors: Ochiai, H., S. Hayashi & J. Otani); A.A. Balkema, Vol.1. pp. 391-396.

Reddy, D.V., 2003 “Long-Term Behaviour of Geosynthetic Reinforced Mechanical Stabilized Wall System”, Department of Civil Engineering, Florida Atlantic University, USA.

Reinforced Earth Company, *2011 Publications on the Design Manual for Reinforced Earth Walls*.

Rimoldi, P. (1988) “Review of Field Measurements of the Behaviour of Geogrids Reinforced Slopes and Walls” *Proc. of Intl. Geotechnical Symp. on Theory and Practice of Earth Reinforcing*, Is Kyushu, Japan, Balkema, pp. 571-578.

Rowe, R.K. and Ho, S.K (1992) “Finite Element Analysis of Geosynthetic Reinforced Soil Walls” *Geosynthetic 1993 Conference*, Vancouver, Canada.

Rowe, R. K. and Skinner, G.D. (2001) “Numerical Analysis of Geosynthetic Reinforced Retaining Wall Constructed on a Layered Soil Foundation” *Geotextiles and Geomembranes*, 19, pp. 387–412.



Saad, B., Mitri, H. and Poorooshasb, H. (2006) "3D FE Analysis of Flexible Pavement with Geosynthetic Reinforcement" *Journal of Transportation Engineering*, 132(5), pp. 402-415.

Schlosser, F. and N.T. Long (1972) "Comport de la Terre Armee dans les Ouvrages de Soutenement" *Proceedings of the 5<sup>th</sup> European Conference on Soil Mechanics and Foundation Engineering*, Vol. 1, pp. 299-306, Madrid, 1972.

Schlosser, F. and Long, N.T. (1974) "Recent Results in French Research on Reinforced Earth", *Journal of ASCE*.

Schlosser, F. and I. Juran (1979) "Parameteres de Calcul des Sols Artificiellement Ameliores: Raport General Séance 8", *Proc. of the 8<sup>th</sup> European Conference on Soil Mechanics and Foundation Engineering*, pp. 1-29, Helsinki.

Schlosser, F., Juran, I, Jacobsen, H. M., "Soil Reinforcement", General Report, 8<sup>th</sup> European Conference on Soil Mechanics and Foundation Engineering, Helsinki, Finland, 1983.

Schlosser, F. and P. Delage (1987) "Reinforced Soil Retaining Structures and Polymeric Material"

Smith, I.M and P. Segrstin (1910) "Inextensible Reinforcements versus extensible ties - FEM Comparative Analysis of Reinforced or Stabilized Earth Structures" *Proc. of the Intl. Symp. on Earth Reinforcement Practice*, Nov. 11-13, 1992 (Editors: Ochiai, H., S. Hayashi & J. Otani); A.A. Balkema, Vol. 1 & 2 pp. 549-554.

Taga, N., S. Tayama, S. Uehara and Y. Doi (1992) "Stability Namograms for Reinforced Earth with Steel Bars against Shallow Sliding of Steep slopes" *Proc. of the Intl. Symp. on Earth Reinforcement Practice*, Nov. 11-13, 1992 (Editors: Ochiai, H., S. Hayashi & J. Otani); A.A. Balkema, Vol. 1 &2 pp.549-554.

Tatsouka, F. (1992) "Role of Facing Rigidity in Soil Reinforcement, Theme Lecture for I.S. Kyushu" *Proc. of the Intl. Symp. on Earth Reinforcement Practice*. Nov. 11-13, 1992)

Vidal H., "the Principle of Reinforced Earth," *Highway Research Record*, No. 282, 1969, pp. 1 - 16.

William Whitcomb and J.R. Bell (1979) Analysis Techniques for Low Reinforced Soil Retaining Walls and comparison of Strips and Sheet Reinforcements", *Proceedings of the 17<sup>th</sup> Engineering Geology and Soil Engineering Symposium*, Moscow.

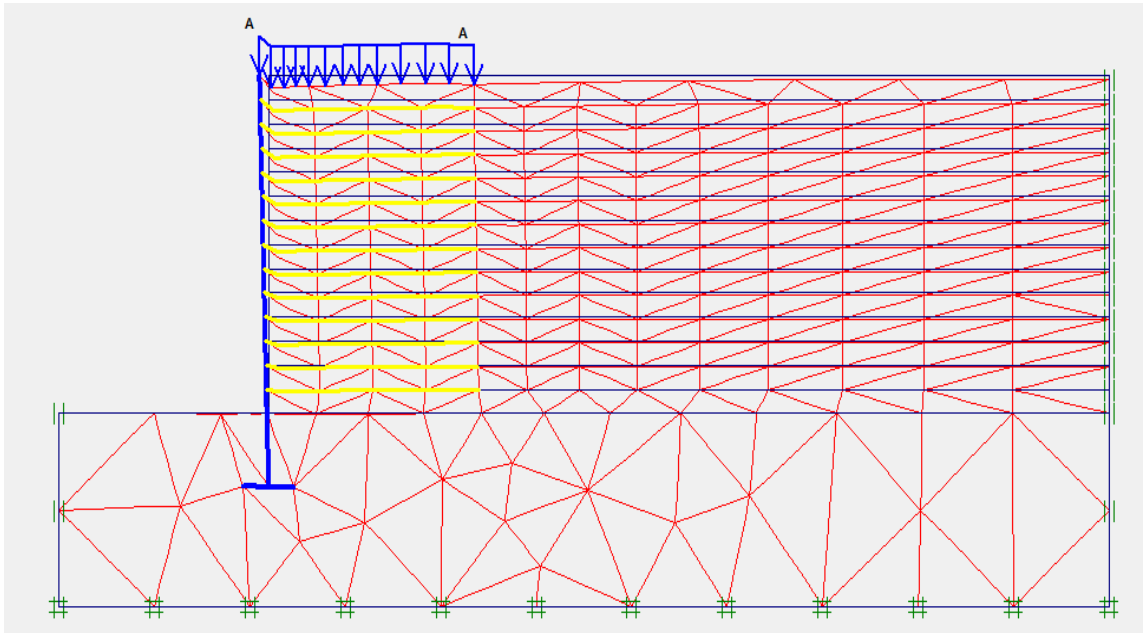
Yako, M.A. and Christopher, B.R. (1988) "Polymerically Reinforced Retaining Walls and Slopes in North America" In: Jarrett, P.M., Mc. Gown, A. (Eds.), *the Applications of Polymeric Reinforcement in Soil Retaining Structures*, Kluwer Academic Publishers, Dordicht, p. 239–283.

Yang, X., (2010) "*Numerical Analyses of Geocell-Reinforced Granular Soils under Static and Repeated Loads*" Ph.D. Dissertation, the University of Kansas: Lawrence, KS., USA.

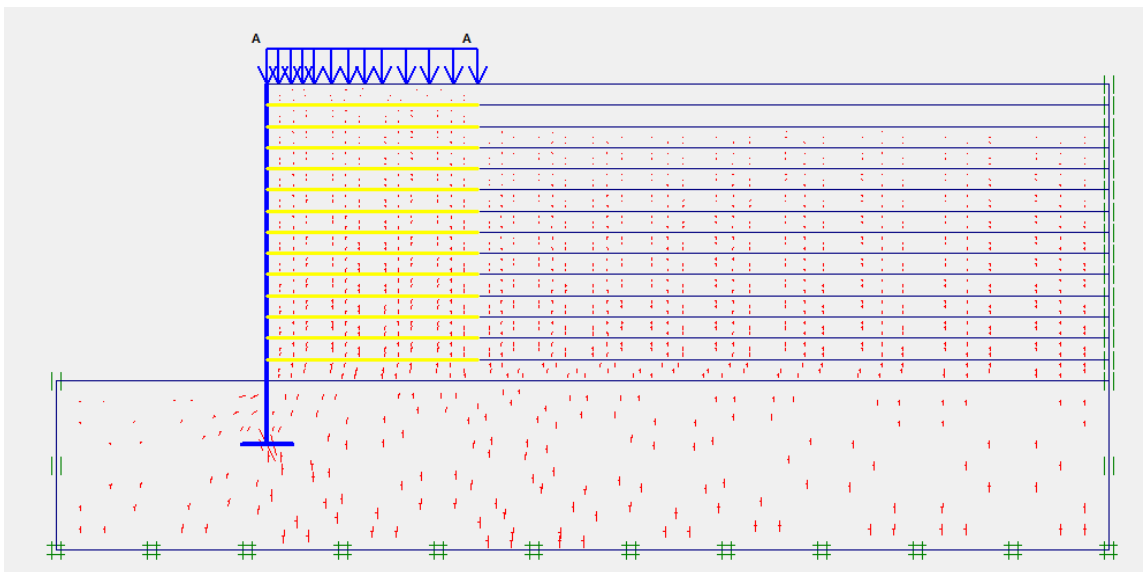
Zeynep Durukan and Semih S. Tezcan (2003) "Cost Analysis of Reinforced Soil Walls" An Online Publication of Science Direct-Geotextiles and Geomembranes, vol. 11, issue 1, pp. 29-43.

## APPENDICES

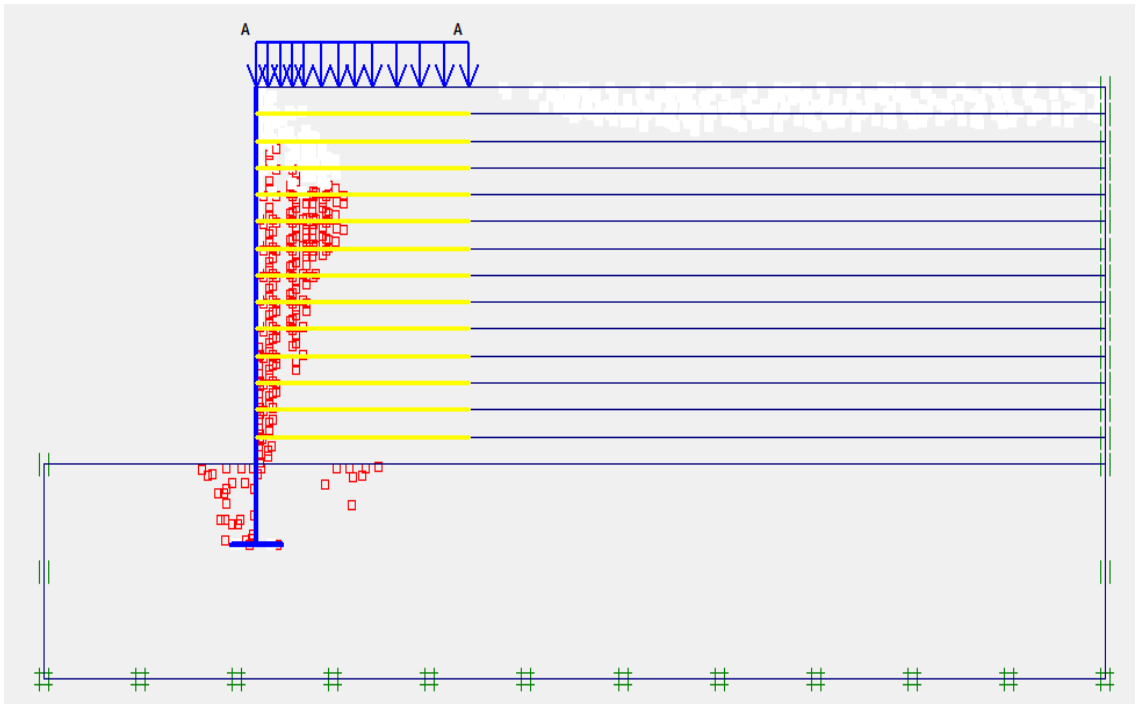
### APPENDIX-1



**Figure 1.1:** Deformed Mesh for the Final Excavation

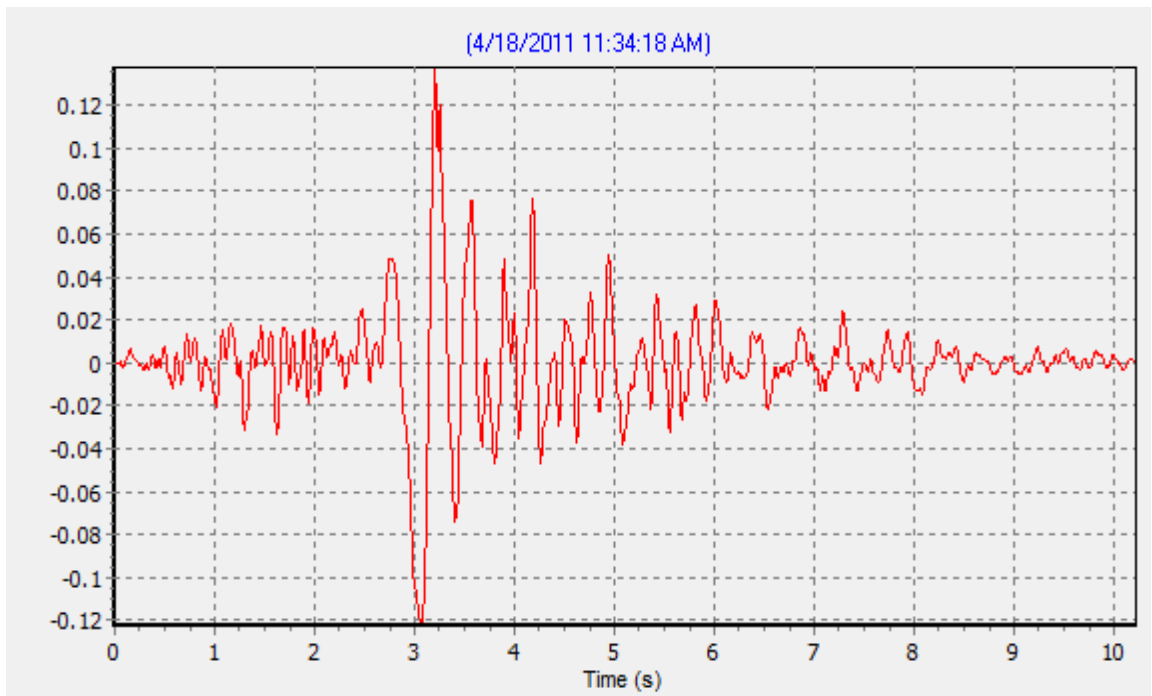


**Figure 1.2:** Effective Stress Contours for the Analysis

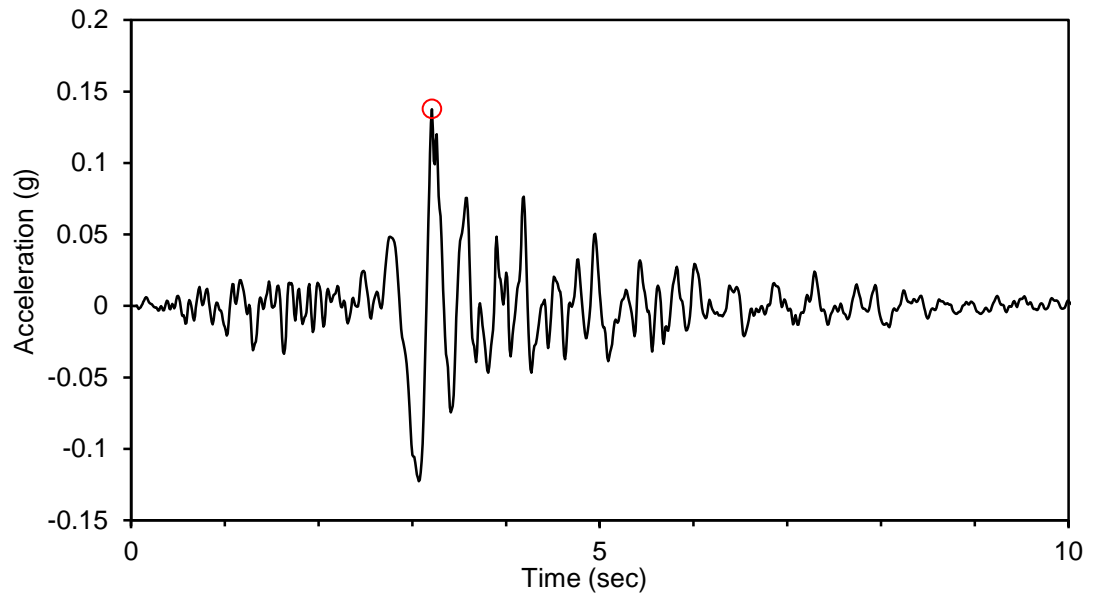


**Figure 1.3:** Plastic Points Contours

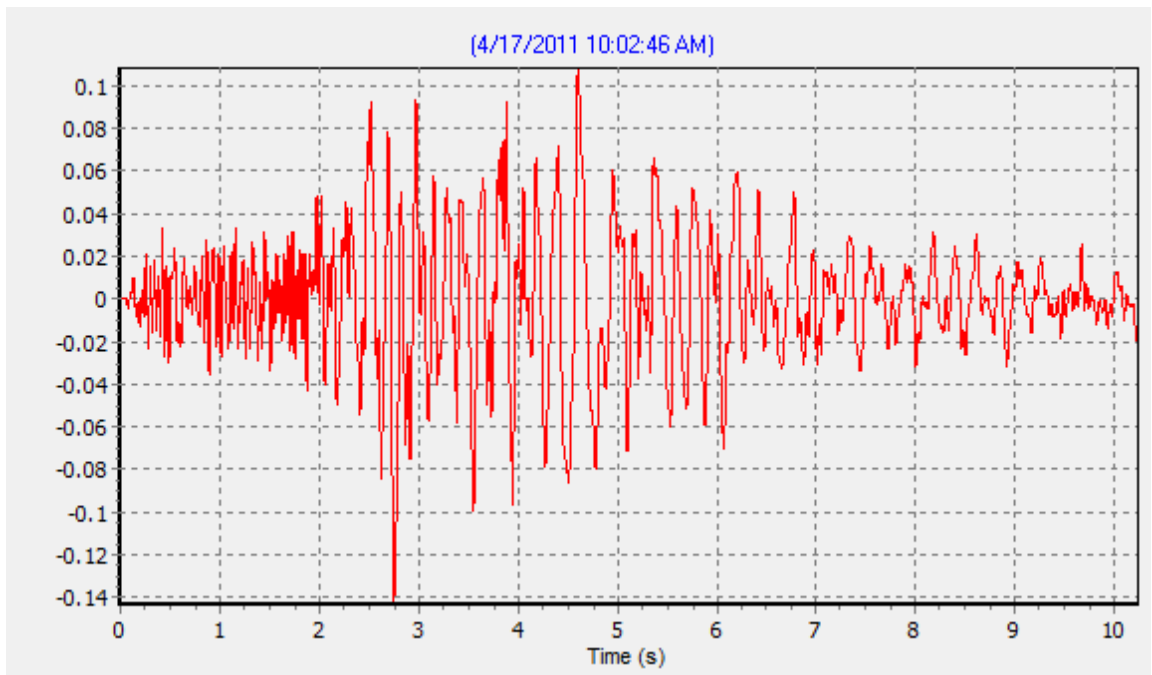
## APPENDIX-2



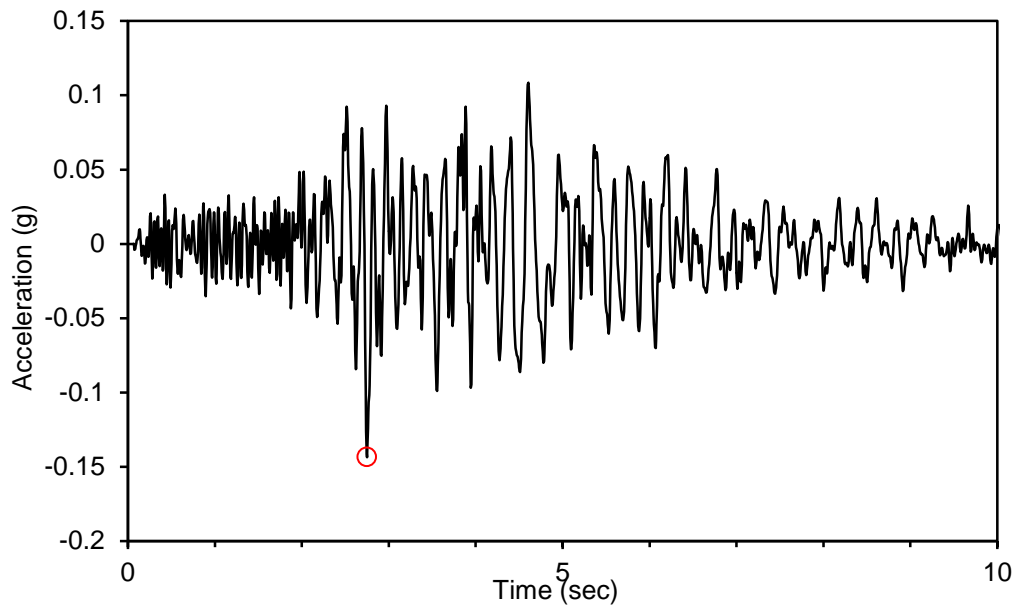
**Figure 2.1:** Dynamic Loading Obtained from Plaxis (Agio Earthquake with  $a=0.12g$ )



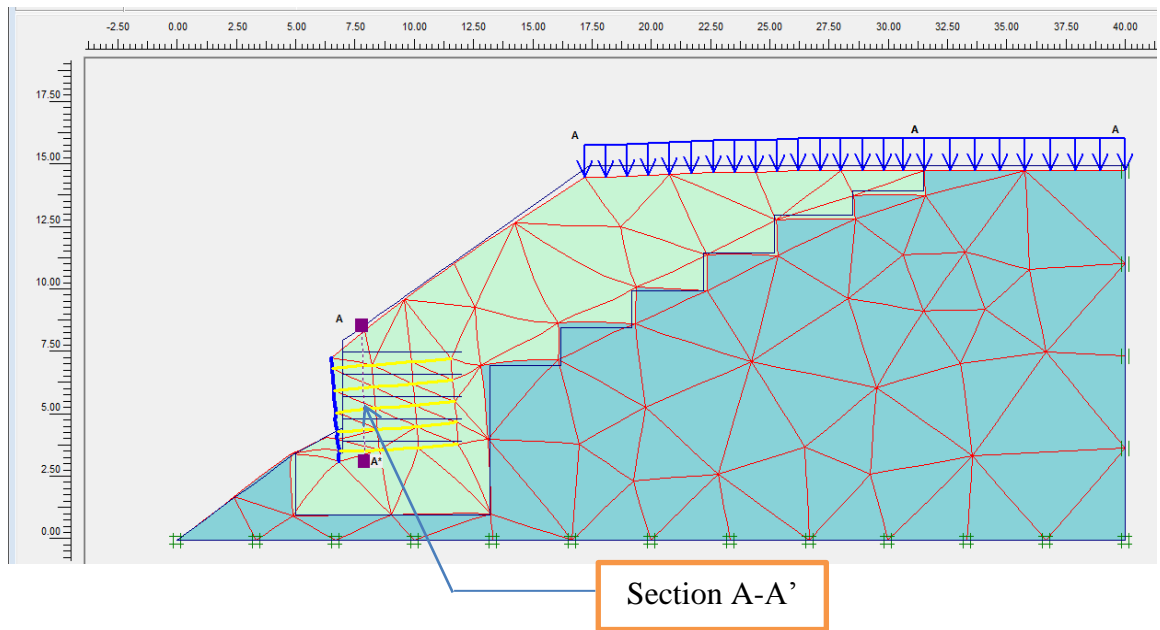
**Figure 2.2:** Dynamic Loading Obtained from EERA - Shake (Agio Earthquake with  $a=0.12g$ )



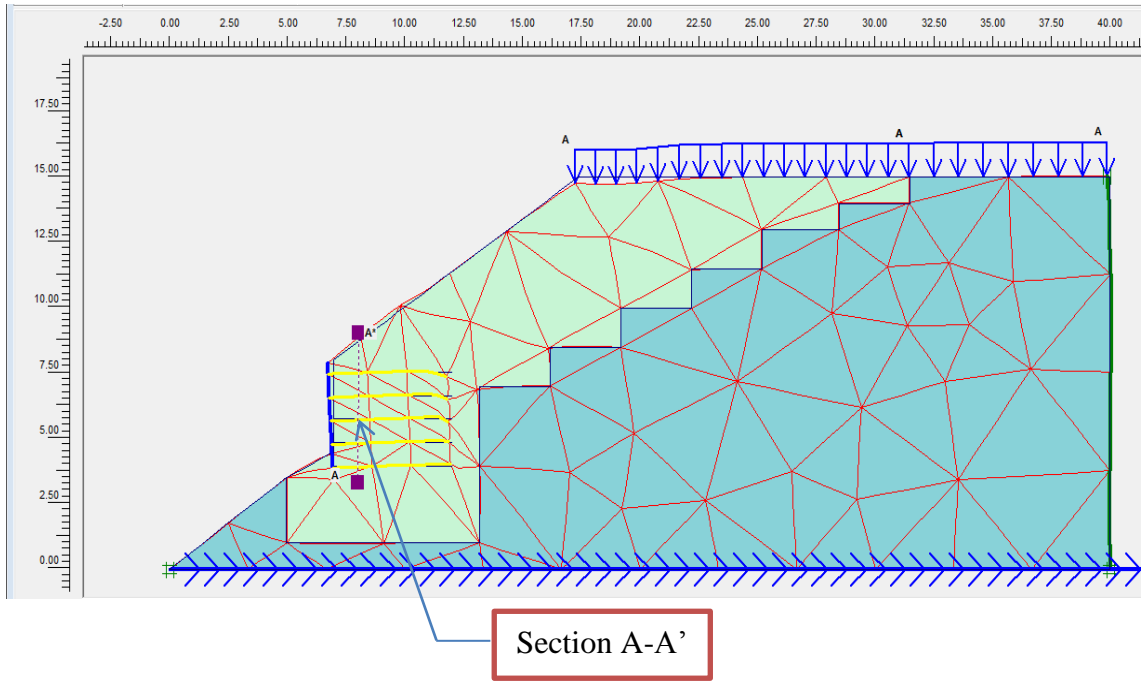
**Figure 2.3:** Dynamic loading obtained from Plaxis (Sepolia Earthquake with  $a=0.12g$ )



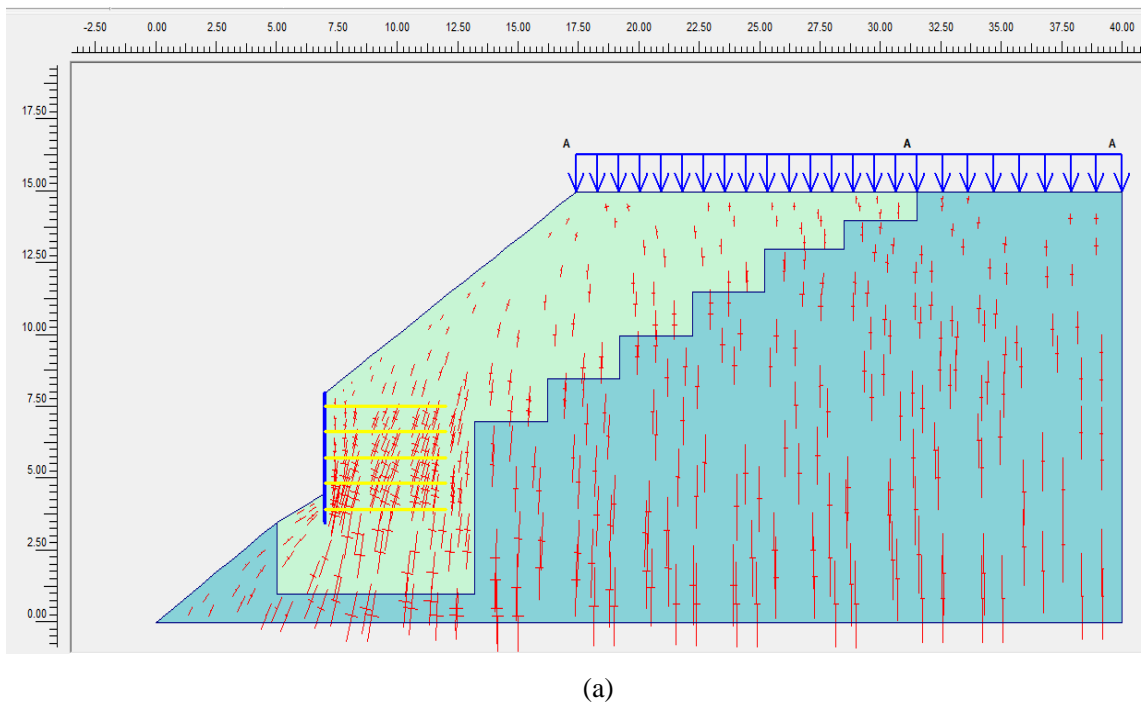
**Figure 2.4:** Dynamic loading obtained from EERA - Shake (Sepolia Earthquake with  $a=0.12g$ )

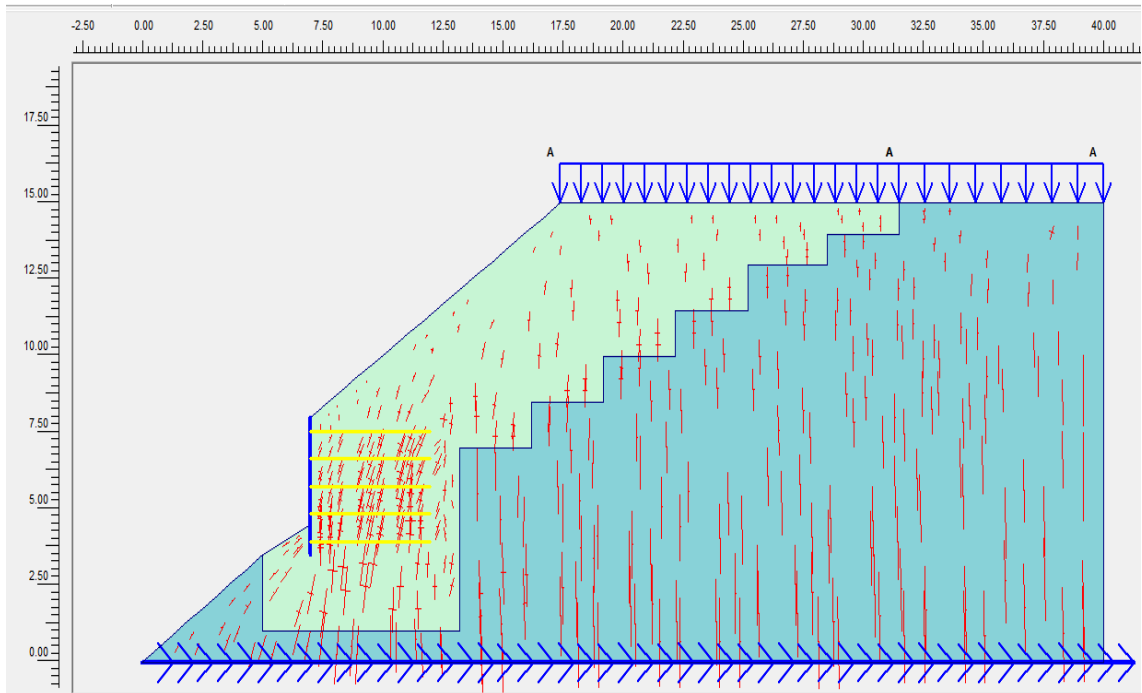


**Figure 2.5:** Deformed Mesh for the Final Excavation (Static Analysis)



**Figure 2.6:** Deformed Mesh for the Final Excavation (Dynamic Analysis)





(b)

Figure 2.7a & b: Effective Stress Contours

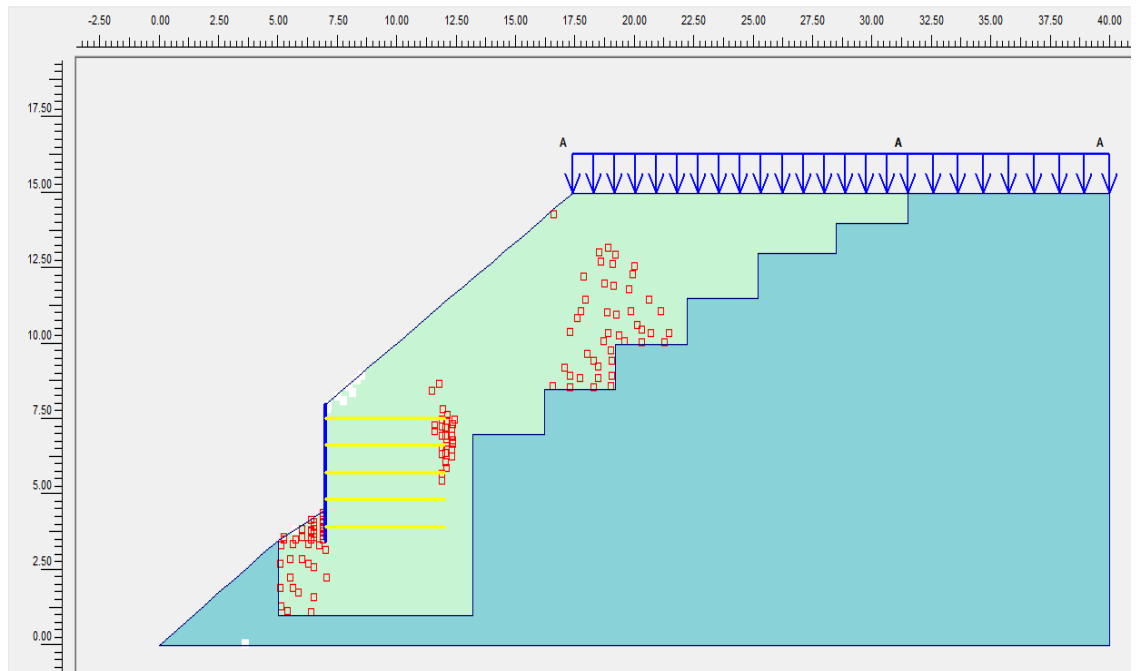


Figure 2.8: Plastic Points Contours



Table 2.1: Detailed Values of Displacements of the Wall Section 1

<b>Node No.</b>	<b>x-coord.</b>	<b>y-coord.</b>	<b>dUx</b> [10 <sup>-3</sup> m]	<b>Ux</b> [10 <sup>-3</sup> m]	<b>dUy</b> [10 <sup>-3</sup> m]	<b>Uy</b> [10 <sup>-3</sup> m]
1	1.875	1.313	3.769	-4.663	4.289	-38.687
2	1.250	0.875	2.063	-4.596	1.483	-20.739
3	0.625	0.438	61.097	-9.435	366.084	-62.328
4	0.000	0.000	0.000	0.000	0.000	0.000
5	0.833	0.000	0.000	0.000	0.000	0.000
6	1.667	0.000	0.000	0.000	0.000	0.000
7	2.500	0.000	0.000	0.000	0.000	0.000
17	4.375	3.063	36.725	3.027	60.371	-7.426
18	3.750	2.625	16.931	8.572	40.362	-3.461
19	3.125	2.188	7.928	-6.828	22.188	-1.511
26	2.500	1.750	5.551	-9.307	10.371	-72.917
27	5.000	1.625	6.969	-3.461	41.169	-8.352
28	5.000	2.250	23.943	-1.945	55.989	-11.264
29	5.000	2.875	47.889	1.167	69.624	-13.170
36	4.167	0.000	0.000	0.000	0.000	0.000
37	5.000	0.000	0.000	0.000	0.000	0.000
38	5.833	0.000	0.000	0.000	0.000	0.000
42	3.333	0.000	0.000	0.000	0.000	0.000
49	6.500	4.250	294.211	6.702	112.155	-26.474
50	6.000	4.000	151.751	5.249	161.880	-20.213
51	5.500	3.750	80.233	4.535	126.017	-16.948
55	5.000	3.500	63.316	6.409	81.950	-14.061
59	7.000	4.088	335.001	3.662	-9.642	-34.287
60	7.000	4.225	350.953	3.987	-9.630	-35.549
61	7.000	4.363	366.912	4.335	-9.620	-37.069
65	7.000	3.950	319.057	3.417	-9.650	-33.077
66	7.000	3.613	279.784	2.167	-9.674	-30.455
67	7.000	3.725	292.867	2.522	-9.668	-31.314
68	7.000	3.838	305.958	2.929	-9.660	-32.187
69	8.250	3.950	85.831	6.270	-183.647	-33.976
70	7.833	3.950	166.430	1.635	-126.311	-34.491
71	7.417	3.950	251.331	2.624	-67.271	-34.482
81	7.000	4.500	382.879	4.735	-9.613	-39.022
82	7.000	4.763	413.361	1.746	-9.596	-44.083
83	7.000	4.675	403.201	2.602	-9.601	-42.704

<b>Node No.</b>	<b>x-coord.</b>	<b>y-coord.</b>	<b>dUx</b> [10 <sup>-3</sup> m]	<b>Ux</b> [10 <sup>-3</sup> m]	<b>dUy</b> [10 <sup>-3</sup> m]	<b>Uy</b> [10 <sup>-3</sup> m]
84	7.000	4.588	393.040	3.574	-9.607	-41.044
91	8.250	4.850	237.778	-1.132	-173.912	-40.929
92	7.833	4.850	324.431	-7.634	-110.917	-41.916
93	7.417	4.850	395.968	16.435	-55.753	-42.957
94	7.000	4.850	423.519	17.468	-9.590	-45.246
95	7.000	5.525	501.583	-3.863	-9.548	-51.411
96	7.000	5.300	475.567	-2.437	-9.562	-49.688
97	7.000	5.075	449.546	-17.291	-9.576	-47.669
107	7.000	5.750	527.597	-5.123	-9.535	-52.916
108	8.250	5.750	433.911	-5.503	-163.372	-46.789
109	7.833	5.750	474.869	-5.296	-100.976	-48.403
110	7.417	5.750	505.338	-5.181	-50.786	-50.380
111	7.000	6.425	605.534	-8.883	-9.500	-56.361
112	7.000	6.200	579.554	-7.703	-9.511	-55.383
113	7.000	5.975	553.576	-6.449	-9.523	-54.240
123	7.000	6.650	631.516	-9.985	-9.489	-57.194
124	8.250	6.650	590.159	-10.061	-156.823	-51.296
125	7.833	6.650	601.758	-10.039	-95.463	-53.024
126	7.417	6.650	613.487	-10.018	-46.871	-54.970
127	7.000	7.325	709.453	-12.905	-9.465	-58.883
128	7.000	7.100	683.473	-12.031	-9.472	-58.437
129	7.000	6.875	657.493	-11.057	-9.480	-57.883
139	5.000	1.000	7.400	-3.447	22.697	-4.160
140	8.075	1.000	-36.773	-2.707	-60.415	27.672
141	7.050	1.000	-16.944	-4.468	-20.563	-2.029
142	6.025	1.000	-1.278	-4.643	8.636	-3.573
149	7.000	3.500	266.708	1.845	-9.678	-29.605
159	6.667	0.000	0.000	0.000	0.000	0.000
163	7.500	0.000	0.000	0.000	0.000	0.000
164	8.333	0.000	0.000	0.000	0.000	0.000
165	9.167	0.000	0.000	0.000	0.000	0.000
181	8.667	3.950	22.599	-16.360	-240.387	-33.174
182	9.917	3.950	-103.337	-1.895	-429.359	-29.648
183	9.500	3.950	-69.166	-1.446	-362.144	-30.996
184	9.083	3.950	-27.985	-8.966	-299.425	-32.175
191	8.667	4.850	163.324	-2.018	-244.173	-39.808
192	9.917	4.850	11.613	-4.001	-485.871	-35.693

<b>Node No.</b>	<b>x-coord.</b>	<b>y-coord.</b>	<b>dUx [10<sup>-3</sup> m]</b>	<b>Ux [10<sup>-3</sup> m]</b>	<b>dUy [10<sup>-3</sup> m]</b>	<b>Uy [10<sup>-3</sup> m]</b>
193	9.500	4.850	53.576	-3.447	-400.055	-37.234
194	9.083	4.850	103.318	-2.789	-319.474	-38.597
207	8.667	5.750	381.894	-5.815	-237.994	-45.338
211	9.083	5.750	325.705	-6.193	-323.188	-43.874
212	9.500	5.750	269.462	-6.608	-417.223	-42.310
213	9.917	5.750	215.911	-7.031	-519.253	-40.585
229	8.667	6.650	571.425	-10.109	-231.550	-49.676
233	9.083	6.650	542.574	-10.221	-319.742	-48.040
234	9.500	6.650	504.938	-10.414	-420.677	-46.318
235	9.917	6.650	463.130	-10.672	-534.034	-44.451
239	7.000	7.550	735.435	-13.684	-9.461	-59.245
240	8.250	7.550	734.142	-13.663	-143.871	-54.116
241	7.833	7.550	734.957	-13.663	-78.809	-55.709
242	7.417	7.550	735.410	-13.674	-29.710	-57.398
243	7.000	7.888	774.411	-14.942	-9.457	-59.552
244	7.000	7.775	761.418	-14.544	-9.458	-59.494
245	7.000	7.663	748.426	-14.123	-9.459	-59.393
255	7.000	8.000	787.406	-15.311	-9.456	-59.570
259	8.071	8.721	1.022	-17.510	-80.759	-56.013
260	7.714	8.480	925.014	-16.874	-30.191	-57.025
261	7.357	8.240	834.551	-16.218	2.336	-58.149
271	9.100	1.000	-58.467	-1.050	-100.359	-26.305
275	12.175	1.000	-130.209	1.224	-242.184	5.369
276	11.150	1.000	-107.388	-8.730	-187.683	2.537
277	10.125	1.000	-82.718	-6.900	-141.202	75.440
281	10.000	0.000	0.000	0.000	0.000	0.000
285	10.833	0.000	0.000	0.000	0.000	0.000
286	11.667	0.000	0.000	0.000	0.000	0.000
287	12.500	0.000	0.000	0.000	0.000	0.000
297	10.333	3.950	-132.587	-2.249	-501.434	-28.131
301	11.583	3.950	-198.189	-2.864	-747.917	-22.289
302	11.167	3.950	-179.344	-2.719	-660.799	-24.472
303	10.750	3.950	-157.326	-2.515	-578.723	-26.395
313	10.333	4.850	-24.827	-4.464	-577.254	-33.942
317	11.583	4.850	-111.013	-5.413	-887.153	-27.064
318	11.167	4.850	-85.569	-5.164	-777.778	-29.674
319	10.750	4.850	-56.811	-4.848	-674.456	-31.948

<b>Node No.</b>	<b>x-coord.</b>	<b>y-coord.</b>	<b>dUx [10<sup>-3</sup> m]</b>	<b>Ux [10<sup>-3</sup> m]</b>	<b>dUy [10<sup>-3</sup> m]</b>	<b>Uy [10<sup>-3</sup> m]</b>
329	10.333	5.750	167.123	-7.439	-629.064	-38.646
333	11.583	5.750	49.471	-8.459	-1.005	-30.983
334	11.167	5.750	84.159	-8.164	-871.944	-33.915
335	10.750	5.750	123.491	-7.819	-746.574	-36.443
345	10.333	6.650	420.725	-10.973	-659.200	-42.382
346	11.583	6.650	303.124	-11.915	-1.100	-34.290
347	11.167	6.650	339.350	-11.620	-942.555	-37.393
348	10.750	6.650	378.982	-11.296	-795.421	-40.055
361	9.917	7.550	723.999	-14.041	-545.273	-47.235
362	9.500	7.550	729.288	-13.877	-423.455	-49.133
363	9.083	7.550	731.497	-13.760	-316.173	-50.888
367	8.667	7.550	732.933	-13.691	-223.371	-52.534
371	8.428	8.961	1.119	-17.170	-139.165	-54.982
375	9.701	9.818	1.557	-17.815	-446.425	-50.450
376	9.276	9.532	1.397	-17.464	-325.518	-52.124
377	8.852	9.247	1.251	-16.888	-223.430	-53.635
381	10.333	7.550	712.898	-14.251	-681.499	-45.153
385	10.750	7.550	694.911	-14.503	-831.700	-42.844
386	11.167	7.550	672.596	-14.778	-995.851	-40.228
387	11.583	7.550	647.679	-15.047	-1.174	-37.221
391	13.333	0.000	0.000	0.000	0.000	0.000
395	14.167	0.000	0.000	0.000	0.000	0.000
396	15.000	0.000	0.000	0.000	0.000	0.000
397	15.833	0.000	0.000	0.000	0.000	0.000
407	13.200	1.000	-149.602	2.608	-305.014	-201.407
408	13.200	3.250	-267.071	-2.043	-952.676	-9.150
409	13.200	2.500	-260.936	1.543	-742.827	-7.120
410	13.200	1.750	-221.651	2.685	-526.943	-4.330
417	12.000	3.950	-212.997	-2.955	-840.531	-19.789
427	12.000	4.850	-131.860	-5.586	-1.002	-24.031
443	12.000	5.750	21.068	-8.680	-1.147	-27.536
453	12.000	6.650	273.240	-12.143	-1.269	-30.613
469	12.000	7.550	622.722	-15.276	-1.364	-33.735
479	10.125	10.104	1.733	-17.860	-587.264	-48.661
483	11.639	11.123	2.484	-17.051	-1.276	-42.762
484	11.135	10.783	2.211	-16.480	-1.012	-44.492
485	10.630	10.443	1.961	-16.436	-782.961	-46.506

<b>Node No.</b>	<b>x-coord.</b>	<b>y-coord.</b>	<b>dUx [10<sup>-3</sup> m]</b>	<b>Ux [10<sup>-3</sup> m]</b>	<b>dUy [10<sup>-3</sup> m]</b>	<b>Uy [10<sup>-3</sup> m]</b>
495	13.200	4.750	-163.188	-5.394	-1.353	-12.036
496	13.200	5.500	-41.326	-9.093	-1.540	-12.961
497	13.200	6.250	132.874	-13.435	-1.714	-13.541
501	13.200	4.000	-236.450	-2.501	-1.156	-10.802
517	13.200	7.000	359.925	-17.305	-1.872	-13.770
518	15.450	7.000	268.992	-8.314	-3.137	23.561
519	14.700	7.000	296.093	-15.435	-2.688	-3.744
520	13.950	7.000	327.878	-16.132	-2.265	-8.725
527	12.144	11.462	2.779	-17.971	-1.581	-41.413
531	13.945	12.674	4.040	-7.393	-3.057	-39.939
532	13.344	12.270	3.581	-10.164	-2.488	-39.862
533	12.744	11.866	3.162	-12.809	-2.000	-40.353
553	16.667	0.000	0.000	0.000	0.000	0.000
554	17.500	0.000	0.000	0.000	0.000	0.000
555	18.333	0.000	0.000	0.000	0.000	0.000
556	19.167	0.000	0.000	0.000	0.000	0.000
569	20.000	0.000	0.000	0.000	0.000	0.000
573	20.833	0.000	0.000	0.000	0.000	0.000
574	21.667	0.000	0.000	0.000	0.000	0.000
575	22.500	0.000	0.000	0.000	0.000	0.000
605	16.200	7.375	386.451	1.805	-3.787	17.910
606	16.200	7.750	518.662	2.189	-3.969	-21.379
607	16.200	8.125	664.228	2.377	-4.150	-34.963
611	16.200	7.000	265.799	1.223	-3.602	38.743
627	16.200	8.500	824.818	2.356	-4.327	-27.791
628	18.450	8.500	829.533	10.781	-6.167	-2.128
629	17.700	8.500	815.201	6.972	-5.561	-97.919
630	16.950	8.500	815.214	3.686	-4.942	65.506
643	14.545	13.078	4.545	-4.520	-3.721	-40.623
644	16.686	14.520	6.881	3.432	-7.237	-47.493
645	15.972	14.039	5.966	1.111	-5.772	-44.600
646	15.259	13.559	5.202	-1.574	-4.658	-42.389
669	19.200	8.875	1.012	12.035	-7.072	-8.037
670	19.200	9.250	1.193	12.822	-7.402	-8.855
671	19.200	9.625	1.389	13.672	-7.737	-9.416
675	19.200	8.500	845.790	11.301	-6.747	-6.750
685	17.400	15.000	8.053	5.399	-9.479	-51.507

<b>Node No.</b>	<b>x-coord.</b>	<b>y-coord.</b>	<b>dUx</b> [10 <sup>-3</sup> m]	<b>Ux</b> [10 <sup>-3</sup> m]	<b>dUy</b> [10 <sup>-3</sup> m]	<b>Uy</b> [10 <sup>-3</sup> m]
689	20.044	15.000	6.134	3.673	-14.558	-53.789
690	19.163	15.000	6.751	3.669	-13.456	-54.575
691	18.281	15.000	7.452	4.304	-11.964	-54.431
701	19.200	10.000	1.601	14.641	-8.077	-9.801
702	21.450	10.000	1.602	15.736	-9.873	-16.800
703	20.700	10.000	1.607	15.756	-9.343	-13.947
704	19.950	10.000	1.606	15.563	-8.744	-11.617
721	23.333	0.000	0.000	0.000	0.000	0.000
725	24.167	0.000	0.000	0.000	0.000	0.000
726	25.000	0.000	0.000	0.000	0.000	0.000
727	25.833	0.000	0.000	0.000	0.000	0.000
753	26.667	0.000	0.000	0.000	0.000	0.000
754	27.500	0.000	0.000	0.000	0.000	0.000
755	28.333	0.000	0.000	0.000	0.000	0.000
756	29.167	0.000	0.000	0.000	0.000	0.000
785	22.200	10.000	1.590	14.416	-10.336	-21.154
786	22.200	10.375	1.785	14.242	-10.772	-23.534
787	22.200	10.750	1.991	14.370	-11.213	-25.095
788	22.200	11.125	2.208	14.606	-11.659	-26.230
801	22.200	11.500	2.435	14.924	-12.109	-27.165
802	24.450	11.500	2.147	14.838	-13.226	-29.318
803	23.700	11.500	2.252	15.443	-12.913	-27.808
804	22.950	11.500	2.349	17.970	-12.544	-27.017
811	20.925	15.000	5.585	4.005	-15.446	-52.737
815	23.569	15.000	4.160	4.622	-17.193	-49.845
816	22.688	15.000	4.596	4.708	-16.725	-50.563
817	21.806	15.000	5.070	4.402	-16.152	-51.575
843	25.200	11.500	2.039	12.626	-13.490	-32.568
844	25.200	11.875	2.197	10.937	-13.957	-35.406
845	25.200	12.250	2.356	9.555	-14.424	-37.325
846	25.200	12.625	2.515	8.194	-14.892	-38.758
859	24.450	15.000	3.759	3.898	-17.576	-49.165
863	27.094	15.000	2.731	5.759	-18.352	-44.708
864	26.213	15.000	3.046	1.216	-18.145	-46.265
865	25.331	15.000	3.388	2.519	-17.890	-47.988
885	30.000	0.000	0.000	0.000	0.000	0.000
889	30.833	0.000	0.000	0.000	0.000	0.000

<b>Node No.</b>	<b>x-coord.</b>	<b>y-coord.</b>	<b>dUx [10<sup>-3</sup> m]</b>	<b>Ux [10<sup>-3</sup> m]</b>	<b>dUy [10<sup>-3</sup> m]</b>	<b>Uy [10<sup>-3</sup> m]</b>
890	31.667	0.000	0.000	0.000	0.000	0.000
891	32.500	0.000	0.000	0.000	0.000	0.000
911	33.333	0.000	0.000	0.000	0.000	0.000
915	34.167	0.000	0.000	0.000	0.000	0.000
916	35.000	0.000	0.000	0.000	0.000	0.000
917	35.833	0.000	0.000	0.000	0.000	0.000
943	27.675	13.000	2.079	8.046	-15.977	-34.966
944	26.850	13.000	2.269	8.243	-15.811	-35.471
945	26.025	13.000	2.468	8.324	-15.607	-36.813
949	25.200	13.000	2.672	6.792	-15.360	-39.946
965	36.667	0.000	0.000	0.000	0.000	0.000
969	37.500	0.000	0.000	0.000	0.000	0.000
970	38.333	0.000	0.000	0.000	0.000	0.000
971	39.167	0.000	0.000	0.000	0.000	0.000
972	40.000	0.000	0.000	0.000	0.000	0.000
973	40.000	0.938	0.000	0.000	-1.221	-2.613
974	40.000	1.875	0.000	0.000	-2.440	-5.195
975	40.000	2.813	0.000	0.000	-3.658	-7.750
1005	28.500	13.250	1.960	5.501	-16.424	-37.455
1006	28.500	13.500	2.016	3.862	-16.735	-38.580
1007	28.500	13.750	2.069	2.206	-17.047	-39.452
1011	28.500	13.000	1.902	7.097	-16.113	-35.913
1024	27.975	15.000	2.439	4.384	-18.519	-43.649
1025	30.619	15.000	1.729	2.398	-18.861	-41.058
1026	29.738	15.000	1.960	2.800	-18.770	-40.600
1027	28.856	15.000	2.200	1.229	-18.656	-41.888
1031	28.500	14.000	2.120	9.284	-17.359	-40.180
1032	30.750	14.000	1.588	5.451	-17.628	-36.705
1033	30.000	14.000	1.760	5.250	-17.555	-36.639
1034	29.250	14.000	1.941	4.308	-17.466	-37.208
1083	40.000	3.750	0.000	0.000	-4.873	-10.278
1087	40.000	4.688	0.000	0.000	-6.086	-12.783
1088	40.000	5.625	0.000	0.000	-7.295	-15.262
1089	40.000	6.563	0.000	0.000	-8.500	-17.718
1093	31.500	15.000	1.527	-1.454	-18.932	-40.971
1094	31.500	14.250	1.457	3.513	-17.997	-38.642
1095	31.500	14.500	1.483	2.040	-18.309	-39.574

<b>Node No.</b>	<b>x-coord.</b>	<b>y-coord.</b>	<b>dUx</b> [10 <sup>-3</sup> m]	<b>Ux</b> [10 <sup>-3</sup> m]	<b>dUy</b> [10 <sup>-3</sup> m]	<b>Uy</b> [10 <sup>-3</sup> m]
1096	31.500	14.750	1.506	8.694	-18.620	-40.335
1097	31.500	14.000	1.430	4.703	-17.686	-37.481
1112	40.000	7.500	0.000	0.000	-9.701	-20.151
1117	35.750	15.000	677.998	2.225	-19.108	-39.114
1118	34.688	15.000	867.205	2.726	-19.081	-39.052
1119	33.625	15.000	1.067	3.411	-19.049	-39.281
1120	32.563	15.000	1.286	3.842	-18.999	-38.988
1139	40.000	11.250	0.000	0.000	-14.457	-29.684
1146	40.000	9.375	0.000	0.000	-12.089	-24.952
1147	40.000	10.313	0.000	0.000	-13.275	-27.326
1151	40.000	8.438	0.000	0.000	-10.898	-22.562
1159	40.000	15.000	0.000	0.000	-19.145	-39.040
1161	40.000	13.125	0.000	0.000	-16.806	-34.373
1162	38.938	15.000	163.230	5.153	-19.143	-39.044
1163	40.000	14.063	0.000	0.000	-17.976	-36.707
1164	36.813	15.000	499.698	1.646	-19.125	-39.079
1166	37.875	15.000	328.948	1.089	-19.136	-39.057

Table 2.2: Detailed Values of the Axial Force at Various Levels in the Wall Section I

<b>Node no.</b>	<b>x-coord.</b> [m]	<b>y-coord.</b> [m]	<b>Nx</b> [kN/m]
107	7.000	5.750	0.000
110	7.417	5.750	11.205
109	7.833	5.750	26.557
108	8.250	5.750	22.025
207	8.667	5.750	18.609
207	8.667	5.750	18.344
211	9.083	5.750	16.985
212	9.500	5.750	16.154
213	9.917	5.750	15.832
329	10.333	5.750	16.048
329	10.333	5.750	15.393
335	10.750	5.750	16.573
334	11.167	5.750	15.970



<b>Node no.</b>	<b>x-coord.</b> [m]	<b>y-coord.</b> [m]	<b>Nx</b> [kN/m]
333	11.583	5.750	12.279
443	12.000	5.750	4.122
<b>Max:</b>			26.557
<b>Min:</b>			0.000

Table 2.3: Detailed Values of the Bending Moments for the Wall Section 1

<b>Node no.</b>	<b>x-coord.</b> [m]	<b>y-coord.</b> [m]	<b>N</b> [kN/m]	<b>Q</b> [kN/m]	<b>M</b> [kNm/m]
255	7.000	8.000	0.231	0.482	0.000
243	7.000	7.888	-0.682	0.823	0.075
244	7.000	7.775	-1.445	0.997	0.179
245	7.000	7.663	-2.050	1.038	0.295
239	7.000	7.550	-2.489	0.977	0.309
239	7.000	7.550	-2.983	-8.777	0.409
127	7.000	7.325	-4.076	-7.937	-1.467
128	7.000	7.100	-5.569	-7.342	-3.181
129	7.000	6.875	-7.044	-7.016	-4.792
123	7.000	6.650	-8.083	-6.987	-6.361
123	7.000	6.650	-8.677	-3.962	-9.352
111	7.000	6.425	-10.509	-2.972	-12.138
112	7.000	6.200	-12.004	-2.128	-15.709
113	7.000	5.975	-13.212	-1.426	-18.106
107	7.000	5.750	-14.179	-0.862	-21.361
107	7.000	5.750	-14.706	-0.492	-24.361
95	7.000	5.525	-16.068	1.263	-21.255
96	7.000	5.300	-17.015	2.261	-18.854
97	7.000	5.075	-17.824	2.800	-15.671
94	7.000	4.850	-18.770	3.176	-14.513
94	7.000	4.850	-19.191	3.603	-13.602
82	7.000	4.763	-19.302	4.298	-12.857
83	7.000	4.675	-19.272	4.753	-12.426
84	7.000	4.588	-19.287	5.077	-10.353
81	7.000	4.500	-19.535	5.380	-8.969
81	7.000	4.500	-18.827	5.244	-7.534

<b>Node no.</b>	<b>x-coord. [m]</b>	<b>y-coord. [m]</b>	<b>N [kN/m]</b>	<b>Q [kN/m]</b>	<b>M [kNm/m]</b>
61	7.000	4.363	-20.065	5.703	-6.225
60	7.000	4.225	-20.871	6.479	-5.383
59	7.000	4.088	-21.341	7.171	-3.447
65	7.000	3.950	-21.569	7.378	-2.436
65	7.000	3.950	-21.435	2.186	-1.436
68	7.000	3.838	-21.570	2.504	-1.185
67	7.000	3.725	-22.182	3.356	-0.848
66	7.000	3.613	-22.448	3.961	-0.439
149	7.000	3.500	-21.548	3.541	0.000
<b>Max:</b>			0.231	7.378	0.409
<b>Min:</b>			-22.448	-8.777	-24.361

Table 2.4: Detailed Values of the Displacements

<b>Node No.</b>	<b>x-coord.</b>	<b>y-coord.</b>	<b>dUx [10<sup>-3</sup> m]</b>	<b>Ux [10<sup>-3</sup> m]</b>	<b>dUy [10<sup>-3</sup> m]</b>	<b>Uy [10<sup>-3</sup> m]</b>
1	1.875	1.313	-249.845	-6.603	-44.431	-9.901
2	1.250	0.875	-133.130	-3.499	-23.888	-6.882
3	0.625	0.438	-45.903	-1.176	-7.816	-22.396
4	0.000	0.000	0.000	0.000	0.000	0.000
5	0.833	0.000	0.000	0.000	0.000	0.000
6	1.667	0.000	0.000	0.000	0.000	0.000
7	2.500	0.000	0.000	0.000	0.000	0.000
17	4.375	3.063	-899.838	-17.159	-155.097	-4.730
18	3.750	2.625	-719.234	-15.967	-122.693	-2.262
19	3.125	2.188	-546.570	-13.459	-93.344	-1.392
26	2.500	1.750	-389.152	-10.129	-67.447	-1.180
27	5.000	1.625	-560.365	-15.223	-144.224	-6.038
28	5.000	2.250	-752.096	-17.753	-175.500	-8.119
29	5.000	2.875	-928.187	-18.517	-189.948	-9.271
36	4.167	0.000	0.000	0.000	0.000	0.000
37	5.000	0.000	0.000	0.000	0.000	0.000
38	5.833	0.000	0.000	0.000	0.000	0.000
42	3.333	0.000	0.000	0.000	0.000	0.000
49	6.500	4.250	-1.534	-14.736	-374.916	-19.487
50	6.000	4.000	-1.359	-15.611	-279.524	-14.477

Node No.	x-coord.	y-coord.	dUx [10 <sup>-3</sup> m]	Ux [10 <sup>-3</sup> m]	dUy [10 <sup>-3</sup> m]	Uy [10 <sup>-3</sup> m]
51	5.500	3.750	-1.199	-16.597	-230.617	-11.506
55	5.000	3.500	-1.076	-16.956	-188.048	-9.559
59	7.000	4.088	-1.610	-16.277	-548.448	-27.422
60	7.000	4.225	-1.672	-16.141	-548.479	-28.399
61	7.000	4.363	-1.733	-15.978	-548.514	-29.530
65	7.000	3.950	-1.549	-16.379	-548.419	-26.503
66	7.000	3.613	-1.399	-16.409	-548.360	-24.274
67	7.000	3.725	-1.449	-16.440	-548.378	-25.020
68	7.000	3.838	-1.499	-16.433	-548.398	-25.763
69	8.250	3.950	-1.698	-13.368	-370.989	-26.554
70	7.833	3.950	-1.649	-14.352	-403.033	-27.228
71	7.417	3.950	-1.601	-15.449	-460.088	-27.438
81	7.000	4.500	-1.794	-15.705	-548.558	-30.908
82	7.000	4.763	-1.912	-18.053	-548.633	-34.862
83	7.000	4.675	-1.873	-17.520	-548.609	-33.705
84	7.000	4.588	-1.834	-16.802	-548.584	-32.393
91	8.250	4.850	-2.082	-16.015	-393.420	-32.904
92	7.833	4.850	-2.039	-16.617	-423.694	-33.736
93	7.417	4.850	-1.996	-17.291	-475.529	-34.469
94	7.000	4.850	-1.951	-18.516	-548.656	-35.880
95	7.000	5.525	-2.251	-21.974	-548.809	-41.470
96	7.000	5.300	-2.151	-20.925	-548.763	-39.892
97	7.000	5.075	-2.051	-19.778	-548.712	-38.057
107	7.000	5.750	-2.352	-22.938	-548.849	-42.865
108	8.250	5.750	-2.439	-20.325	-406.409	-38.098
109	7.833	5.750	-2.411	-21.084	-428.102	-39.423
110	7.417	5.750	-2.381	-21.967	-473.603	-40.934
111	7.000	6.425	-2.652	-25.809	-548.945	-46.227
112	7.000	6.200	-2.552	-24.881	-548.918	-45.248
113	7.000	5.975	-2.452	-23.925	-548.886	-44.131
123	7.000	6.650	-2.752	-26.702	-548.969	-47.076
124	8.250	6.650	-2.735	-24.805	-427.133	-42.119
125	7.833	6.650	-2.733	-25.406	-434.362	-43.620
126	7.417	6.650	-2.736	-26.042	-465.326	-45.222
127	7.000	7.325	-3.052	-29.274	-549.022	-48.844
128	7.000	7.100	-2.952	-28.457	-549.008	-48.384
129	7.000	6.875	-2.852	-27.599	-548.990	-47.794

<b>Node No.</b>	<b>x-coord.</b>	<b>y-coord.</b>	<b>dUx</b> [10 <sup>-3</sup> m]	<b>Ux</b> [10 <sup>-3</sup> m]	<b>dUy</b> [10 <sup>-3</sup> m]	<b>Uy</b> [10 <sup>-3</sup> m]
139	5.000	1.000	-356.252	-11.037	-99.146	-2.861
140	8.075	1.000	-446.963	-9.621	-141.200	3.918
141	7.050	1.000	-417.517	-12.373	-140.394	7.677
142	6.025	1.000	-391.647	-12.925	-124.171	-1.433
149	7.000	3.500	-1.348	-16.352	-548.345	-23.523
159	6.667	0.000	0.000	0.000	0.000	0.000
163	7.500	0.000	0.000	0.000	0.000	0.000
164	8.333	0.000	0.000	0.000	0.000	0.000
165	9.167	0.000	0.000	0.000	0.000	0.000
181	8.667	3.950	-1.748	-12.389	-356.888	-25.633
182	9.917	3.950	-1.897	-9.333	-390.172	-21.702
183	9.500	3.950	-1.848	-10.360	-368.604	-23.211
184	9.083	3.950	-1.798	-11.387	-356.972	-24.520
191	8.667	4.850	-2.125	-15.360	-382.452	-31.816
192	9.917	4.850	-2.254	-13.212	-434.018	-27.374
193	9.500	4.850	-2.211	-13.946	-404.873	-29.095
194	9.083	4.850	-2.168	-14.668	-387.075	-30.565
207	8.667	5.750	-2.467	-19.677	-403.651	-36.784
211	9.083	5.750	-2.497	-19.094	-415.189	-35.344
212	9.500	5.750	-2.529	-18.558	-439.416	-33.705
213	9.917	5.750	-2.563	-18.066	-475.218	-31.802
229	8.667	6.650	-2.743	-24.274	-431.507	-40.604
233	9.083	6.650	-2.757	-23.817	-447.525	-38.974
234	9.500	6.650	-2.777	-23.448	-475.269	-37.154
235	9.917	6.650	-2.802	-23.166	-515.076	-35.076
239	7.000	7.550	-3.152	-30.042	-549.033	-49.178
240	8.250	7.550	-2.900	-28.673	-457.371	-44.704
241	7.833	7.550	-2.912	-29.054	-450.278	-46.122
242	7.417	7.550	-2.995	-29.493	-446.665	-47.517
243	7.000	7.888	-3.302	-31.102	-549.041	-49.427
244	7.000	7.775	-3.252	-30.769	-549.039	-49.378
245	7.000	7.663	-3.202	-30.414	-549.037	-49.295
255	7.000	8.000	-3.352	-31.410	-549.041	-49.442
259	8.071	8.721	-2.979	-32.490	-468.890	-46.505
260	7.714	8.480	-2.978	-31.910	-452.399	-47.355
261	7.357	8.240	-3.068	-31.582	-433.234	-48.188
271	9.100	1.000	-488.219	-6.874	-139.910	3.396

<b>Node No.</b>	<b>x-coord.</b>	<b>y-coord.</b>	<b>dUx</b> [10 <sup>-3</sup> m]	<b>Ux</b> [10 <sup>-3</sup> m]	<b>dUy</b> [10 <sup>-3</sup> m]	<b>Uy</b> [10 <sup>-3</sup> m]
275	12.175	1.000	-641.165	-1.853	-198.869	9.380
276	11.150	1.000	-592.463	-4.530	-168.210	6.408
277	10.125	1.000	-539.892	-5.484	-147.782	4.808
281	10.000	0.000	0.000	0.000	0.000	0.000
285	10.833	0.000	0.000	0.000	0.000	0.000
286	11.667	0.000	0.000	0.000	0.000	0.000
287	12.500	0.000	0.000	0.000	0.000	0.000
297	10.333	3.950	-1.946	-8.330	-420.524	-19.976
301	11.583	3.950	-2.084	-5.643	-557.396	-12.838
302	11.167	3.950	-2.039	-6.412	-504.711	-15.587
303	10.750	3.950	-1.993	-7.311	-458.935	-17.931
313	10.333	4.850	-2.298	-12.487	-473.266	-25.353
317	11.583	4.850	-2.430	-10.598	-645.025	-16.751
318	11.167	4.850	-2.386	-11.150	-579.253	-20.131
319	10.750	4.850	-2.342	-11.792	-521.865	-22.967
329	10.333	5.750	-2.599	-17.618	-521.986	-29.570
333	11.583	5.750	-2.717	-16.582	-724.746	-20.016
334	11.167	5.750	-2.677	-16.871	-647.000	-23.792
335	10.750	5.750	-2.637	-17.218	-579.336	-26.933
345	10.333	6.650	-2.831	-22.973	-567.006	-32.675
346	11.583	6.650	-2.936	-22.932	-795.622	-22.660
347	11.167	6.650	-2.899	-22.856	-707.317	-26.579
348	10.750	6.650	-2.864	-22.869	-631.094	-29.873
361	9.917	7.550	-2.957	-27.697	-548.258	-37.267
362	9.500	7.550	-2.937	-27.824	-506.310	-39.474
363	9.083	7.550	-2.920	-28.038	-477.536	-41.419
367	8.667	7.550	-2.909	-28.329	-461.530	-43.148
371	8.428	8.961	-2.994	-33.198	-468.758	-45.487
375	9.701	9.818	-2.990	-35.318	-549.287	-40.215
376	9.276	9.532	-3.000	-34.778	-508.881	-42.266
377	8.852	9.247	-3.001	-34.035	-482.646	-44.029
381	10.333	7.550	-2.983	-27.660	-603.803	-34.752
385	10.750	7.550	-3.011	-27.708	-673.262	-31.871
386	11.167	7.550	-3.043	-27.842	-756.782	-28.549
387	11.583	7.550	-3.078	-28.049	-854.494	-24.686
391	13.333	0.000	0.000	0.000	0.000	0.000
395	14.167	0.000	0.000	0.000	0.000	0.000

Node No.	x-coord.	y-coord.	dUx [10 <sup>-3</sup> m]	Ux [10 <sup>-3</sup> m]	dUy [10 <sup>-3</sup> m]	Uy [10 <sup>-3</sup> m]
396	15.000	0.000	0.000	0.000	0.000	0.000
397	15.833	0.000	0.000	0.000	0.000	0.000
407	13.200	1.000	-683.152	2.018	-237.753	4.653
408	13.200	3.250	-1.928	-1.282	-693.827	3.252
409	13.200	2.500	-1.555	1.505	-551.369	3.407
410	13.200	1.750	-1.141	2.886	-400.006	3.827
417	12.000	3.950	-2.127	-5.043	-616.640	-9.592
427	12.000	4.850	-2.472	-10.183	-718.937	-12.709
443	12.000	5.750	-2.758	-16.358	-812.393	-15.434
453	12.000	6.650	-2.974	-23.086	-895.928	-17.927
469	12.000	7.550	-3.114	-28.301	-966.512	-20.155
479	10.125	10.104	-2.969	-35.541	-605.412	-37.952
483	11.639	11.123	-2.789	-32.996	-957.093	-30.024
484	11.135	10.783	-2.869	-34.415	-810.859	-32.433
485	10.630	10.443	-2.928	-35.285	-694.650	-35.136
495	13.200	4.750	-2.552	-9.730	-957.079	3.514
496	13.200	5.500	-2.798	-14.944	-1.079	3.888
497	13.200	6.250	-2.998	-20.784	-1.193	4.432
501	13.200	4.000	-2.261	-5.131	-828.824	3.257
517	13.200	7.000	-3.147	-27.126	-1.298	5.244
518	15.450	7.000	-3.292	-19.144	-2.251	18.510
519	14.700	7.000	-3.258	-25.246	-1.901	14.444
520	13.950	7.000	-3.208	-27.059	-1.582	9.831
527	12.144	11.462	-2.688	-31.139	-1.137	-28.037
531	13.945	12.674	-2.115	-22.774	-2.115	-24.597
532	13.344	12.270	-2.347	-25.783	-1.722	-25.133
533	12.744	11.866	-2.536	-28.585	-1.399	-26.272
553	16.667	0.000	0.000	0.000	0.000	0.000
554	17.500	0.000	0.000	0.000	0.000	0.000
555	18.333	0.000	0.000	0.000	0.000	0.000
556	19.167	0.000	0.000	0.000	0.000	0.000
569	20.000	0.000	0.000	0.000	0.000	0.000
573	20.833	0.000	0.000	0.000	0.000	0.000
574	21.667	0.000	0.000	0.000	0.000	0.000
575	22.500	0.000	0.000	0.000	0.000	0.000
605	16.200	7.375	-3.361	-7.936	-2.760	19.513
606	16.200	7.750	-3.403	-7.406	-2.895	19.818

<b>Node No.</b>	<b>x-coord.</b>	<b>y-coord.</b>	<b>dUx</b> [10 <sup>-3</sup> m]	<b>Ux</b> [10 <sup>-3</sup> m]	<b>dUy</b> [10 <sup>-3</sup> m]	<b>Uy</b> [10 <sup>-3</sup> m]
607	16.200	8.125	-3.431	-7.425	-3.029	20.172
611	16.200	7.000	-3.305	-9.101	-2.623	19.191
627	16.200	8.500	-3.445	-7.928	-3.162	20.700
628	18.450	8.500	-3.312	4.588	-4.694	18.843
629	17.700	8.500	-3.388	-2.622	-4.186	20.705
630	16.950	8.500	-3.431	-6.962	-3.670	20.583
643	14.545	13.078	-1.833	-19.530	-2.593	-24.498
644	16.686	14.520	-264.978	-11.022	-5.333	-29.566
645	15.972	14.039	-915.249	-13.504	-4.149	-27.481
646	15.259	13.559	-1.435	-16.388	-3.288	-25.964
669	19.200	8.875	-3.197	11.243	-5.445	12.217
670	19.200	9.250	-3.171	12.374	-5.714	11.881
671	19.200	9.625	-3.128	13.449	-5.988	11.773
675	19.200	8.500	-3.208	10.015	-5.180	12.853
685	17.400	15.000	712.092	-8.952	-7.205	-32.685
689	20.044	15.000	26.827	-6.238	-11.419	-31.747
690	19.163	15.000	251.067	-7.844	-10.533	-33.535
691	18.281	15.000	515.242	-8.790	-9.322	-34.512
701	19.200	10.000	-3.069	14.464	-6.268	11.855
702	21.450	10.000	-2.593	15.162	-7.751	2.645
703	20.700	10.000	-2.760	15.204	-7.322	5.854
704	19.950	10.000	-2.922	15.136	-6.826	8.976
721	23.333	0.000	0.000	0.000	0.000	0.000
725	24.167	0.000	0.000	0.000	0.000	0.000
726	25.000	0.000	0.000	0.000	0.000	0.000
727	25.833	0.000	0.000	0.000	0.000	0.000
753	26.667	0.000	0.000	0.000	0.000	0.000
754	27.500	0.000	0.000	0.000	0.000	0.000
755	28.333	0.000	0.000	0.000	0.000	0.000
756	29.167	0.000	0.000	0.000	0.000	0.000
785	22.200	10.000	-2.427	13.966	-8.116	-1.931
786	22.200	10.375	-2.344	13.708	-8.473	-3.556
787	22.200	10.750	-2.247	13.990	-8.832	-4.570
788	22.200	11.125	-2.136	14.404	-9.195	-5.221
801	22.200	11.500	-2.011	14.821	-9.559	-5.678
802	24.450	11.500	-1.642	15.410	-10.363	-8.847
803	23.700	11.500	-1.755	15.765	-10.148	-7.189

<b>Node No.</b>	<b>x-coord.</b>	<b>y-coord.</b>	<b>dUx [10<sup>-3</sup> m]</b>	<b>Ux [10<sup>-3</sup> m]</b>	<b>dUy [10<sup>-3</sup> m]</b>	<b>Uy [10<sup>-3</sup> m]</b>
804	22.950	11.500	-1.877	15.678	-9.883	-6.041
811	20.925	15.000	-144.099	-4.269	-12.106	-29.768
815	23.569	15.000	-530.222	7.180	-13.405	-25.180
816	22.688	15.000	-426.694	-5.672	-13.071	-26.298
817	21.806	15.000	-298.413	-2.300	-12.647	-27.890
843	25.200	11.500	-1.536	13.176	-10.536	-12.552
844	25.200	11.875	-1.449	11.172	-10.903	-14.656
845	25.200	12.250	-1.358	10.020	-11.268	-16.017
846	25.200	12.625	-1.263	9.021	-11.631	-16.945
859	24.450	15.000	-611.569	1.238	-13.669	-24.232
863	27.094	15.000	-741.237	3.702	-14.157	-20.289
864	26.213	15.000	-719.907	2.393	-14.036	-21.317
865	25.331	15.000	-674.625	1.483	-13.877	-22.919
885	30.000	0.000	0.000	0.000	0.000	0.000
889	30.833	0.000	0.000	0.000	0.000	0.000
890	31.667	0.000	0.000	0.000	0.000	0.000
891	32.500	0.000	0.000	0.000	0.000	0.000
911	33.333	0.000	0.000	0.000	0.000	0.000
915	34.167	0.000	0.000	0.000	0.000	0.000
916	35.000	0.000	0.000	0.000	0.000	0.000
917	35.833	0.000	0.000	0.000	0.000	0.000
943	27.675	13.000	-1.009	10.109	-12.342	-15.247
944	26.850	13.000	-1.061	10.037	-12.255	-14.841
945	26.025	13.000	-1.112	9.489	-12.140	-15.336
949	25.200	13.000	-1.166	7.883	-11.991	-17.642
965	36.667	0.000	0.000	0.000	0.000	0.000
969	37.500	0.000	0.000	0.000	0.000	0.000
970	38.333	0.000	0.000	0.000	0.000	0.000
971	39.167	0.000	0.000	0.000	0.000	0.000
972	40.000	0.000	0.000	0.000	0.000	0.000
973	40.000	0.938	0.000	0.000	-857.084	-1.626
974	40.000	1.875	0.000	0.000	-1.727	-3.118
975	40.000	2.813	0.000	0.000	-2.609	-4.510
1005	28.500	13.250	-919.577	7.420	-12.644	-18.368
1006	28.500	13.500	-889.882	6.195	-12.882	-19.257
1007	28.500	13.750	-861.731	4.967	-13.120	-19.930
1011	28.500	13.000	-951.597	8.965	-12.405	-17.191



<b>Node No.</b>	<b>x-coord.</b>	<b>y-coord.</b>	<b>dUx</b> [10 <sup>-3</sup> m]	<b>Ux</b> [10 <sup>-3</sup> m]	<b>dUy</b> [10 <sup>-3</sup> m]	<b>Uy</b> [10 <sup>-3</sup> m]
1024	27.975	15.000	-751.016	4.645	-14.250	-20.513
1025	30.619	15.000	-690.027	4.301	-14.405	-19.807
1026	29.738	15.000	-715.124	4.963	-14.369	-19.988
1027	28.856	15.000	-733.926	4.826	-14.319	-20.685
1031	28.500	14.000	-834.796	3.655	-13.356	-20.468
1032	30.750	14.000	-728.965	7.054	-13.461	-18.782
1033	30.000	14.000	-766.456	7.173	-13.437	-18.395
1034	29.250	14.000	-798.740	6.778	-13.403	-18.417
1083	40.000	3.750	0.000	0.000	-3.501	-5.836
1087	40.000	4.688	0.000	0.000	-4.402	-7.131
1088	40.000	5.625	0.000	0.000	-5.310	-8.421
1089	40.000	6.563	0.000	0.000	-6.222	-9.738
1093	31.500	15.000	-644.167	9.861	-14.425	-22.793
1094	31.500	14.250	-670.467	4.861	-13.713	-20.949
1095	31.500	14.500	-659.500	3.710	-13.951	-21.684
1096	31.500	14.750	-650.683	2.426	-14.188	-22.293
1097	31.500	14.000	-683.371	6.079	-13.475	-20.080
1112	40.000	7.500	0.000	0.000	-7.137	-11.084
1117	35.750	15.000	-370.723	3.248	-14.448	-21.927
1118	34.688	15.000	-452.774	3.873	-14.449	-21.633
1119	33.625	15.000	-528.145	4.451	-14.451	-21.497
1120	32.563	15.000	-593.310	4.815	-14.444	-21.138
1139	40.000	11.250	0.000	0.000	-10.801	-16.637
1146	40.000	9.375	0.000	0.000	-8.971	-13.837
1147	40.000	10.313	0.000	0.000	-9.887	-15.230
1151	40.000	8.438	0.000	0.000	-8.054	-12.455
1159	40.000	15.000	0.000	0.000	-14.437	-22.343
1161	40.000	13.125	0.000	0.000	-12.622	-19.483
1162	38.938	15.000	-96.074	8.903	-14.438	-22.315
1163	40.000	14.063	0.000	0.000	-13.530	-20.916
1164	36.813	15.000	-282.850	2.489	-14.444	-22.086
1166	37.875	15.000	-190.823	1.685	-14.440	-22.226